Encapsulation of Lactobacillus rhamnosus GG into hybrid alginate-silica microparticles

Haffner Fernanda Bianca

Collégium Sciences & Technologies
Pôle Scientifique Chimie Physique Moléculaires
Ecole Doctorale SESAMES ED 412

THÈSE

Présentée pour l'obtention du titre de **Docteur en Chimie**

de l'Université de Lorraine

par

Fernanda B. Haffner

Encapsulation of *Lactobacillus rhamnosus* GG into hybrid alginate-silica microparticles

Soutenue le 07 Juillet 2017

Membres du jury :

Rapporteurs :	Jens Risbo	Professeur associé Université de Copenhague, Danemark
	Thu-Hoa Tran-Thi	Directrice de Recherche CEA-Saclay, France
Examinateur:	Cécile Nouvel	Professeure Université de Lorraine, France
Invités:	Tom van de Wiele	Professeur associé Université de Gand, Belgique
	Nadia Canilho	Maître de Conférences Université de Lorraine, France
	Roudayna Diab	Maître de Conférences Université de Lorraine, France
Directrice de thèse :	Andreea Pasc	Maître de Conférences (HDR) Université de Lorraine, France

Equipe NANO – UMR 7565 SRSMC CNRS – Université de Lorraine
Faculté des Sciences et Technologies BP 239, 54506 Vandoeuvre-lès-Nancy Cedex
Projet financé par l'Europe (Programme FP7/2007-2013, n° 606713 BIBAFOODS)

Table of contents

Acknowledgements

First of all I would like to thank my main supervisor Andreea for her trust, guidance and knowledge sharing. She is definitely an inspiring female leader who is not only smart scientifically speaking but also has a precious emotional intelligence. And thank you Nadia for being there all times too – under the storms and the sunny days. The success of this PhD study is undoubtedly related to a great teamwork between the three of us along with the generous Marie Curie grant. By the way, this project has received funding from the European Union's Seventh Framework Program for research; technological development and demonstration under grant agreement no. 606713.

My profound gratitude for the acceptance as reviewers of this work goes to Thu-Hoa Tran-Thi and Jens Risbo. I am very flattered to have both of you in my jury along with Tom van de Wiele, Cecile Nouvel and Nadia Canilho.

Many researchers and staff at the University of Lorraine crossed my path along these 3-years and they were all very important to my research progress. Thanks for your time: Jean-Bernard Regnouf-De-Vains, Timothé Vucko, Sandrine Lamandé-Langle, Mathieu Etienne, Maciek Mierzwa, Carole Gardiennet, Stéphane Fontanay, Stéphanie Philippot, Mihayl Varbanov, Catherine Colson, Manu Chenin, Arnaud Risler, Paule Bazard, Francis Hoffmann, Paul (Magasin de Chimie), Stéphane Parrant, Lionel Richaudeau, Dominique Dodin, Francis Hoffmann, Lionel Aranda, Lise Salsi, Andreï Lecomte, Sébastien Hupont, Xavier Assfeld and Séverine Bonenberger. A very special thanks goes to Raphaël Duval who provided me with his lab's infrastructure for the microbiological work.

I also had the pleasure to be hosted in other European Institutions or enterprises and therefore I would like to thank some people for their great assistance. My special gratitude goes to Bruno Medronho from University of Algarve; Tom van de Wiele, Christine Graveel, Jana De Bodt and Tim Lacoere from University of Ghent; Ana Rascon from Aventure AB and Stefan Ulvenlund from CR Competence in Sweden.

The Bibafoods fellows will always be a cheerful memory on my PhD's journey too. Thank you all for the nice time spent together in the schools, secondments, trainings,

conferences and so on: Federico, Maryam, Cigdem, Poonam, Tomasz, Racha, Maria, Yoran, Federica, Surender, Sofia, Ileana and Davide. Another thanks for the fun company of all the European supervisors too: Tommy, Jens, Marité, Dennis, Tom, Björn, Maria, Bruno, Filipe, Gemma, Carmen, Jordi, Motomu, Stefan K., Hans, Stefan U. and Anna.

All the happy hours and laughs with the chemistry theoreticians were indeed very helpful for my sane state of mind, and therefore for the achievement of this work ☺ I started definitely to get a bit more interested in programing now thanks to these super fun guys: Antonio, Hugo, Benjamin, Thibaud, Audrey, Marco, Toni, Maria-Chiara, Sébastien, Chris, François, Mounir and Xavier.

And well, well, well, I would not have survived these 3-years without some other very important lovelies and I am definitely more than glad to have met you during my studies: Maura, Agnes, Sijin, Maxime, Lucie, Sanghoon, Marine, Émilie, Apolline, Luis, Jeanne, Oona, Marie-Chantal and Étienne. A special high-five from my heart goes to Hugo and Lara who are two extraordinary little aliens! Many memories will accompany my soul for life. Thank you both for all the laughs, tears, chats, happy hours, roller-skating, badminton, and all the stargazing adventures.

The last but not least: I thank my family for given me wings to embrace my own decisions with passion and courage, yet always remembering to keep my integrity. My final acknowledgment goes to a very special person: Thank you Alex for all your encouragement, understanding and love.

“We only live once, but if we do it right, then once is enough” (Mae West)

Scientific contributions

Peer-reviewed articles:

1. **Core-shell alginate@silica microparticles encapsulating probiotics**.
   Haffner, F. B., Girardon, M., Etienne, M., Fontanay, S., Canilho, N., Duval, R. E., Mierzwa, M., Diab, R., Pasc, A.*
   J. Mater. Chem. B, **2016**, 4, 7929-7935 (IF 4.8).

2. **Encapsulation of probiotics: insights into academic and industrial approaches**.
   Haffner, F. B., Diab*, R., Pasc, A.
   AIMS Materials Science, **2016**, *3*(1), 114–136.

3. **Silica-based systems for oral delivery of drugs, macromolecules and cells.**
   Diab, R., Canilho, N., Pavel, I. A., Haffner, F. B., Girardon, M., Pasc* A.
   Adv. Colloid Interface Sci., **2017**, doi.org/10.1016/j.cis.2017.04.005 (IF:7.8)

Book chapter:

4. **Clinical and preclinical use of nanomedicines: a status report.**
   Diab,* R., Kim, S., Pavel, I.-A., Canilho, N., Haffner, F. B., Li, S., Celzard, A., Varbanov, M., Lamouroux, E. and Pasc, A.
   Biomedical Application of Nanoparticles, Ed. B. Rihn, CRC Press Taylor & Francis Group, 2017, ISBN : 9781498750011

Submitted articles:

5. **Original behavior of *L. rhamnosus* GG encapsulated in freeze-dried alginate-silica microparticles revealed upon simulated gastrointestinal conditions.**
   Haffner, F. B., van de Wiele, T., Pasc* A.
   J. Mater. Chem. B (ms TB-ART-04-2017-000930)

Articles in preparation:

6. ***In situ* follow-up of hybrid alginate-silicate microbeads formation by linear rheology.**
   Haffner, F. B., Canilho, N., Medronho, B., Gardiennet-Ducet, C., Gansmüller, A., Pasc, A.*

7. **Unexpected *L. rhamnosus* GG survival in apple juice and beer.**
   Haffner, F. B., Pasc* A.

Oral presentations:

1. Haffner, F. B, Pasc, A. Encapsulation of Probiotics: A glimpse into academic vs industrial approaches. ***Journée Francophone des Jeunes Physico-Chimistes***, 13th to 17th of October 2014, Dammerie-Le-Lys, France.

2. Haffner, F. B., Diab, R., Girardon, M., Fontanay, S., Duval, R. E., Pasc, A. Encapsulation of *L. rhamnosus* GG in Alginate-silicate hybrid beads. **10th International Scientific Conference on Probiotics and Prebiotics – IPC2016**, 21th to 23rd of June 2016, Budapest, Hungary.

3. Haffner, F. B., Diab, R., Canilho, N., Fontanay, S., Duval, R. E., Pasc, A. Core-shell Alginate-Silica microparticles as carriers of probiotics. **Formula VIII Congress**, 4th to 7th of July 2016, Barcelona, Spain.

4. Haffner, F. B., Diab, R., Girardon, M., Fontanay, S., Duval, R. E., Pasc, A. Core-shell Alginate-Silica microparticles encapsulating probiotics. **6th EuCheMS Chemistry Congress**, 11th to 15th of September 2016, Seville, Spain.

5. Haffner, F. B., Wiele T. Van de, Pasc, A. Original behavior of *L. rhamnosus* GG encapsulated in freeze-dried alginate-silica microparticles revealed upon simulated gastrointestinal conditions. **Women and their Microbes**, 2nd of June 2017, Amsterdam, The Netherlands.

Outreach activities:

1. One-minute video aiming to outreach my PhD subject. Find it online https://www.youtube.com/watch?v=05UMxpP_nZk or read with your smartphone the barcode to your left with the 'Barcode Scanner' App.

2. Hands-on science teaching to pre-school kids in Nancy, France (2016) and experiments about 'Functional Foods' to adults in Barcelona, Spain (2016).

3. A 15 minutes science talk about my PhD research in a 'Happy Hour' context to the bachelor, master and scientific students of the University of Lorraine, Nancy, France (2016).

4. President of the French Chemical Society Youth Office - Lorraine section (Nov. 2014 to Nov. 2016).

5. Founder, Writer and Editor of Esperluette: for more info on the project, please read the Appendix II.

Abbreviations

APTMS: (3-Aminopropyl)trimethoxysilane
ATR-FTIR: Attenuated total reflectance - Fourier transform infrared spectroscopy
BCCM: Belgian coordinated collections of microorganisms
CFU mL^{-1}: Colony forming units per milliliter
CFU g^{-1}: Colony forming units per gram
CLSM: Confocal laser scanning microscopy
CMC: Critic micellar concentration
DCs: Dendritic cells
DGGE: Denaturing gradient gel electrophoresis
DNA: Deoxyribonucleic acid
EFSA: European food and safety authority
FC: Flow cytometry
FDA: Food and drug administration
FMT Fecal microbiota transplants
GABA: *Gamma*-aminobutyric acid
GALT: Gut-associated lymphoid tissues
GIT: Gastrointestinal tract
GRAS: Generally recognized as safe
HLB: Hydrophilic-lipophilic balance
IBD: Inflammatory bowel disease
IC: Ion chromatography
LGG: *Lactobacillus rhamnosus* GG
LUV: Large unilamellar vesicles
MRS: Man, Rogosa and Sharpe broth
NMR: Nuclear magnetic resonance
O/W: Oil-in-water emulsion
PBS: Phosphate buffer saline
PCR: Polymerase chain reaction
PGPR: Polyglycerol polyricinoleate
qPCR: Quantitative polymerase chain reaction
QPS: Qualified presumption of safety
SEM: Scanning electron microscopy
SHIME: Simulator of human intestinal microbial ecosystem
TEM: Transmission electron microscopy
TEOS: Tetraethyl orthosilicate
TMOS: Tetramethyl orthosilicate
W/O: Water-in-oil emulsion
W/O/W: Water-in-oil-in-water emulsion

Structure of the thesis

Chapter 1. General Introduction

A brief overview contextualizing the background of this work along with the aim and the main objectives of the thesis is in this section.

Chapter 2. State-of-the-art

It is composed of a large view of the importance of the microbiome research and its impact on major societal diseases followed by the interest of probiotics and their encapsulation. A literature review on encapsulation techniques and materials is assessed in more details. The chapter finishes with perspectives on the microbiome research field.

Chapter 3. Experimental part

The chemicals, methods and steps utilized for the accomplishment of this work are detailed in the experimental part.

Chapter 4. Results and Discussions

The results obtained from two LGG encapsulation strategies are discussed in this section, composed of two parts: (I) emulsification and (II) electrospraying. In brief, in the first part, the hybrid alginate-silicate material obtained via emulsification was not successful in keeping a large amount of viable LGG under confinement. Additionally, the bacteria could not be released from these microbeads. Despite the fact that this strategy does not look appropriate for encapsulation of cells, the formation mechanism of those beads was investigated. The findings are of interest in the fundamental comprehension of the formation of composite materials with potentiality in other domains. Finally, we show that in-situ rheology measurements were particularly adapted to monitor the various processes taking place during the complex mineralization/gelation process. In the second part of the study, core-shell alginate-silica microparticles were obtained by electrospraying, strategy that allowed us to obtain a plausible bacterial carrier in wet and lyophilized conditions. The synthesized beads had the LGG viability assessed in an *in vitro* gut model and in two food matrices, apple juice and beer. Beer, which contained 5 vt% alcohol, could be seen as a potential new probiotic food matrix targeting a wider public or eventually a new niche of customers.

Chapter 5. General Conclusions and Perspectives

Main conclusions and perspectives on encapsulation of probiotics are discussed on this section.

Appendix I. Characterization Techniques

The working principles of the main characterization techniques utilized during the thesis studies are explained in details in this section, *i.e.* scanning electron microscopy, transmission electron microscopy, confocal laser scanning microscopy, flow cytometry, rheology, polymerase chain reaction, denaturing gradient gel electrophoresis, DNA extractions, Sanger sequencing.

Appendix II. ESPERLUETTE - Research Outreach

All articles published on campus prior to the impression of the thesis manuscript are attached in this section along with an explanation of the *Esperluette* project – a personal initiative aiming to outreach research done at University of Lorraine in Nancy.

INTRODUCTION/

GENERAL INTRODUCTION

1. INTRODUCTION

Au cours des dernières années, des efforts considérables ont été investis pour comprendre et prouver les effets positifs de l'utilisation des bactéries probiotiques pour traiter divers problèmes de santé qui s'étendent des maladies gastriques jusqu'à la dermatite. Les formulations développées à base de probiotiques ont été destinées aux traitements par voie orale ou topique.[1] Plus précisément, on estime que le tractus gastro-intestinal d'un individu adulte est colonisé par 10^{14} cellules, parmi cela, il se trouve des probiotiques et des bactéries potentiellement néfastes.[2] La symbiose entre les micro-organismes gastro-intestinaux est dictée par le régime alimentaire de l'hôte, l'apport médicamenteux, l'hygiène et l'état pathologique. Par conséquent, le microbiote d'un individu est constitué d'une communauté diversifiée selon les habitudes diététiques et sanitaires d'une personne.[3-5]

Des études récentes évoquent le rôle considérable joué par le microbiome intestinal dans la prédisposition à différents phénotypes de maladies, qui sont souvent accompagnées de dysbiosis, et sont des problèmes majeurs de santé publique, comme c'est le cas pour l'obésité, le diabète et les syndromes intestinaux, par exemple.[3,5,6] Dans ce contexte, les probiotiques jouent un rôle dans la modification des expressions génétiques impliquées dans l'immunomodulation, l'absorption des nutriments, la suppression des agents pathogènes, le métabolisme énergétique et dans le fonctionnement de la barrière intestinale, où ils stimulent aussi la prolifération des cellules épithéliales ou induisent la sécrétion de mucine.[1,7-9] Les avantages positifs sur la santé dérivés de ces cellules probiotiques sont principalement dépendants de la souche bactérienne et de la maladie développée.

Pour restaurer l'équilibre du microbiote, l'apport de probiotiques par la voie orale est une méthode de choix. Dans ce cas, la microencapsulation des cellules est souvent nécessaire afin de fournir une protection externe aux microorganismes qui doivent conserver leur viabilité jusqu'à l'intestin, après avoir traversé les conditions difficiles du passage gastro-intestinal, c'est-à-dire, le pH acide, la présence de sels biliaires et d'enzymes.

Dans ce contexte, **l'objectif général** proposé dans ce travail était de synthétiser des microparticules d'alginate et de silice pour véhiculer une souche probiotique modèle, *Lactobacillus rhamnosus* GG (LGG), jusqu'à l'intestin. Pour la première fois, des supports combinant dans la même matrice, un polymère bio-protecteur, l'alginate, et un déshydratant alimentaire inorganique, la silice amorphe, ont été obtenus. La silice est généralement ajoutée à des formulations agroalimentaires préparées sous forme de poudre, pour servir d'agent antiagglomérant ou régulateur du taux d'humidité, afin d'assurer un stockage à long terme sans altération. Dans le cas des microcapsules, la silice devrait renforcer leur résistance mécanique et diminuer la diffusion des sucs acides dans les particules pendant le passage gastro-intestinal, permettant ainsi une meilleure protection des bactéries encapsulées.

Néanmoins, pour réaliser ce projet, plusieurs **objectifs principaux** ont été définis pour structurer et jalonner cette recherche et atteindre l'objectif général. Les différentes étapes pour mener à bien ce travail ont été définies comme suit :

- Encapsuler des LGG viables dans des microparticules d'alginate et de silice
- Développer des micro-supports alimentaires en tenant compte la compatibilité alimentaire
- Conserver une viabilité cellulaire élevée dans les microcapsules
- Modéliser la libération des cellules viables avec un modèle gastro-intestinal *in vitro*

Après cette introduction posant le contexte dans lequel s'inscrit ce projet de recherche doctorale, le deuxième chapitre de ce manuscrit de thèse fait un bilan bibliographique des travaux effectués sur le microbiote et les techniques d'encapsulation de micro-organisme. Puis, le troisième chapitre détaille les techniques et protocoles expérimentaux employées et établis pour obtenir les résultats présentés et discutés dans le quatrième chapitre de cet ouvrage. Enfin, le bilan des résultats majeurs et conclusions scientifiques seront résumés dans le cinquième chapitre de ce manuscrit qui fera également état des perspectives de recherches à poursuivre.

Références

1 T. Iannitti and B. Palmieri, *Clinical Nutrition*, 2010, **29**, 701–725.

2 W. H. Holzapfel, P. Haberer, J. Snel, U. Schillinger and J. H. J. Huis in't Veld, *International Journal of Food Microbiology*, 1998, **41**, 85–101.

3 V. Tremaroli and F. Bäckhed, *Nature*, 2012, **489**, 242–249.

4 P. Hemarajata and J. Versalovic, *Therapeutic Advances in Gastroenterology*, 2013, **6**, 39–51.

5 A. Woting and M. Blaut, *Nutrients*, 2016, **8**, 202.

6 F. De Vadder, P. Kovatcheva-Datchary, D. Goncalves, J. Vinera, C. Zitoun, A. Duchampt, F. Bäckhed and G. Mithieux, *Cell*, 2014, **156**, 84–96.

7 P. D. Cani, S. Possemiers, T. Van de Wiele, Y. Guiot, A. Everard, O. Rottier, L. Geurts, D. Naslain, A. Neyrinck, D. M. Lambert, G. G. Muccioli and N. M. Delzenne, *Gut*, 2009, **58**, 1091–1103.

8 E. Larsson, V. Tremaroli, Y. S. Lee, O. Koren, I. Nookaew, A. Fricker, J. Nielsen, R. E. Ley and F. Bäckhed, *Gut*, 2012, **61**, 1124–1131.

9 C. L. Maynard, C. O. Elson, R. D. Hatton and C. T. Weaver, *Nature*, 2012, **489**, 231–241.

1. GENERAL INTRODUCTION

Overview

In the past years there have been extensive efforts in understating and proving the positive effects in the use of probiotic bacteria for different types of health issues spanning from oral to topical formulated products and to treat from gastric diseases to dermatitis.[1] More specifically in the case of the gastrointestinal tract, an estimation of about 10^{14} viable cells from probiotics to potentially harmful bacteria are thought to harbor an adult individual.[2] Their harmonic relationship is dictated by the host's diet, medication intake, hygiene habits and diseased state. Consequently, an individual's microbiome holds a unique diverse community implying in its health maintenance.[3-5]

Recent evidences evoke the considerable role played by the gut microbiota in the predisposition to different disease phenotypes, which are often accompanied by dysbiosis, and are of major public health issues, *e.g.* obesity, diabetes and intestinal syndromes.[3,5,6] In this context, probiotics play a role in modification of the gene expressions, which are involved in immunomodulation, nutrient absorption, suppression of pathogens, energy metabolism and intestinal barrier function such as stimulation of epithelial cell proliferation or induction of mucin secretion.[7-9] Yet the positive health benefits provided by these probiotic cells are essentially strain-dependent as well as disease-dependent.

To restore an imbalance in the microbiota, the oral intake of probiotics is a practice. In this case, cells microencapsulation is oftentimes necessary in order to provide external protection to the load that must arrive viable to the intestines after going through the harsh conditions of the gastrointestinal passage, *i.e.* low pH, presence of bile salts and enzymes.

Aim

We proposed in the present work to synthesize alginate-silica beads as carriers of a model probiotic strain, *Lactobacillus rhamnosus* GG (LGG). For the first time, carriers combining within the same matrix, a bio protective polymer, alginate, and a desiccant,

amorphous silica, were obtained. The later is usually added to dried formulations in order to regulate the water activity as an anti-caking agent, and to insure thus, a long-term storage of the living material. Silica should provide extra mechanical protection and lower HCl diffusion into the beads during the gastrointestinal passage allowing a better protection of the encapsulated bacteria.

Main Objectives

- Encapsulate viable LGG in alginate beads with silica to reinforce the carriers
- Develop food microcarriers taking into account food compatibility
- Keep high cell viability while under confinement
- Release viable cells under an *in vitro* gut model

References

1 T. Iannitti and B. Palmieri, *Clinical Nutrition*, 2010, **29**, 701–725.

2 W. H. Holzapfel, P. Haberer, J. Snel, U. Schillinger and J. H. J. Huis in't Veld, *International Journal of Food Microbiology*, 1998, **41**, 85–101.

3 V. Tremaroli and F. Bäckhed, *Nature*, 2012, **489**, 242–249.

4 P. Hemarajata and J. Versalovic, *Therapeutic Advances in Gastroenterology*, 2013, **6**, 39–51.

5 A. Woting and M. Blaut, *Nutrients*, 2016, **8**, 202.

6 F. De Vadder, P. Kovatcheva-Datchary, D. Goncalves, J. Vinera, C. Zitoun, A. Duchampt, F. Bäckhed and G. Mithieux, *Cell*, 2014, **156**, 84–96.

7 P. D. Cani, S. Possemiers, T. Van de Wiele, Y. Guiot, A. Everard, O. Rottier, L. Geurts, D. Naslain, A. Neyrinck, D. M. Lambert, G. G. Muccioli and N. M. Delzenne, *Gut*, 2009, **58**, 1091–1103.

8 E. Larsson, V. Tremaroli, Y. S. Lee, O. Koren, I. Nookaew, A. Fricker, J. Nielsen, R. E. Ley and F. Bäckhed, *Gut*, 2012, **61**, 1124–1131.

9 C. L. Maynard, C. O. Elson, R. D. Hatton and C. T. Weaver, *Nature*, 2012, **489**, 231–241.

ETAT DE L'ART/
STATE-OF-THE-ART

2. ETAT DE L'ART

L'écosystème de l'intestin humain commence à se développer dès la naissance grâce au microbiote vaginale de la mère lorsque le naurrison nait par voie basse ou bien grâce à l'environnement lorsque la naissance a lieu par césarienne.[1,2] Les cellules bactériennes profitent de la disponibilité abondante de nutriments et de la température corporelle constante pour proliférer dans les intestins. Un exemple sont les bactéries de la famille de bifidobacteria et des lactobacillus qui prospèrent dans ce milieu stérile grâce à la présence d'oligo-saccharides du lait maternel. Les intestins seront donc colonisés par des bactéries probiotiques, ou 'pro-life', et des bactéries potentiellement néfastes, mais les deux types de micro-organismes s'équilibrent et contribuent à la bonne santé de l'individu. Le développement du microbiote d'un nourrisson aura un impact durable sur sa santé du début à la fin de sa vie.[3,4] En effet, un être humain subira des modifications au niveau de la diversité de ces bactéries qui colonisent les 32 m^2 de surface du tractus gastro-intestinale.[5,6] Ces changements sont finalement liés à une co-évolution de l'hôte et des micro-organismes sous l'influence des facteurs internes et externes à l'individu, comme l'âge et le pays de résidence par exemple.[1,7,8] Les résultats obtenus à l'issue du projet de recherche appelé « microbiome humain » ont abouti à un concept intéressant en ce qui concerne le microbiote gastro-intestinal. En effet, il semblerait que le microbiome soit composé d'un ensemble de microbiotes communs à plusieurs individus (appelé noyau), combiné à des microbiotes plus spécifiques à l'hôte, appelé microbiome périphérique. Ce dernier est lié à des variables externes telles que le mode de vie de l'hôte, l'environnement, le système immunitaire, la physiologie et le génotype, tandis que le microbiome noyau reflète plutôt le groupe de gènes présents dans le tractus gastro-intestinal dans la grande majorité des humains.[3,9]

La protection générale de la santé de l'hôte par la colonisation intestinale est connue depuis la fin des années soixante-dix, alors que le concept de microbiome humain n'a été reconnu par la communauté scientifique que très récemment dans ce 21ème siècle.[5,10,11] Cependant, à l'époque, les chercheurs avaient déjà observé un plus grand développement des maladies sévères de type botulisme ou salmonellose, chez les souris sans germes.[7,8,12] Les nombreuses études, menées lors de ces dernières décennies dans le domaine, ont finalement toutes convergées vers une même conclusion: les sujets

malades possèdent une diversité microbienne réduite dans les intestins. Néanmoins, à ce jour, le mécanisme biologique permettant de spécifier quels métabolites bactériens sont associés au développement de maladies métaboliques, dans le cas d'un microbiome moins diversifié, n'est pas encore clarifié.[9,13] C'est pourquoi, la corrélation entre les maladies et le microbiote est un sujet de recherche en expansion pour notamment essayer de trouver des traitements permettant de guérir certaines maladies sociétales en pleine évolution telles que l'obésité, les maladies inflammatoires de l'intestin, le diabète, et les allergies, par exemple.

Pour rétablir l'équilibre du microbiote chez l'individu, l'apport de probiotiques par la voie orale est de plus en plus pratiqué. C'est le mode d'administration le moins coûteux à ce jour et le plus accessible pour la population. Néanmoins, l'encapsulation de ces souches probiotiques destinées à l'ingestion est souvent nécessaire pour maintenir leur viabilité jusqu'à l'arrivée du cargo dans le colon, par exemple. Effectivement, le passage gastro-intestinal impose des obstacles à la survie des souches, majoritairement liés au pH gastrique, aux sels biliaires et aux enzymes.

En ce qui concerne les principales stratégies utilisées dans la formation de microcapsules, quatre méthodes peuvent être citées : l'extrusion, l'émulsion, la pulvérisation et la lyophilisation[10,11,14] de polysaccharides ioniques (alginate et chitosane), d'exopolysaccharides microbiens (gellan et les gommes de xanthane) et des protéines de lait qui sont des exemples d'agents encapsulant les plus couramment utilisés.[12,15] Sachant que les micro-organismes ont une longueur d'environ quelques micromètres, les tailles finales des microparticules sont évidemment du même ordre de grandeur mais peuvent contenir une seule souche ou un consortium de souches.

En ce qui concerne la formulation, les matériaux à base d'alginate sont de loin les plus explorés en raison de leur biocompatibilité, de leur biodégradation, de leur très bonne cytocompatibilité et de leurs propriétés mucoadhésives.[13,16] Une autre classe de matériaux à base de protéine, combinant des polysaccharides et / ou des fibres non digestibles appelées aussi prébiotiques font également l'objet de nombreuses études.[14,17] Dans l'intérêt de conserver l'intégrité des capsules alginiques ou protéiques face notamment au pH gastrique mais aussi aux enzymes rencontrées au cours du

passage gastro-intestinal, des stratégies de protection, développées en conditions simulées, sont rapportées dans la littérature. Ainsi, on trouve essentiellement les quatre méthodes de protection suivantes : i) Alginate revêtu par des protéines de lait. Dans ce cas, l'uniformité de la microstructure de la protéine et la structure de l'ensemble de la microcapsules formée après lyophilisation sont à l'origine d'une bonne performance de protection;[15] ii) Alginate revêtu de chitosane contenant des prébiotiques, tels que l'inuline et galactooligosaccharide. Le chitosane confère une protection supplémentaire aux cellules encapsulées tandis que les prébiotiques semblent avoir un effet synergique à l'origine de l'augmentation du nombre de cellules et / ou leur activité;[16] iii) Encapsulation de *L. acidophilus* La-5 dans du lactosérum ou dans de la crème de lait ;[17] et iv) Encapsulation de *L. plantarum* dans une formulation associant un prébiotique, des fructooligosaccharides et un extrait de protéines de lait[2,18] v) Enfin, une approche plus sophistiquée qui consiste à confiner des bactéries probiotiques dans une émulsion de type Pickering stabilisée par des nanoparticules de silice hydrophobisées a été rapportée par Wijk *et al.* Ce travail ouvre de nouvelles voies dans l'encapsulation des bactéries.[4,19]

Cependant, seulement peu d'études ont été réalisées sur animaux, probablement du à leur coût et à leur complexité. En outre, l'encapsulation d'un cocktail de souches bactériennes dans des transporteurs individuels, est de nos jours, la dernière tendance dans les recherches inhérentes à l'étude du microbiote. Les cellules peuvent agir de manière synergique, une souche pouvant stimuler le bénéfice probiotique des autres et vice versa. Dans ce contexte, les leaders de la recherche en probiotique dans le secteur privé, comme *Chr. Hansen*, cherchent à trouver de nouvelles souches potentielles de probiotiques au sein du microbiote humain. Les défis de ce type de recherche s'intensifient en raison de la multitude d'espèces de micro-organismes qui restent à découvrir puis à cultiver dans les conditions qui leur sont propres et donc sont loin d'être complètement connues à ce jour.

Les experts des domaines scientifiques liés au microbiome se sont réunis à la 18ème Conférence du Café Nature en novembre 2016 à Tokyo où les conférences ont permis une meilleure compréhension de l'impact de la recherche sur les microbiotes dans notre vie quotidienne. Le Dr Evan Elinav, du Weizmann Institute of Science (Israël), a

exposé les résultats préliminaires du «Projet de nutrition personnalisé» lancé il y a cinq ans. L'étude vise à déterminer les facteurs qui stimulent la réponse glycémique aux aliments. Jusqu'à présent, les réponses se révèlent spécifiques à chaque patient et, par conséquent, «un régime alimentaire unique n'est pas approprié. Le microbiome intestinal est plus unique que ce que nous pensions », a-t-il conclu. D'autre part, le professeur Kenya Honda et ses collègues de l'école de médecine de l'Université Keio (Japon) ont commencé à étudier comment les bactéries buccales modifient le système immunitaire intestinal. Il a ajouté: « chaque jour, un individu produit 1,5 litre de salive, qui contient une grande quantité de bactéries orales qui s'infiltrent dans l'intestin. Les premiers signes de la maladie de Crohn peuvent être observés par la dysbiosis provenant de bactéries dérivées par voie orale. »

Ce sont certainement des moments passionnants pour le domaine de recherche sur le microbiote / probiotiques, puisque les scientifiques commencent à comprendre la diversité, la nature dynamique et la distribution du microbiome. La recherche est à l'aube de nouvelles découvertes, car récemment des résultats on été publiés sur l'impact des bactéries intestinales sur le fonctionnement du cerveau et sur son influence dans les troubles tels que l'anxiété et la dépression.[20,21] Pourtant, l'utilisation de probiotiques comme supplément quotidien pour l'entretien de la santé est encore discuté par la communauté scientifique. Certaines raisons reposent sur des désaccords sur les définitions, par exemple, de ce qu'est un microbiome sain, voir même, est-il possible pour un individu de devenir plus sain? Les recherches en cours et à venir aboutiront aux futurs traitements et à de nouveaux aliments fonctionnels. Peut-être qu'un jour, le microbiome deviendra à l'image de l'empreinte digitale, une sorte de «empreinte intestinale» ou un indicateur médical de notre état de santé.

Références

1 T. Yatsunenko, *et al. Nature*, 2012, **486**, 222–228.

2 C. L. Maynard, C. O. Elson, R. D. Hatton and C. T. Weaver, *Nature*, 2012, **489**, 231–241.

3 P. J. Turnbaugh, R. E. Ley, M. Hamady, C. M. Fraser-Liggett, R. Knight and J. I. Gordon, *Nature*, 2007, **449**, 804–810.

4 T. Matsuki, K. Yahagi, H. Mori, H. Matsumoto, T. Hara, S. Tajima, E. Ogawa, H. Kodama, K.

Yamamoto, T. Yamada, S. Matsumoto and K. Kurokawa, *Nat Comms*, 2016, **7**, 11939.

5 P. Hemarajata and J. Versalovic, *Therapeutic Advances in Gastroenterology*, 2013, **6**, 39–51.

6 H. F. Helander and L. Fändriks, *Scandinavian Journal of Gastroenterology*, 2014, **49**, 681–689.

7 F. M. Collins and P. B. Carter, *Infection and Immunity*, 1978, **21**, 41–47.

8 L. J. Moberg and H. Sugiyama, *Infection and Immunity*, 1979, **25**, 653–657.

9 A. Woting and M. Blaut, *Nutrients*, 2016, **8**, 202.

10 M. T. Cook, G. Tzortzis, D. Charalampopoulos and V. V. Khutoryanskiy, *Journal of Controlled Release*, 2012, **162**, 56–67.

11 R. I. Corona-Hernandez, E. Álvarez-Parrilla, J. Lizardi-Mendoza, A. R. Islas-Rubio, L. A. de la Rosa and A. Wall-Medrano, *Comprehensive Reviews in Food Science and Food Safety*, 2013, **12**, 614–628.

12 R. Li, Y. Zhang, D. B. Polk, P. M. Tomasula, F. Yan and L. Liu, *Journal of Controlled Release*, 2016, **230**, 79–87.

13 A. Sosnik, *ISRN Pharmaceutics*, 2014, **2014**, 1–17.

14 Q.-Y. Dong, M.-Y. Chen, Y. Xin, X.-Y. Qin, Z. Cheng, L.-E. Shi and Z.-X. Tang, *International Journal of Food Science and Technology*, 2013, **48**, 1339–1351.

15 Y. Jiang, Z. Zheng, T. Zhang, G. Hendricks and M. Guo, *International Journal of Food Sciences and Nutrition*, 2016, **67**, 670–677.

16 W. Krasaekoopt and S. Watcharapoka, *LWT - Food Science and Technology*, 2014, **57**, 761–766.

17 G. M. Maciel, K. S. Chaves, C. R. F. Grosso and M. L. Gigante, *Journal of Dairy Science*, 2014, **97**, 1991–1998.

18 R. Rajam and C. Anandharamakrishnan, *LWT - Food Science and Technology*, 2015, **60**, 773–780.

19 J. van Wijk, T. Heunis, E. Harmzen, L. M. T. Dicks, J. Meuldijk and B. Klumperman, *Chem. Commun.*, 2014, **50**, 15427–15430.

20 J. A. Foster and K.-A. McVey Neufeld, *Trends in Neurosciences*, 2013, **36**, 305–312.

21 M. Crumeyrolle-Arias, M. Jaglin, A. Bruneau, S. Vancassel, A. Cardona, V. Daugé, L. Naudon and S. Rabot, *Psychoneuroendocrinology*, 2014, **42**, 207–217.

2. STATE-OF-THE-ART

2.1. Gastrointestinal microbiota

The human gut ecosystem starts to build up mostly by the mother's vaginal microbiota when the neonate is delivered via natural birth, or by the surrounding environment if it is delivered via caesarean section.[1] The bacterial cells take advantage of the abundant availability of substrates and the constant body temperature in order to perpetuate in the intestines. For instance, *Bifidobacterium* and *Lactobacillus* thrive in at first sterile habitat due to the content of the breast milk, mostly oligosaccharides. The microbiota development of an infant will have a durable impact on its own health.[2] Essentially, along its lifespan, a human will experience modifications in the diversity of these bacterial community that occupy the 32 m^2 of gastrointestinal surface.[3] These changes are ultimately related to a coevolution of host and microorganisms by virtue of internal and external factors, as one's age and geography for example.[4] The "human microbiome project" proposed an interesting concept in respect to the gastrointestinal microbiota: the presence of a core and a peripheral microbiome. The later is related to external variables such as host lifestyle, environment, immune system, physiology and genotype while the core microbiome reflects the group of genes present in the gastrointestinal tract in the ample majority of humans.[5]

It is very much curious to observe that 90 % of the cells found in the human body are mostly prokaryotic cells[6] meaning that they are not the ones building our own muscles, skin or organs. They are smaller in size and are present in the compartments of our body mostly inhabiting our intestines, where an amount of about 10^{14} viable cells for a adult human was estimated.[7] More than 1000 distinctive bacterial species are spread across the gastrointestinal sections weighing between 1 to 2 kilograms.[8] The intestinal sections differ however in terms of bacterial composition and activity. The stomach has a very limited amount of bacteria due to its low pH, but the small intestine contains in majority facultative anaerobic and aerotolerant strains whereas the large intestine holds a wider and more complex ecosystem with hundreds of different species. This fact results from the transit time in each of the sections, accounting for longer ones in the

large intestine, which implies in a greater breaking down of the nutrients favoring cells growth.[9] Figure 1 exemplifies the sections of the intestines with its microbiota and pH specificities. Species in the Firmicutes and Bacteroidetes sum up more than 90 % of total gut microbiota.[10]

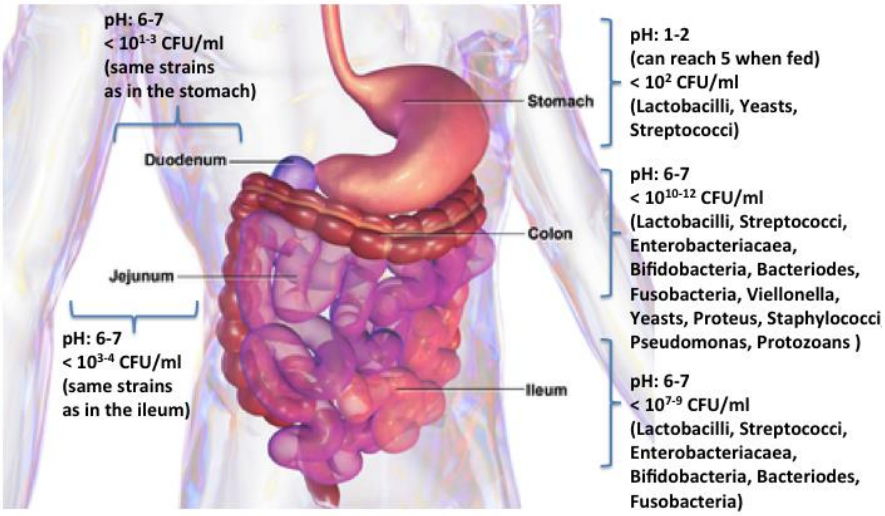

Figure 1: Adapted gastrointestinal passage scheme showing the pH and bacterial community in each section.[11,12]

The harmonic relationship of these bacteria in the most metabolic active organ in our body is dictated by several factors such as the host's diet, medication intake, hygiene habits, diseased state, among others. Consequently, an individual's microbiome holds a unique diverse community implying in its health maintenance.[9,13,14] Recent evidences evoke the considerable role played by the gut microbiota in the predisposition to different disease phenotypes, which are often accompanied by dysbiosis, and are of major public health issues, *e.g.* obesity, diabetes and intestinal syndromes.[13,15] With that being said, Figure 2 exemplifies schematically what it could be the microbiota development of healthy and diseased subjects during the course of their lives.

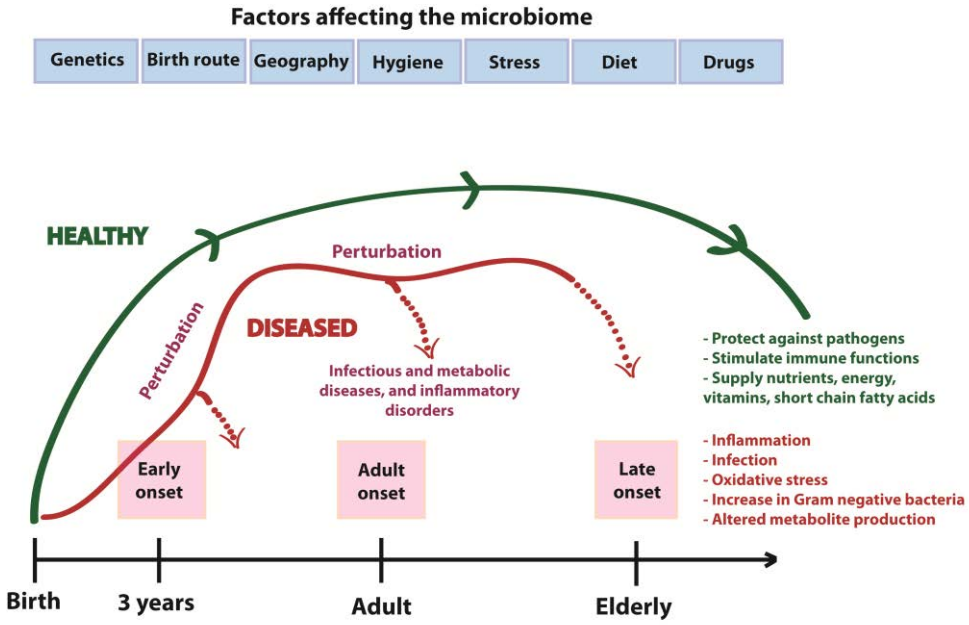

Figure 2: An overview of the evolution of a healthy and a diseased microbiome of an individual during a life period. Adapted from Kostic *et al.*[9]

2.2. Gut microbiome and host health

The general protection of the host health by normal gut colonization was known as far back as the late seventies although the concept of human microbiome arose only in the twenty-one century.[14] Back then however, researchers had already observed the greater inclination of germ-free mice in developing severe illnesses, such as Botulism and Salmonellosis.[16,17] In the next decades, substantial studies in the domain came into the spotlight and they all converged to the same conclusion: diseased subjects hold a reduced microbial diversity in the intestines. Yet, up to date, there is still a lack of understanding of the relation between development of metabolic diseases and specific bacterial metabolites in a less diverse microbiome.[15]

The bacterial cells and the host collaborate during their lives in a rather symbiotic relationship. On a broad perspective, the microbes thrive by virtues of the constant body temperature along with the obtention of the energy sources and nutriments through the host's diet required for their proliferation. To keep a healthy size bacterial community, they will need to compete among themselves resulting in the continue presence of the most adapted bacteria. The host itself will profit from the degradation of

larger molecules into smaller ones performed by the bacterial enzymes during their survival competition, which would otherwise not be available to the maintenance of the metabolic functions of the host. The ultimate fate resumes into either a successful- or mal-functioning of both partners that will equally suffer the consequences. Thus, in a more specific perspective, the functional contributions of these bacterial cells are the following: (i) depolymerization and degradation of indigestible fibers such as resistant starch or plant cell wall polysaccharides, resulting in short-chain fatty acids;[18] (ii) utilization of intestinal glycan mucins as growth substrates when other polysaccharides are absent;[19] (iii) degradation of dietary proteins, which are a source of carbon, nitrogen and energy;[20] (iv) conversion of polyphenols, secondary plant compounds that recently showed attention as being health promoters[21] and (v) degradation of bile salts, which significantly inhibit Bacteroidetes and Actinobacteria when present in elevated amounts.[22]

The correlation of diseases with the microbiota of the patients is an increasing research topic. Obesity, inflammatory bowel disease (IBD), diabetes and allergies are herein discussed in more details.

Obesity

The scientific attention towards obesity is not a novel field of research, however the understating of this metabolic disorder experienced great progression in the last decade thanks to the differences observed in the gut composition of obese and lean mice. The microbiota of the obese rats holds more Firmicutes and less Bacteroidetes, which follows the same trend in the fecal analysis of the human phenotypes. Interestingly, weight loss by fat- or carbohydrate-restricted diets, favors the augmentation of Bacteroidetes levels, indicating that these bacteria respond to calorie intake.[23] Another study observed the weight augmentation of germfree mice after fecal transplantation of microbiota from obese into the lean mice without any changes in their diets.[24] The obese microbiome seems to be capable in harvesting more energy from food. Lean mice that received the fecal transplantation from equal lean mice kept the same body mass.[25] Thus, the microbes seem to play a decisive role in the obtention of energy, carbon and nutrients from one's diet along with fat deposition. In an evolution point of view,

modern societies need less energy input to accomplish their regular activities as if compared to their ancient peers. The daily carbohydrate- or fat-rich food intake is elevated however in modern western diets followed by sedentary habits, which govern the establishment of an obese-like gut ecosystem.[13,24]

Inflammatory bowel diseases (IBD)

More than 3.6 million people in North America and Europe suffer from IBD including ulcerative colitis and Crohn's diseases.[26] IBD augments the risk of such individuals in developing colorectal cancer.[9] Studies show altered interactions between the gut immune system and the microbiota as being the cause of the illness progression. Firstly, it is of importance to note that healthy subjects have a difference in the mucus layer of the lumen in the small intestine and the colon, where the colon holds an inner and an outer layer. The inner is strongly attached to the epithelial cells and it is sterile avoiding any contact of bacteria with the body cells. The commensal microbes inhabit the outer part.[27] In subjects holding Crohn's disease, there is a dense community of adherent-invasive *Escherichia Coli* able to infect epithelial cells, *i.e.* present in the inner layer, and replicate within macrophages.[28] Another genus of bacteria present in abnormal quantities is *Fusobacterium* inducing mucosal erosion.[29] In order to epithelial cells to keep their metabolism active, short-chain fatty acids such as acetate, propionate and butyrate, are necessary[30] and these can be provided by dietary fibers, which are hydrolyzed by beneficial bacteria such as *Bifidobacterium* or *Lactobacillus*.

Diabetes

Type-2 diabetes is a major modern disorder accounting for heavy governmental costs worldwide. Genetic and environmental factors are contributors to the individual's health state. Individuals with this pathology possess only a moderate gut dysbiosis in comparison to patient's holding inflammatory bowel disease. However, a decrease in the proportion of the phylum Firmicutes and the Clostridia class was observed.[31] Additionally, butyrate-producing bacteria diminishes, which may be directly related to the increase in opportunistic pathogens. These bacteria were reported to have protective effects against several diseases.[32] Even more interestingly is the increase in

intestinal permeability observed in obese and diabetic mice when they are treated with a high-fat diet.[33] Such a diet rebounds into a decrease in the presence of *Bifidobacteria* that usually hydrolyzes intestinal lipopolysaccharides and in this particular case results into a lesser effective intestinal barrier function.[34,35]

Allergies

Over the last decades we observe a great increase in allergic disorders especially in the modern developed countries. Curiously enough, such societal conditions overlap with a progressive hygiene care, smaller family sizes, diet changes and overuse of medication.[36] Already back in the late nineties, Wold *et al.* postulated that an excessive hygienic lifestyle would restrict the immune system from inducing and maintaining oral tolerance of inoffensive antigens specially in early life. In reality, children reach an adult-like gut microbiome only at the age of three years old.[4] Additionally, not only genetics play a role in the infant microbiome development, but also external factors such as country of origin, breastfeeding or delivery mode. Natural birth and early guts colonization is in fact thought to be beneficial to children against allergies in a later stage of their lives. In a study, allergic children hold significantly less *Lactobacillus rhamnosus, L. casei, L paracasei, Bifidobacterium adolescentis* and *Clostridium difficle* during their first two months of lives.[37] Along the same lines, another study in mice showed that the gut-associated lymphoid tissues (GALT) do not develop correctly if the normal microbial colonization is somehow perturbed in the first months of life leading to a continual immune dysregulation.[38] It is still unknown however if the gut microbiota dysbiosis is the cause of allergies or if it is a consequence. Nevertheless, more and more studies have been showing the importance of the mother's microbial environment during pregnancy as well, and how it may modulate the offspring's immune development even before birth.[39]

Other disorders are on the radar of this domain too. For instance, alcohol ingestion induces changes in the mucus barrier of the intestinal epithelium developing into a so-called 'leaky gut'.[33] The stool microbiome of patients dealing with cirrhosis contains extensively more bacteria from the Alcaligenaceae and Enterobacteriaceae taxa when compared to healthy controls. Poor cognition performance was related to the first taxa

whereas Enterobacteriaceae aggravated inflammation.[40,41] The increase of intestinal permeability was observed during stress states too where the bacterial cells obtain free access to interact with immune and neuronal cells.[8] This example introduces us to another fascinating and rather *in vogue* area of research: the gut-brain axis. The term falls back from 1880s when William James and Carl Lange introduced the concept built around the bidirectional communication between the central nervous system and the intestinal organs. This communication has not only an influence in the maintenance of gastrointestinal homeostasis and digestion, but also it affects mood, cognitive functions, and the stress- and pain modulation systems.[6,42,43] Lately, pathologies such as Parkinson, autism, anxiety and depression have been discussed in more details. For instance, dysfunction in the signaling of the *gamma*-aminobutyric acid (GABA) inhibitory neurotransmitter leads to anxiety and depression.[8] As a matter of fact, the capability of *Lactobacillus* sp. in metabolizing glutamate and therefore producing GABA under culture conditions was already described in the literature.[44] The *in vivo* verification of Higuchi *et al.* study was performed feeding mice with *Lactobacillus rhamnosus* and there was indeed a decrease in the emotional behaviors of the rodents.[45]

All these encouraging findings will lead to novel approaches in health treatments in the very near future. This fact can be already exemplified by the unconventional fecal microbiota transplants (FMT) use to treat antibiotic-resistant strains of *Clostridium difficile*. In the first randomized trials conducted by van Nood and colleagues the result was extremely promising. About 94 % was the efficacy for patients suffering from recurrent bacterial infections while of only about 38 % for patients treated with the regular antibiotic vancomycin.[46]

The gut microbiota research will keep certainly expanding enormously taking into account all the axes it encompasses from metabolic diseases to neurosciences in which collaboration and multidisciplinary are still very much desired in order to advance in a undeniable complex domain. Technological advances of molecular and metagenomic tools are also of importance to propel the frontiers of the microbiome knowledge. As a general perspective of mine, with such scientific studies reaching more and more a broader audience, there will be eventually more people questioning modern standards such as the actual excessive hygienization, which reflects in some ways in an

individual's poorer immune system, and consequentially predisposition to several pathologies.

2.3. Probiotics

History

Probiotics have been with us for quite some time, more precisely since we have been eating fermented milk: centuries before Christ. The association of these bacterial cells with health benefits and the first findings are however fairly recent and dating back to about a century ago.[47] The Russian Nobel Prize Eli Metchnikoff was the first one to suggest the beneficial role of the gastrointestinal bacteria. He based his hypothesis on the observation of the longevity of Bulgarian peasants and their frequent intake of fermented dairy products. Metchnikoff postulated that the lactic acid bacteria replaced the pathogenic microorganisms in the guts and the result was a decrease in certain illnesses.[48] At the same period of time, Henry Tissier, a French pediatrician, observed the low numbers of a peculiar Y-shaped bacterium in the stools of infants facing diarrhea while healthy subjects had plenty of these 'bifid' microorganisms, which led him to suggest its administration to restore the microbiota of the ill children. Metchnikoff and Tissier were thus the pioneers of the probiotic field, although the term probiotic was not utilized until 1974 with the studies of growth promoting supplements in the animal feed. Few years later, the first successful fecal transplants trials for patients suffering from *Clostridium difficile* recurrence supported evidences on the beneficial role provided by a healthy gut microbiota.[49] By the late eighties, *in vitro* inhibition of *Clostridium botulinum* from isolates of intestinal bacteria confirmed further the importance of certain species of bacteria populating out gastrointestinal tract, which only gained more and more attention to up-to-date.

According to the Food and Agriculture Organization of the United Nations/World Health Organization (FAO/WHO), probiotics are living microorganisms that promote the host health when administered in adequate amounts.[48] Commonly the scientific community accepts a daily consumption of 10^8 to 10^9 CFU g^{-1} (Colony Forming Units per gram) of probiotic viable cells as being the minimum amount required to confer the desired benefits.[50]

Overall, under natural circumstances, humans should not need probiotic supplements with the exception of the public holding any type of special condition, *e.g.* reestablishment of gut microbiota after a long-term use of antibiotics. However, changes in the behaviors of our society challenge the inhabitants of the gut. Sterile food consumption, increased hygienization and medication overuse are some of the antagonists of our commensal microbiota, which can be potentially normalized by the ingestion of probiotics.

In terms of legislation, it is of importance to note that firstly probiotics can hold a food supplement or a drug label. The latter guarantees still up to today a higher product quality in terms of strain efficacy and manufacturing processes. Thus, the pharmaceutical industry must comply with all the compulsory strict and costly analyses to launch a product holding any health claim. In the case of food supplements, the current regulation (EC1924/2006) states that any health claim must be based on scientific evidences that are then analyzed by the European food safety authority (EFSA) before any commercialization.[51]

In terms of economics, the global scenario of probiotics is very encouraging. Probiotic ingredients and supplements reached approximately $23.1 billion in 2012; and the growth forecast is in the $36.7 billion range to 2018.[52] Given this context, pharmaceutical and food industries are both interest in grasping a share in this market. Table 1 exemplifies the probiotic strains already used for commercial applications to date. In respect to actual food products, a wide range, mainly dairy, are in the market, and more are yet to come, especially non-dairy novelties.[53] The low-cholesterol diets, lactose intolerance and milk protein allergy public, vegans and vegetarians are some of the future potential customers for these products. Herein some examples: table olives;[54] apple juice;[55] goat's milk ice cream;[56] green tea;[57] kefir;[58] dry apple snack;[59] orange, pineapple and cranberry juices;[60] pomegranate and cranberry juices;[61] carrot and watermelon juice;[62] fresh apple wedges;[63,64] chocolate[65] and cereals.[66,67]

Table 1: Adapted list of several probiotic strains used in commercial applications to date.[68]

Company	Probiotic strain
Chr. Hansen	*L. acidophilus* LA1/LA5, *L. delbrueckii* ssp. *bulgaricus* Lb12, *L. paracasei* CRL431, *B. animalis* ssp. l*actis* Bb12
Danisco	*L. acidophilus* NCFMs, *L. acidophilus* La, *L. paracasei* Lpc, *B. lactis* HOWARUTM/Bl
Winclove	*B. lactis* W51, *B. lactis* W52, *E. faecium* W54, *L. acidophilus* W22, *L. paracasei* W20, *L. plantarum* W21, *L. salivarius* W24, *Lc. Lactis* W19
DSM Food Specialties	*L. acidophilus* LAFTIs L10, *B. lactis* LAFTIs B94, *L. paracasei* LAFTIs L26
Nestle	*L. johnsonii* La1
Snow Brand Milk	*L. acidophilus* SBT-20621, *B. longum* SBT-29281
Institute Rosell	*L. rhamnosus* R0011, *L. acidophilus* R0052
Yakult	*L. casei* Shirota, *B. breve* strain Yaku
Foneterra	*B. lactis* HN019 (DR10), *L. rhamnosus* HN001 (DR20)
Probi AB	*L. plantarum* 299v, *L. rhamnosus* 271
Danone	*L. casei* Immunitas, *B. animalis* DN173010
Essum AB	*L. rhamnosus* LB21, *Lactococcus lactis* L1A
Biogaia	*L. reuteri* SD 2112
Morinaga Milk Industry Co. Ltd.	*B. longum* BB536
Lacteol Laboratory	*L. acidophilus* LB
Medipharm	*L. paracasei* F19
Merck	*L. rhamnosus* GR-1, *L. reuteri* RC-14

Probiotic strain

The idea behind delivering helpful bacteria into the intestines is genuine, but holds few prerequisites. In order to be considered as a probiotic at first, the bacterial strain should comprise with minimum the following: (i) non-pathogenic, (ii) tolerated by the immune system, *i.e.* do not have any carcinogenic nor allergic effect and (iii) be able to get down to its site of action alive and preferably being able to recolonize and/or proliferate in that specific location. The bacterial surface plays therefore a key role in establishing narrow interactions within the ecosystem present at the site of action. Figure 3 illustrates for instance the differences in the cell wall structure of gram-positive and

gram-negative bacteria. Often the probiotic species are gram positive. The work of Tripathi *et al.* studied in more details the constituents of a gram-positive lactic acid bacterium.[69]

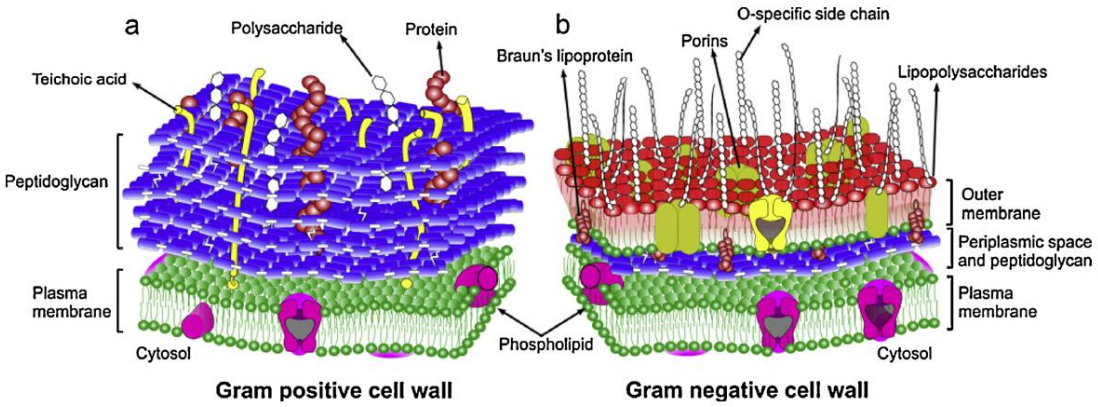

Figure 3: Comparison of the structures of the cell wall of a) a gram-positive, and b) a gram-negative bacteria.[69]

When probiotics are considered as food additive, there are few other essential key points to be considered. It should not create unpleasant flavors or texture and should hold the American label 'generally recognized as safe' (GRAS) or the European label 'qualified presumption of safety' (QPS). Up to recently, the genera of bacteria (or yeast) used to promote the host health were mostly Leuconostoc, Pediococcus, Enterococcus, Bifidobacteria and Lactobacillus**,** where the two last ones account for a long and safe use in the dairy industry.[70] New insights gained over the last years into metabolic syndromes have drawn the attention of scientist to a so-called 'next generation of probiotics'. The use of high-throughput sequencing has been allowing studies of the human microbiome in greater details. In such a context, it is certain that novel strains with enormous potential as probiotics will emerge in the next years. A today's example is *Akkermansia muciniphila*, a mucin-degrading bacteria that was found to be present in lower levels in obese and diabetes type-2 individuals.[71]

Bifidobacterium

Tissier at the Pasteur Institute in France was the first one to isolate these bacteria. They are anaerobic, gram-positive, immobile and non-spore-forming, holding a curved rod shape or a Y-shape and producing mostly acetic and lactic acids as end-products from

glucose fermentation.[72] Several strains have been isolated from feces of human such as *B. longum, B. breve, B. infantis, B. bifidum, B. adolescentis* and *B. pseudonatenulatum,* but also from animals such as *B. animalis.*[73] Curiously, the animal strains do not colonize humans or vice-versa. However, as *B. animalis* is more acid-resistant, it has been used in various yogurts types.[74]

Lactobacillus

Lactic acid bacteria are gram-positive, non-spore-forming, holding a rod-shape and producing mostly lactic acid as the end-product of the fermentation of carbohydrates. They are part of the normal human microbiota and colonize the mouth, intestines and the female genitourinary tract. Some of the most frequent isolated from the feces of humans are *L. brevis, L. casei, L. acidophilus, L. plantarum, L. fermentum, L. salivarius* and *L. rhamnosus.*[75]

Lactobacillus rhamnosus GG (LGG)

As its counterparts, LGG is a non-spore-forming, gram-positive, rod-shaped, facultative anaerobe producing mostly lactic acid as end-product of the carbohydrate fermentation (Figure 4). It has been isolated from the gastrointestinal tract of a healthy human by Goldin and Gorbach in 1983 explaining its GG label. It hold the dimensions of ca. 0.8 to 1.0 by 2.0 to 4.0 μm depending on culture conditions.[76] It can be seen as single units or in chains. The stationary phase in the bacteria life-cycle is reached after 24 h at 35 °C in MRS broth.[77]

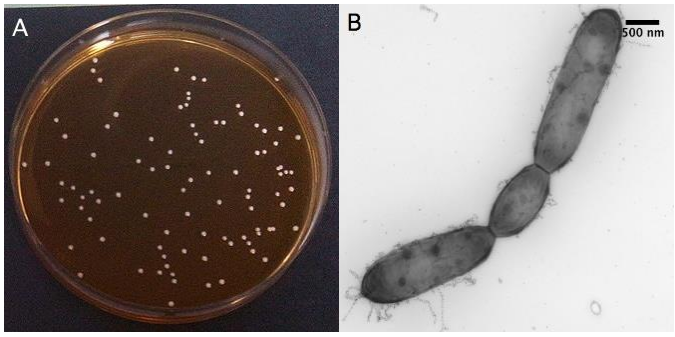

Figure 4: A) typical LGG colonies on MRS-agar plate, B) LGG in a chain with its pili in evidence.[78]

Its probiotic proprieties were first postulated as a result of its resistance to acid and bile along with excellent adhesion to human epithelial cells due to the presence of

fimbria-like appendages most known as pili, which plays an important role in gut colonization.[79] The beneficial effects of this strain came after extensive clinical trials and human intervention studies. For instance, LGG is generally recognized as safe (GRAS) and it is used in the treatment of acute gastroenteritis, Crohn's disease, diarrhea and also urogenital infections.[12] Due to its well-documented history in the literature for its probiotic properties, LGG was therefore chosen in our study.

Probiotics mechanisms of action

There are three main mechanisms in which probiotics appear to get involved in to exert beneficial effects.[1,12,33,80,81] Figure 5 exemplifies schematically these mechanisms. Yet, to keep in mind, the positive health benefits provided by these probiotic cells are essentially strain-dependent.

The three mechanisms are:

i) Antimicrobial effects: inhibition of pathogens by hydrolyzing complex carbohydrates and producing metabolites such as short chain fatty acids (mainly butyrate, propionate and acetate), bacteriocins and hydrogen peroxide. The organic acid producing bacteria are important in maintaining the pH of the luminal region to an optimal level preventing the proliferation of other pathogens.[82] The bacteriocins produced by lactic acid bacteria are proteins or protein complexes with antibacterial activity towards gram-positive bacteria. The range of inhibition of these strains is generally narrow, which means only closely related to the producing microorganism.[83]

ii) Immune modulation: interacting with host cell types such as dendritic cells (DCs), T cells, regulatory T cells, monocytes/macrophages, immunoglobulin A producing B cells, natural killer cells, and by induction of T-cell apoptosis.[81]

iii) Mucosal barrier: induction of mucin secretion maintaining the integrity of the intestinal epithelium. Compromised epithelium tight junctions allow macromolecules permeability, which may trigger autoimmune responses in predisposed individuals. In fact, subjects suffering from infectious diarrhea, inflammatory bowel disease and even diabetes type-1 have a higher mucosa permeability.[84-86]

Some probiotics strains are able to adhere to the epithelial cells by electrostatic interactions, hydrophobic and steric forces. Doing so, they prevent the pathogens to invade the body system while competing also for nutrients.[87]

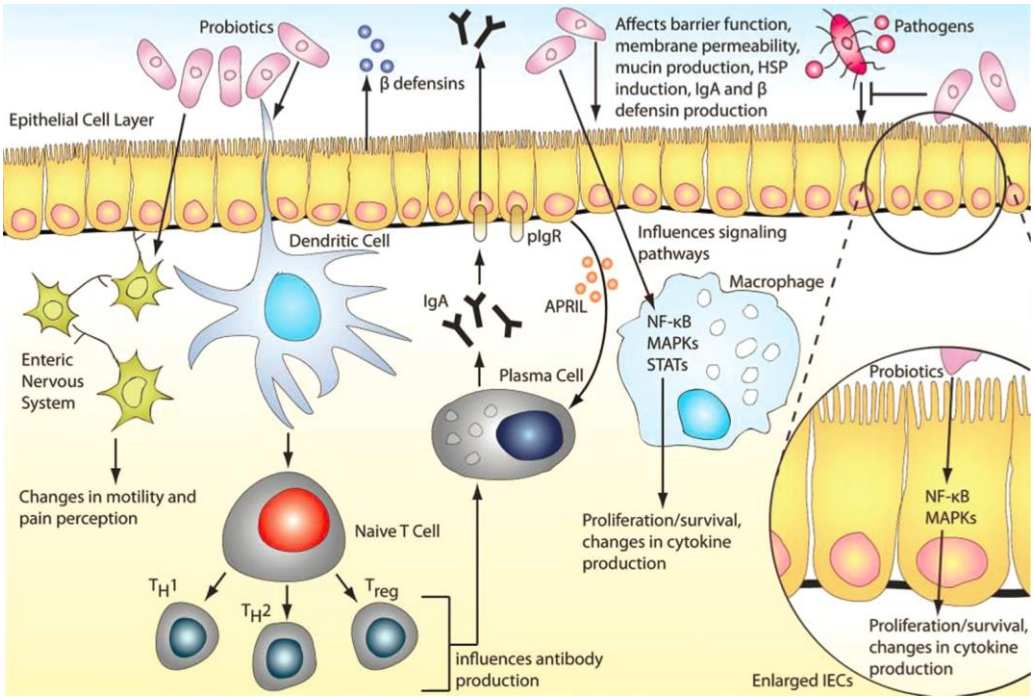

Figure 5: Scheme of the main mechanisms in which probiotics are thought to get involved in.[14]

As a final observation, despite the fact that several strains support beneficial health effects for the treatment of specific diseases, the usual outcome of the reviews is: more studies are needed to settle conclusions. An example is the case of LGG with 21 studies accounting in total with 3979 participants showing clinical efficacy in treating acute gastroenteritis.[51] Overall we could affirm that this specific strain in its free state has the potential in treating this specific disease. However, what is of paramount importance, and still less addressed currently, is the beneficial effect of the same strain under confinement conditions in the case of the encapsulated systems since the carrier synthesis may influence the metabolic activities of the microbial cells. Indeed, the encapsulation efficiency may be less important if the cells lose their probiotic efficacy.

2.4. Encapsulation techniques

Encapsulation is a physicochemical or mechanical process aiming in keeping a substance under confinement for a certain period of time. In general, bacteria are encapsulated in order to protect them from stresses encountered during the technological processes of food preparation and during the gastrointestinal passage. Figure 6 exemplifies some of the most important key stress factors.

The stresses during the technological process of a given product and their final impact on the probiotic strain are dependent undoubtedly on the product itself and the strain in question. For example, a pineapple juice would impose great acidity stresses during storage while alcohol content will be detrimental to cells if added to alcoholic beverages. During consumption, the acidity of the stomach is usually the first most destructive factor on cells and its negative impact will depend mostly on the bacterial strain type.

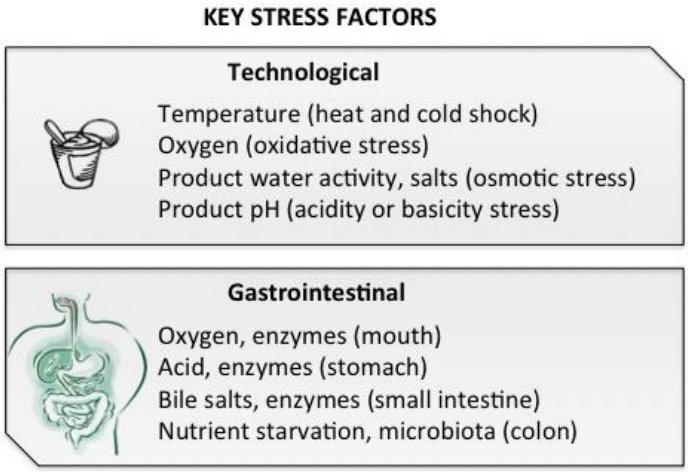

Figure 6: The cells key stress factors during the technological and gastrointestinal processes. Adapted from Ruiz *et al.*[88]

Overall Lactobacilli are acid-tolerant bacteria and are able to maintain viability at a pH range of 4.5 to 7.0. When the extracellular pH gets to very low values, the cells utilize a proton-translocating ATPase in order to maintain cytoplasmatic pH homeostasis.[89] Nevertheless, LGG showed in the past an extraordinary ability to survive the GIT passage.[90] Its was capable of surviving a pH as low as 2.5 after 4 h.[91] Corcoran *et al.* came to the conclusion that the presence of glucose in the media enhances LGG

survivability in simulated gastric juices.[92] The same result was not observed in the case for other strains such as *Lactobacillus gasseri*. Table 2 exemplifies the influence of the acidity in the survivability of some non-encapsulated bacterial strains.

Yet the poor survivability of non-encapsulated bacteria is an issue not only during the GIT passage, but also in ready-to-consume probiotic products available in the market. If the probiotic cells are not viable prior to consumption, then the problematic needs to be addressed even before its ingestion. In food products, the viability is not only strain-dependent, but also depends on interactions with other species present in the product, culture conditions and production of metabolites affecting the final acidity of the product. Several reports have drawn the attention of scientists to the poor survival of strains at the time of consumption of yogurts.[93] Three out of six samples in a dairy product study contained no traces of live bacteria.[94] These insights highlight the importance of providing protection to bacteria strains before addition to food carriers and consumer consumption. For such, scientists assess a multitude of technological approaches in order to obtain microcapsules. The choice of a particular technique will depend mostly on the encapsulation agents, the desired size of final material and bacterial strain. Additionally, mild processes reduce cell injury during the encapsulation and allow higher cell viability in the final material.

Table 2: Acidity influence on the survivability of non-encapsulated bacteria.

Bacterial strain	Incubation time & pH	Impact on survivability	Reference
B. infantis	30 min & pH 2.5	None survived	[95]
L. acidophilus *B. infantis*	3 h & pH 2.0	5 log loss 3 log loss	[96]
Nine *Bifidobacteria* strains	2 h & pH 2.0	*B. lactis* Bb-12 showed best performance: 1 log loss	[97]
L. acidophilus *B. lactis* Bb-12	2h & pH 1.0 & 2.0	pH 1.0: none survived pH 2.0: around 1.5 log loss for both	[98]
L. rhamnosus GG	45min & pH 2.0	about 7 log loss when glucose is not present	[92]

The most common encapsulation techniques are briefly described in the next paragraphs along with examples of studies.

Spray-drying

This atomization technology is the most widely used encapsulation technique in the food industry due to its continuous production feasibility and tailor-made characteristics depending on feed and encapsulating agent.[94] The configuration of a basic spray dryer consists of a drying chamber, which receives a liquid spray, and it is rapidly evaporated as soon as it encounters the hot air flow. The liquid is broken into fine dried droplets. Spray driers are used frequently to entrap oils, aroma, enzymes and pharmaceutical drugs. A large amount of research has been put into encapsulating probiotic bacteria in a laboratory scale; however, final cell viability in food carriers can still be an issue for industrial application due to temperature, osmotic extremes and water activity (a_w).

High outlet temperature causes overall damages to probiotics. Behboudi-Jobbehdar *et al.* observe an increase in the survival rate of *L. acidophilus* from 2.5 to 84 % when the outlet temperature was reduced from 91.5 to 60 °C.[99] Additionally, the authors concluded that a more elevated flow rate typically reduces cell membrane damage. Yet, the heat-tolerance of the cells seems to be very much related to the moment of cell harvesting as well. Corcoran *et al.* spray-dried *L. rhamnosus* in lag, early log and stationary phases and compared the strain viability independently of the type of feed carrier used. The order of survivability is stationary, early log and lag with 50 %, 14 % and 2 % respectively.[100]

In order to keep high cell viability in the spray-dried powder, studies on storage are important. The survival of *L. acidophilus* after 35 days of storage at 25 °C was investigated by Yonekura *et al*.[101] and the viability of *B. animalis* ssp *lactis* after 12 weeks at 4 °C.[102]

The development of spray-dried probiotic bacteria has been limited in large commercial scale to the best of our knowledge. Despite the high production rates and relatively low operating costs, *i.e.* 4 to 7 times cheaper than freeze drying,[103] most of the probiotic

strains do not survive in large quantities after the heat stress and dehydration. The high temperatures result in high mortality and inactivation of microorganisms damaging cytoplasmatic membrane, cell wall, ribosomes and DNA.[104,105] Another industrial limitation is the shell material, which needs to be soluble in water at an acceptable level due to usual water aqueous formulations. Stable spray dried culture starters are attractive to the fermented probiotic business as they could be added directly into finished food, suppressing the need of liquid starter stocks and resulting in less storage costs.[106]

Spray-cooling (or spray chilling)

In spray-cooling, the active ingredient is dispersed in a molten material, usually fats, serving as the carrier. The cold air injected into the chamber enables the solidification of the microcapsules.[107] The advantages of this technique are: (i) the least expensive with scale-up potential for probiotics,[108,109] (ii) application of lower temperatures enabling its use with thermosensitive microorganisms, (iii) capsules are generally insoluble in water due to the use of wax and oil as carriers. Their solubility will depend on the hydrophilic and lipophilic characteristics of the carrier.[110] On the other hand, few eventual hurdles are: (i) displacement of the core material during storage due to the solidification and crystallization process of lipids,[108] (ii) hydrophobic characteristic of the material can be an issue for certain applications, (iii) difficulty to obtained a delayed release of a water soluble ingredient over 30 minutes when the food carrier has high water activity.[109]

Promising systems have been developed in the past years. Pedroso *et al.* observe the impact of spray-cooling on *B. animalis* ssp *lactis* and *L. acidophilus* and concluded that the process conditions did not impact negatively either cell viability. In a 90-days storage at 7 °C, about 72 % of the encapsulated *B. animalis* ssp *lactis* remained viable while only 20% for *L. acidophilus*.[108] Another study looked into 120-days storage of *L. acidophilus* at -18 °C or 7 °C with a relative humidity of 11 %. Their formulation with polydextrose presented the best cell viabilities, which were quite similar, about 7.0 CFU g^{-1}, for both temperatures.[111]

The expanding scenario of probiotics gains overtime more attention in the animal feed industry as well where the rules for antibiotics administration become stricter and the intention of enhancing animal health and productivity is a reality.[112] Lallemand Health Solutions commercializes Bactocell®, a product based on viable *Pediococcus acidilactici,* an additive that reduces bone deformation in fishes.[113] In another commercial approach, there have been trials on co-encapsulation of few strains in the same carrier. DuPont Pioneer owns a patent where *Enterococcus faecium*, *Lactobacilli* or yeast are the community in question and the product is targeted to animals. The microspheres can be stored for a period of 3 to 6 months and cell viability is maintained even if there is exposure to some moisture or antibiotics.[114]

Spray-coating

Spray coating consists of forming a uniform layer onto solid particles. It is utilized with a vast variety of shell materials such as polysaccharides, proteins, fats, yeast cell extract, or even complex formulations. This versatility translates into potential controlled release features.[109] In the basic configuration, powdered probiotic bacteria are kept in motion in the chamber and a coating is sprayed over them. The final material will have different characteristics depending on the applied spray coating configuration.[115]

Fluidized bed drying is a type of spray coating invented and patented in 1963 by Würster commonly used in the food industry. This technology allows the use of milder temperatures compared to spray drying due to optimal heat and mass transport resulting in higher cell survival.[116] This system was utilized by Schell *et al.* to encapsulate *L. reuteri* with different coatings. Interestingly, they observed a better survival at pH 1.5 to 4.5 when the coating in question was shellac, a FDA-approved resin used in the coating of candies and fruits, which is secreted by the female insect *Laccifer Lacca*. In terms of the operating parameters, Semyonov *et al.* observed that the inlet air temperature was the most detrimental accounting with a 250-fold decrease in survival rate of *L. paracasei* when the temperature increased from 47 °C to 62 °C.[117]

The rehydration of a powder before its addition to a given product may affect the viability to the encapsulated cell. Champagne *et al.* evaluated various homogenization, rehydration and plating practices of spray-coated and freeze-dried *L. rhamnosus* and *B.*

longum. This study points out that *L. rhamnosus* has a better survival rate to freeze drying than *B. logum* and spray-coated cultures rehydrated slower and only partially.[118]

Advances using this technology can be seen already in the market. Lallemand Health Solutions has developed an encapsulation technology named Probiocap®. The molten hydrophobic coating is injected in a rotational vessel containing agglomerates of living dehydrated probiotics.[119] One of the advantages of the process includes suitability with a wide range of coating materials, which can have a higher melting point than the temperature of the human body avoiding an early stage disintegration of the capsules. The same company developed Star®, a water-based enteric-coating with excellent barrier protection that allows manufacturers to add lower concentration of microorganisms per capsule, allowing in any case the maintenance of the load efficacy.

Liposomes

Liposomes are spherical bilayers composed of phospholipids similar to cellular membranes. Hydrophilic molecules are entrapped in the water-soluble interior of the liposome, and hydrophobic in the oil-like portion. They hold the neat potentiality of delivering hydrophilic and hydrophobic active ingredients in one single cargo. The large unilamellar vesicles (LUV) are the most pertinent for the food industry due to their high encapsulation efficiency and over time better stability. Main drawbacks of such technique are upscaling costs and often the formulations are kept in rather dilute aqueous suspensions, which translate into additional costs.[109]

There are still several issues to be addressed in order to liposomes be successfully utilized in the probiotic industry. Chemical degradation, stability and oxidation are main downsides. The use of liposomes in value-added products is however current and well established in the pharmaceutical industry. For the beverage industry, one smart development to avoid the lipid degradation is by freeze-drying it. Curcusome®, a freeze-dried liposomal formulation can be kept in release caps. Since liposomes are not stable at low pH or high temperatures, often parameters of the beverage industry, the liposomal powder is released from the cap into the beverage right at consumption. Innovations as such can bridge the liposomes research to probiotics in like manner.

Coacervation

Coacervation is a widely studied technique applied with several hydrocolloid systems such as gelatin/acacia gum, carrageenan, chitosan, soy protein and gelatin/carboxymethylcellulose. Coacervation can achieve rather high payloads, on the other hand the process is cost-expensive and frequently crosslinking substances are involved, such as glutaraldehyde or enzymes.[109] One (simple coacervation) or more (complex coacervation) hydrocolloids are dispersed in an aqueous solution with an active substance. With a pH change, the opposite charged colloids link together forming a layer around the active substance. The complex coacervation has been widely used to encapsulate flavors and unsaturated fatty acids with the goal of enhancing their shelf life.

A successful encapsulation system will protect the probiotics against the gastrointestinal passage, but the cells should withstand the storage as first place. Shoji *et al.* microencapsulated *L. acidophilus* by complex coacervation employing pectin and casein followed by spray-drying and further addition to buffalo milk yogurt. The bacteria survived in 10^7 CFU g^{-1} in buffalo milk presenting a shelf life of around 120 days at 7 °C. However, adequate amounts did not survive the simulated pH conditions of the stomach.[120] Gerez *et al.* encapsulated *L. rhamnosus* combining ionotropic gelation and complex coacervation using pectin and whey protein. The authors observed an effective protection of *L. rhamnosus* resulting in a survival rate of 10^7 CFU mL^{-1} in pH 2.[121]

Emulsification

The emulsification is often investigated since it is a straightforward process with no need of expensive equipment. Overall in an emulsifying process, the surfactant type and the energy given during the agitation process are the main drivers in the final emulsion droplets sizes.[122] The drawback here is the difficulty in controlling the droplets size distribution with a standard emulsification process, and this fact results in polydispersity of the final material. There is, however, an emerging technology called membrane emulsification, where one of the emulsion phases is pushed trough a holey foil generating spherical droplets that are enclosed by the phase of the emulsion containing the surfactant. It produces uniform droplets holding potential for cell

encapsulation.[123] However, the high cost of final product is still a hurdle for the production of ordinary foodstuff.

The role of the surfactant in the preparation of an emulsion is to decrease the interfacial tension, defined as the work that must be expended to increase the size of the interface between two adjacent phases, which do not mix completely with one another. The adsorption of the surfactant within the interface of the droplets allows a greater "stability" of the system that is anyhow thermodynamically unstable and tends to a phase separation. In resume, the surfactant slows the rate of the physical mechanisms that lead to phase separation granting a kinetic stability of the system.[124]

The surfactant has two parts with different polarity: an apolar or hydrophobic part holding an affinity to oils and a polar and hydrophilic holding an affinity to water. One or more aliphatic hydrocarbon chains, linear or branched, aromatic or alkyl aromatics might constitute the hydrophobic part. Its hydrophobicity varies with the number of carbons, insaturations and ramifications. One or more polar groups, ionic or nonionic constitute the hydrophilic head. Choosing an adequate surfactant to stabilize an emulsion means either having affinity towards the continuous phase, *i.e.* hydrophobic character for a W/O emulsion or hydrophilic character for an O/W emulsion. This is known as 'Bancroft rule'.[125] The hydrophilic-lipophilic balance (HLB) is a concept used to define the nature of the surfactant in terms of its hydrophilicity (20) or hydrophobicity (0). Thus, the scale goes from 0 to 20 depending on the molecular structure of the surfactant and it can be calculated as below:

$$HLB = 20 * \left(\frac{Mh}{M}\right)$$

where Mh is the molecular mass of the hydrophilic portion of the surfactant molecule, and M is the molecular mass of the whole molecule.

In other words, the HLB values are a guidance for the obtention of a W/O emulsion (HLB between 0 and 9) or an O/W emulsion (HLB between 11 and 20). It is of importance to note that the HLB is only a feature of the surfactant itself and the

proprieties of the system will depend for example on temperature, composition or electrolytes concentration as well.[124]

In this study, two surfactants were used to obtain the final materials: a hydrophobic one, PGPR (HLB: 4.0) and a hydrophilic one, Tween 40 (HLB: 15.6). Polyglycerol polyricinoleate (PGPR) is a power nonionic hydrophobic emulsifier used in the food industry for the preparation of W/O emulsions. It is manufactured in four steps, *i.e.* preparation of the castor oil fatty acids followed by their condensation, preparation of polyglycerol followed by the partial esterification of the condensed castor oil fatty acids with the polyglycerol.[126] Its excellent water-binding capacities are attributed to the long hydrophilic polyglycerol chain. In terms of consumption, the normal metabolism of lipids in the human body is not interfered by the PGPR since its digestibility is up to 98 %. Additionally, it is considered GRAS by the FDA.[127]

Polyoxyethylene sorbitan monopalmitate (Tween 40) is a nonionic hydrophilic emulsifier produced from ethylene oxide, sorbitol and palmitic acid. It is considered a food additive with very low acute toxicity, thus being safe for consumption in the levels of 10 mg/kg of bw/day.[128]

Emulsion-based techniques are on the radar of many researchers. Dianawati *et al.* prepared fifteen different emulsion systems to evaluate the survival of *B. longum* after freezing steps. Overall milk proteins and sugars were more protective. One explanation may be due to the easier interaction of the hydroxyl groups of sugars with the polar sites of phospholipid bilayers composing the cell membranes.[129] Amine *et al.* studied the survival of extruded or emulsified *B. longum* added to cheddar cheese with a 21-days storage at 4 °C. The emulsion method showed a superior survival with however a 2 log CFU mL^{-1} reduction.[130] The work of Mantzouridou *et al.* looked into cell viability of *L. paracasei* ssp *paracasei* entrapped in corn oil droplets. The cell freely suspended in the continuous phase and stabilized with egg yolk had the highest cell viability after a 4-week refrigerated storage when compared to the cells imprisoned in oil droplets.[131]

In terms of patents, Unilever holds an invention for a salad dressing of a W/O/W edible emulsion containing probiotic bacteria in the internal water phase. Although its

composition is not detailed, the constituents are water, yogurt, sunflower oil, PGPR, tween 60, vinegar, sugar, xanthan gum and salt. The emulsion has an acceptable level of viable cells after 3 weeks of storage at 8 °C.[132]

Extrusion

Generally speaking, this method consists in allowing the bacteria slurry flow through a dripping nozzle and the droplets harden simultaneously when contacting the receiving solution. The regular extrusion gave rise to other more elaborated methods, such as co-extrusion, rotating disk with jet break-up, electrospraying and JetCutting (Figure 7).[104]

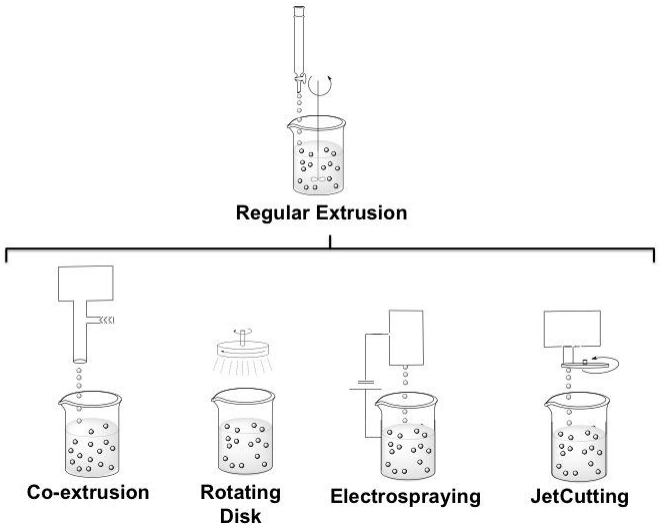

Figure 7: Scheme of some extrusion methods used for probiotic encapsulation.

One of the preferred polymers used in extrusion systems is alginate and coatings are applied onto the beads in order to enhance protection. Borges *et al.* evaluated the effect of microencapsulation on the viability of *L.casei*, *L. paracasei*, *L. acidophilus* and *B. animalis* in an alginate matrix. Results concluded that survival is strain-dependent. Among these strains, free and encapsulated *L. acidophilus* demonstrated the highest survival rates when lethal conditions of temperature and pH were applied.[133] The authors discuss the final bead size and its protection role. The requirement of the food industry to avoid organoleptic drawbacks in a given product is of 100 μm and in fact humans can detect particles of sizes small as 25 μm.[134] However, smaller sizes confer less protection. Finally, the balance between final size and intended protection is debatable and it will ultimately depend on the characteristics of the food carrier.

Nualkaekul *et al.* compared alginate and pectin beads for improving the survival of *L. plantarum* and *B. longum* during storage in pomegranate and cranberry juices. The influence of various coating materials on cell survival was assessed and the double gelatin coated pectin beads coffered the highest protection in the juices. The effect may be attributed to the formation of a dense polyelectrolyte complex, which eventually increased the buffering effect of the beads. For instance, the coating protected the beads against the penetration of gallic acid.[61] Khan *et al.* entrapped *B. adolescentis* in capsules composed of biopolymer mixtures of chickpea, faba, lentil or pea protein isolates with alginate. Shelf life studies with a plain yogurt as a model showed a reduction of 3 log CFU mL^{-1} for entrapped cells with all capsules designs in a period of 7 days whereas free cells had 8 log CFU mL^{-1} reduction.[135] The use of legume proteins along with alginate opens up the ingredient market to non-dairy applications. Laelorspoen *et al.* investigated the use of electrospraying in a zein-alginate core-shell system containing *L. acidophilus*. The increase of the voltage decreased beads sizes confirming Poncelet's *et al.* work, and only minor changes in viability were suffered with the voltage adjustment.[136] De Prisco *et al.* used a vibrating technique to encapsulate *L. reuteri* in alginate/chitosan matrixes with further freeze-drying. The authors report a narrow bead size of 110 ± 5 μm and encapsulation efficiency higher than 90 % for the four systems studied. There was an observation of a 100 % cell survival after freeze-drying with no changes on the structure of the beads.[137] Graff *et al.* encapsulated *Saccharomyces boulardii* in an alginate/acrylic acid matrix coated with chitosan using the laminar jet break-up. The use of acrylic acid minimized the aggregation and sticking of the beads.[138] Coghetto *et al.* electrosprayed *L. plantarum* with alginate or alginate-pectin. After a 21 days refrigeration storage, the encapsulated cells showed cell survival around 9 log CFU mL^{-1} whereas the free cells hold only 1 log CFU mL^{-1}.[139] Pitigraisorn *et al.* coated electrosprayed alginate *L-acidophilus* with egg albumen and stearic acid as first layer followed by cassava starch as second layer in order to improve moist-heat-resistance.[140]

Extrusion is largely applied in research, but not only, since it has been present in the market as well. BRACE GmbH proposes a vibrating nozzle system for the encapsulation of a variety of different ingredients.[141] The company holds a patent for production of spherical alginate beads in industrial scale. Based on the BRACE technology, Vésale

Pharma developed Intelicaps®, uniform probiotic microcapsules with an alginate-based shell and typical sizes of 600 to 800 µm. Morishita Jintan Co. Ltd produces Bifidobacteria capsules of 2 mm with a three-layer shell of gelatin to be blended with yogurts. The company owns the patent of Asada *et al.* who created multilayer capsules composed of cells capable of growing in the confined state.[142]

Freeze-drying (or lyophilisation)

The freeze-drying technique is often assessed when long-term preservation of cultures is necessary. It is still the most satisfactory method for storage, and it can be used to preserve the lactic acid bacteria starter cultures in the dairy industry for example.[143-145]

In a typical freeze-drying process, the excessive moisture of the samples is removed under low temperatures. The liquid material containing the bacteria is first frozen with further decrease of the chamber pressure enabling the frozen water to sublimate. It is an energetic costly procedure, but on the other hand it avoids oxidation of the cells and it provokes less harm to the cells when compared to the high drying temperatures. An eventual concern associated with this technique is the formation of ice crystals during slow freezing, which may lead to significant cell damage and ideally must be avoided.[146]

A successful freeze-drying followed by high cell viability in a rehydration step is a result of several parameters. For instance, the microencapsulation matrix,[143,147] the physiological state of the cells,[148] the freezing rate,[149] the initial cell concentration,[150] the rehydration conditions and the use of cryoprotectants are of importance in freeze-drying tolerance.[151] Moreover, exposure of bacterial cells to sub-lethal stresses increases the robustness of the cells.[88] In such a context, Nguyen *et al.* studied the consequences of exposing *B. bifidum* to 42 °C prior to freeze-drying. Indeed the authors confirm the increase of cell resistance to lyophilisation and overall downstream processing, which seemed to be correlated to exopolysaccharide excretion by the bacteria.[152]

In nature, microorganisms withstand dehydration by accumulating disaccharides intracellularly, mostly sucrose and trehalose, which allow them to protect vital cell structures.[153] Disaccharides are thought to stabilize the lipid membrane and proteins by

hydrogen bonds preventing denaturation and cell wall disruption.[154] With this being said, disaccharides seem to be important in the intra- and extracellular milieu. Thus, the cell loss is attenuated as a result of lowering the freezing point of water and formation of amorphous matrixes. The amorphous state has a higher viscosity translating into lower molecular motility and therefore less chemical deterioration along with serving as a shielding barrier around the cells.[155]

Ideal cryoprotectants should be food grade, permeate through the cell wall and contain non-toxic solutes. The efficacy of several chemicals as protectants has been investigated over the years. Often the outcome of these studies highlights the fact that each specific strain behaves differently in the presence of the same chemical.[145] In the work of Siaterlis *et al,* LGG received better protection with sucrose when compared to sorbitol or trehalose.[156] This outcome was in agreement with Ananta *et al*,[157] but oppose the work of Miao *et al*. Sucrose in this case was the least effective cryoprotectant when compared to lactose, trehalose, and maltose. In addition, the best outcome came from the mixture of lactose and maltose where 98.7 % of LGG survived the freeze-drying procedure.[158] Such results reinforce the fact that the same strain behaves in a unique manner depending most likely on harvesting time, growth media, initial cell concentration and small protocol variations. The complexity increases when an encapsulation matrix with or without cryoprotectant is entrapping the cells. As an example, Hugo *et al.* confirmed the formation of stable cold-set gels with viable *L. delbrueckii* ssp *lactis* when adding $CaCl_2$ to high pressure-treated and freeze-dried soybean protein isolates.[67] In such context, the cell viability response will depend on the encapsulation material and technique along with all the other parameters mentioned beforehand.

Oftentimes the high cost of this technique is highlighted as a drawback. However, when considering the bacterial loss in the cost analysis of different drying methods, freeze-drying seems a competitive approach. At present day, the industry uses this technique to dry components for value-added products, *e.g.* enzymes, probiotic pills for the reestablishment of the gut microbiota and bacterial strains used in research.

2.5. Encapsulation materials

Polymers are organic or inorganic macromolecules constituted of smaller chemical units (monomers) covalently linked one to another. Their chemical structure and the chains conformation will confer them specific functionalities such as gel formation or water absorption capabilities. There is a wide choice in terms of encapsulating materials ranging from organic and natural such as plant and algae based, organic and synthetic such as polyacrylamide, or inorganic options such as silica (SiO_2). Table 3 exemplifies the most common utilized cell encapsulation materials and they are correlated with the previously described encapsulation techniques.

Generally speaking, cells confinement impose great challenges since the matrix must be biocompatible, but also support cell survival, which depends on inducing minimal cell stress during the synthesis, *i.e.* mild temperatures, pH and ionic strength. For these reasons, natural hydrogels are of interest.

Natural hydrogels are highly hydrophilic polymers able to get truly hydrated while forming a tridimensional network supported by electrostatic or covalent interactions between the polymer and a crosslinker. The biological-like structures formed by the hydrogels are similar to the extracellular milieu of the human cells conferring them great potential in the encapsulation of living materials.[159] Additionally, the diffusion of molecules in and out of the gel allows the communication of the entrapped cells with the external environment. The cross-linkage degree and polymer composition have however an important impact in the final encapsulation efficiency and cellular viability. Ordinarily, the hydrogel is composed of two distinct phases: the sol phase of a water-based free flowing slurry containing the bacterial cells and the polymer, and the gel phase with the formed network being hold commonly by electrostatic forces between the polymer and the ions introduced in the system. Their disadvantage lies on the rather porous matrix holding a more fragile final mechanical structure. Alginate is a good example of a hydrogel extensively used in microbial cells encapsulation. In order to overcome the rather flexible and porous matrix, which leads to loss of viability during gastrointestinal passage, the system is often reinforced with a coating.[160] Additionally, in an acidic environment, such as in the gastric stage where pH can drop to less than 2

for as long as 2 h, alginate can also be hydrolyzed into D-mannuronic and α-L-guluronic acids,[161] allowing bacteria release before they reach the lower intestinal tract.

Table 3: Correlation of encapsulation technologies with capsules sizes, currently encapsulation materials, pros and cons.[162]

	Usual capsules sizes	Most current encapsulation agents	Pros	Cons
Spray-drying	5 to 150 μm[111]	Inulin,[163,164] acacia gum,[103] locust bean gum,[165] starch,[55] soy protein,[103] whey protein,[99,101,102,164] skim milk,[163] chitosan,[101,166] alginate[101]	1. Mass production 2. Continuous process 3. Material monodispersity 4. Well established in the food industry for other applications 5. Inexpensive	1. Loss of cell viability due to high temperatures 2. Mostly used with aqueous suspensions, i.e. shell material should be soluble in water
Spray-cooling	20 to 200 μm[110]	Cocoa butter,[111] Palm oil,[111] Palm kernel oil[111]	1. Mass production 2. Continuous process 3. The least expensive encapsulation technique 4. Mild temperatures setup	1.Lower load (10-20%) when compared to spray drying (5-50%) 2.Encapsulated ingredient may be on the surface and in contact with environment 3.Difficulty to delay the release of water-soluble ingredient over 30min
Freeze-drying	-	Starch,[167] soy protein,[67,129] casein,[129] whey protein,[129] skim milk[129]	1. Excellent final dried material suitable for most food applications 2. Suitable for sensitive materials as probiotics	1.High costs 2. Cell damage with eventual crystal formation if not done correctly 3.Eventual need of cryoprotectants
Spray-coating	5 μm to 1 mm[94]	Shellac,[116] fat[118]	1. Control release with addition of different coatings 2. Increase in storage stability	1. May introduce forces that can damage the cells 2. Although temperature is lower, the exposure could be longer along with oxygen exposure
Emulsification	200 nm to 1 mm[94]	Inulin,[131] K-carrageenan,[168] alginate[130]	1.Easy technique 2.Usual high survival rate of bacteria	1.Costly to scale-up 2.Polydispersity of material 3.Shape variation of material 4.Prolonged shear forces may cause damage to cells
Liposomes	few nm to few μm[94]	Phospholipids[94]	1.Improve taste issues (*e.g.* flavor encapsulation) 2.Provide good protection to	1. Most costly and complex technique among the ones described in this section

			sensitive agents 3. Can carry hydrophobic and hydrophilic molecules in the same cargo 4.Mucoadhesive	2. It uses organic solvents 3. Formulations are kept in dilution aqueous solution 4. Stability issues at high and room temperature as well as low pH
Coacer-vation	1μm to 1 mm[94]	Pectin,[120] gelatin[169]	1. High payloads (up to 99%) 2. Mild preparation conditions 3. High shell integrity	1. Expensive technology 2. Usual use of non-food grade crosslinkers or enzymes 3. Natural small differences in the structure of the polysaccharides influence the final capsule structure (quality control challenge)
Extru-sion	100 μm to 3 mm[94]	Locus bean gum,[165] pectin,[61,139] chicory,[170] sugarbeet,[170] whey protein,[171-173] gelan gum,[174] xanthan gum,[174] gelatin,[61] chitosan,[61] K-carregeenan,[168] alginate[61,130,135,139,140,170,175,176]	1. Monodispersity 2. Scale-up potential 3. Mild conditions 4. Continous process	1. Frequently other technologies are further used in order to obtain a final dry material 2. Larger capsules

Alginate

From all polymers used in cell encapsulation, alginate is by far the most studied since its successful employment in the entrapment of pancreatic islets reported by Lim and Sum as a result of its remarkable biocompatibility and mucoadhesiveness.[177] Several examples were already mentioned on the extrusion section.

In terms of classifications, alginates fall in the soluble dietary fibers and prebiotics categories. It means these polysaccharides are relevant in the reduction of blood cholesterol, regulation of insulin and improvement on nutrient and mineral absorption (dietary fibers category) or promoting benefits to the fecal metabolism of the microbiota in humans (prebiotics category).[178] On another perspective, interestingly, some bacteria are able to secrete alginate as an exopolysaccharide, which role is to protect it from surroundings adversities and enhance adhesion to solid surfaces. An example is *Pseudomonas aeruginosa* that is present in soil and freshwater.[179] All these

evidences reinforce the potential use of this anionic polysaccharide in the encapsulation of probiotic bacteria.

Alginate in food

From a regulatory point of view, the FDA recognizes alginate as GRAS. In Europe, alginates are enlisted as food additives in category 4 from E400 to E495, *e.g.* E400 (alginic acid), E401 (sodium alginate) or E402 (potassium alginate). Their use is versatile and they can be employed as thickeners, stabilizers, gel-producer, film-forming agents in milk puddings, syrups, purees, desserts, dry mixes, icing, and so on. The work of Glicksman examines the several applications of alginate in different food systems.[180]

Gel formation: the egg-box model

Alginic acid is a natural linear polymer commercially extracted from brown seaweed and often used in the food and pharma industries due to its gel and viscosity properties. Various proportions of covalently linked 1,4-β-D-mannuronic acid (M) and α-L-guluronic acid (G) residues compose alginate. The M/G ratio depends on the source of the alginic acid and vary according to geographic location, species, algae age and harvesting season.[181] In terms of structure, alginates are irregularly arranged homopolymeric blocks (MM or GG) or heteropolymeric blocks (MG) (Figure 8).[182-185] Its ability to form stable hydrogels results from its crosslinking properties once in aqueous solution containing di- or trivalent cations.[186] The network is formed by the electrostatic interactions between the oxygenated functions of the G residues and the ion, forming a so-called egg-box model described for the first time by Grant *et al.* (Figure 9).[187] The gel formation and its viscoelastic properties are linked to the affinity of the ion with the G residues as a result of electrostatic forces and steric hindrance. Therefore, the affinity varies with the molecular weight of alginate and its M/G ratio as well as the concentration and type of the ion in solution. For instance, the strength of the binding is greater with Ca^{2+} than with Mg^{2+}.[188] Thus being the major reason why Ca^{2+} predominates the description on the literature of the mechanism of gelification of alginate.

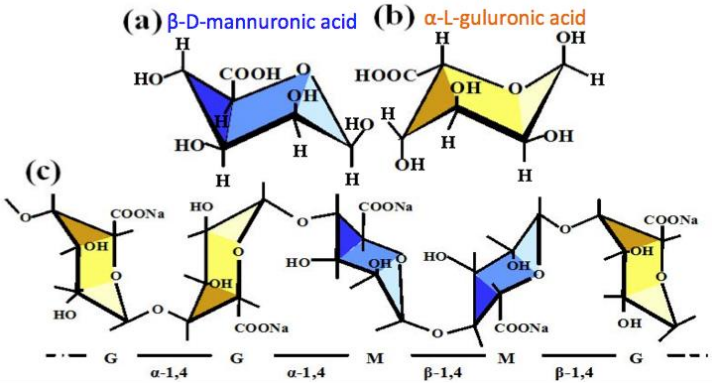

Figure 8: Composition of alginate: a) β -D-mannuronic acid (M), b) α-L-guluronic acid (G), c) Molecular structure of sodium alginate.[185]

The mechanism proposed on Figure 9 happens once the disorderly GG-blocks become orderly by the lateral association of two GG-blocks at their junction zones where a Ca^{2+} is trapped and the solution gelifies.[186] This phenomenon, so-called 'zipper mechanism', forms stable junctions for a minimum of 8 consecutive G units in the case of Ca^{2+}. The study of Sikorski *et al.* allowed the confirmation of the phenomenon via structural analysis using X-ray diffraction.[189]

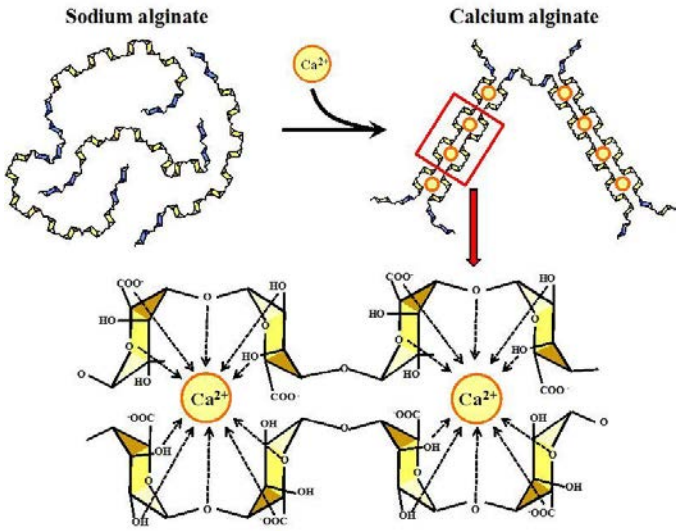

Figure 9: Egg-box model: Gelation of a homopolymeric block (GG) of α-L-guluronic acid with calcium ions.[185]

Additionally, Fang *et al.* studied the binding process and formation of the egg-box junctions as a function of the concentration of Ca^{2+} and the different rations of guluronate/mannuronate. They report three sequential steps with the increase of

cations in solution: (i) formation of a monocomplex by the interaction of Ca^{2+} with a single guluronate unit, (ii) pairing of the monocomplexes and formation of the egg-box and, (iii) lateral association of the egg-boxes (Figure 10). This ascertainment is valid when Ca^{2+} is introduced slowly and homogeneously to the system. Otherwise, if the solution of alginate is extremely concentrated, the gelation is quick, strong and irreversible, leading to heterogeneous gels.[190]

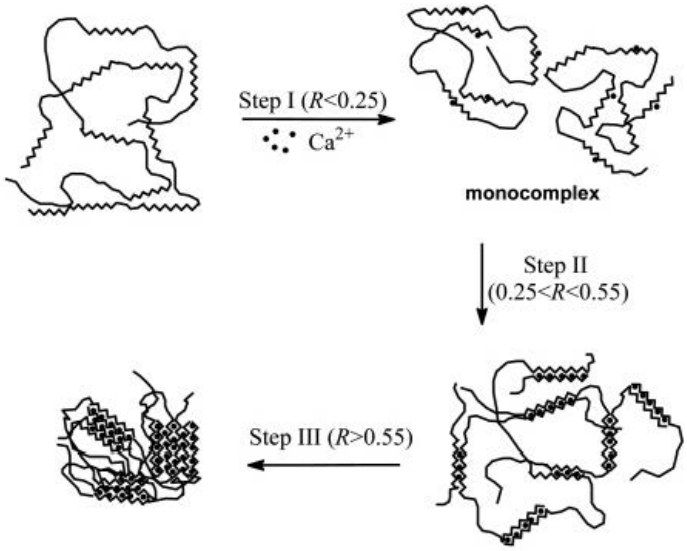

Figure 10: Schematic representation of the three steps binding of Ca^{2+} for a long-chain alginate. R represents the ratio of Ca^{2+} to G units.[190]

Alginate chains disintegration

The stability of alginates will strongly depend on temperature, pH, impurities in solution and the packing of the linked units. The glycosidic bonds are susceptible of rupturing in acid and basic conditions. As an example, if the pH gets below 5, the alginate chains get cut inducing a decline of the viscosity of the solution due to the hydrolysis of the bonds resulting in a shorter chain. In acidic and basic conditions, the decrease in the degree of polymerization follows a first order kinetic reaction:

$$\frac{1}{PDi} - \frac{1}{PDo} = kt$$

where PD_i and PD_0 are polymerization degree at a time t or t_0, respectively.

Haug *et* al. observed the intrinsic viscosity of an alginate solution over the pH range of 4 to 14. Indeed, the inverse of the viscosity is proportional to the number of broken bonds in the polysaccharide chain with a slower degradation between the pH of 5 to 10.[191] Erosion is favored therefore below pH 5 and above pH 10. Another possibility for gel disintegrating is with the addition of chelating agents that sequestrates the Ca^{2+} out of the box. Two examples of molecules capable of dismantling the gel are ethylenediaminetetraacetic acid (EDTA) and sodium citrate.

Silica

The second most abundant element on earth is silicon that occurs as silicates and silica in fresh water, seawater, soils and stones such as basalt or granite. Many living species, *e.g.* diatoms or eukaryotic algae, utilize silicon for major metabolic processes or even to build their external structures conferring them mechanical protection while allowing material exchange crucial in cellular growth.[192] The phenomenon of deposition of oxides on living matter is known as biomineralization and in nature certain bacteria, an example is *Bacillus subtilis*, can have a mineral crust (*e.g.* silica or iron-hydroxide depending on the water composition) formed around themselves protecting against predators or even dehydration. It is on the light of such natural phenomenon that silica was chosen as inorganic material to confer mechanical strength and chemical stability to encapsulated alginate beads containing LGG.

Amorphous silica in food

Plants, and more specifically cereals, contain high amounts of silicon in the form of SiO_2 whereas food from animal sources contains rather lower levels. The main readily available source of silicon to humans is orthosilicic acid $Si(OH)_4$ that is widely present in drinking water and beer, and rapidly eliminated by the kidneys when ingested.[193] Silicates and amorphous silica are approved as food additives by the European Food and Safety Authorities (EFSA) and are enlisted as E551 (amorphous SiO_2), E552 (calcium silicate), E553a(i) (magnesium silicate), E553a(ii) (magnesium trisilicate), E553b (talc) and E554 (sodium aluminosilicate). A consumption of amounts up to 1500 mg per day of silica is assumed to be harmless by the regulating organizations. Its main

role in dried food formulations relates to the insurance of long-term storages of the product as a water-activity regulator, a so-called anti-caking agent in food additive terms. Silicon is a structural component of connective tissues and it is key for the healthy maintenance of bones, skin, cartilages, and nails.

In academic research, there have been attempts on using silica as encapsulating agent for food purposes. For instance, hybrid core-shell approaches, such as alginate-silica, were explored by Callone *et al.* for the confinement of *Oenococcus oeni* or yeast cells with applications in the wine fermentation process.[194] Additionally, mesoporous silica loaded with folic acid was elaborated aiming the enrichment of yogurts[195] and fruit juices.[196]

Chemical silica structures

Silica or silicon dioxide is a solid mineral with the chemical formula of SiO_2. Generally speaking it can be natural or synthetic, crystalline or amorphous. The silicon atoms in quartz for instance are arranged in a highly ordered microscope structure given to it a crystalline property. Figure 11 illustrates the crystalline and amorphous bulk arrangements of some SiO_2 units. In both cases, the bulk of silica is composed of SiO_4 tetrahedral units that form siloxane rings of different Si–O sizes. The size of the silica rings present on the silica surface generally ranges from flexible 12-membered rings to strained 4-member Si–O rings, and the distribution of such siloxane rings generally depends on the calcination/activation temperature of silica.[197]

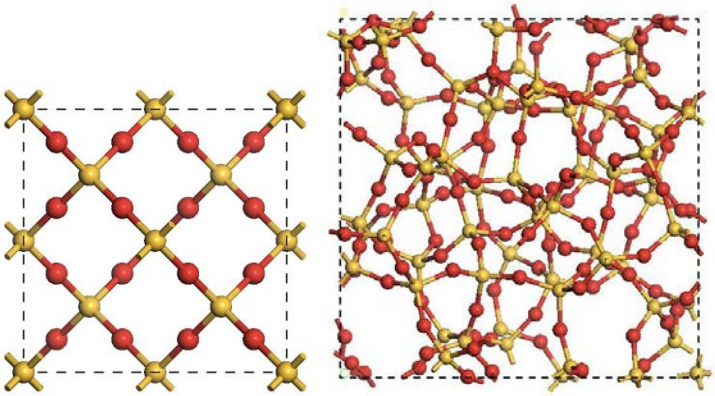

Figure 11: Unit cells of bulk structures of: (left) crystalline SiO_2 with 8 units and (right) amorphous SiO_2 with 64 units.[197]

At the surface, different kinds of silanols can be found and they can be classified as isolated (non-H-bonded), geminal, vicinal, and interacting (H-bonded) silanols (Figure 12). In the isolated silanol groups (Q^3), silicium forms three covalent bonds with oxygen atoms and a fourth bond with a surface hydroxyl. In the vicinal silanol (Q^3), two hydroxyl functions are bond to different silicium atoms and they are close enough to interact via hydrogen bonding among them. In the geminal silanol (Q^2), two hydroxyl functions are bond to the same silicium. They are actually two close to establish a hydrogen bond. Such group is usually in minority. In the siloxane bridge, four oxygen atoms are covalently linked to one silicium (Q^4).[198] In the NMR ^{29}Si spectroscopy, the different silicium atoms are designated as Q^n where n represents the number of other silicate structures linked to the one in question. The ^{29}Si chemical shifts (-δppm) for silica structures are in the order of: -90 ppm (Q^2), -100 ppm (Q^3) and -110 ppm (Q^4). [199]

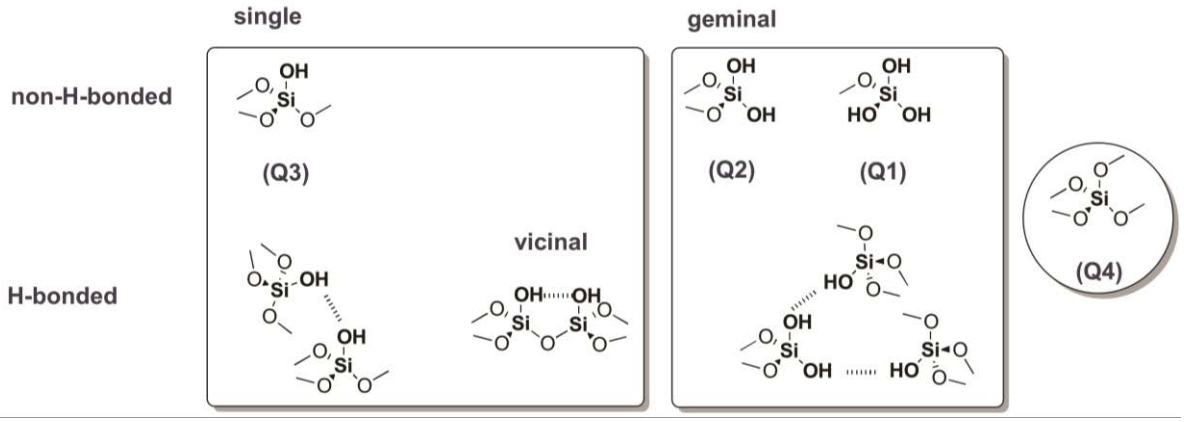

Figure 12: Types of silanol and silica bridges.

In the case of crystalline silica, only three kinds of silanols can be found at the surface: geminal, vicinal and isolated silanols while in the case of amorphous silica, all kinds of silanols are present. This property explains the highest reactivity of amorphous silica surfaces *vs* crystalline ones. Moreover, depending on the reaction conditions, such as temperature or condensation degree, the OH density at the surface of the material can be tuned between less than 1 to 7 OH/nm^2. There are several types of synthetic amorphous silica and their final properties are mostly related to the different fabrication processes the material goes through. Yet the sol-gel route is the most studied specially in the entrapment of living materials.[200]

Silica formation: the sol-gel process

The sol-gel route could be seen as a biomineralization process. In nature, orthosilicic acid $Si(OH)_4$ is present in water and this molecule gives rise to silica that is formed by the condensation of the silanol groups (Si−OH) of two molecules forming an oxo bridge (Si−O−Si) while releasing a water molecule.[201]

$$Si{-}OH + HO{-}Si \Rightarrow Si{-}O{-}Si + H_2O$$

The building blocks of a silica network are formed by four oxygen atoms at the corner of a regular tetrahedron holding a silicon ion in the center (SiO_4). The Si−O bond formed at this stage is the most stable of all Si−X bonds. Usually the overall reaction can be written as it follows:

$$Si(OH)_4 \Rightarrow SiO_2 + 2H_2O$$

However, the synthesis of synthetic silica are usually undertaken with alkoxide precursors $Si(OR)_4$, where R is an alkyl group instead of $Si(OH)_4$. Figure 13 illustrates the formation mechanism of silica and the release of ethanol during the hydrolysis/condensation reactions of tetraethyl orthosilica (TEOS).[202]

In the present study, the two silica alkoxide precursor used are tetramethyl orthosilica (TMOS) and (3-aminopropyl)trimethoxisilane (APTMS) (Figure 14). Silica is mainly formed in three steps: (i) The precursors are hydrolyzed in the presence of water to orthosilicic acid $Si(OH)_4$ while methanol is released, (ii) spontaneous condensation of silanol groups give rise to a colloidal dispersion of silica particles in the solution known as sol, (iii) and the hydrolysis and condensation progresses simultaneously. The growth of the silica particles and their linking into branched chains gives rise to a 3D network, a continuous solid skeleton within the solution, known as gel.

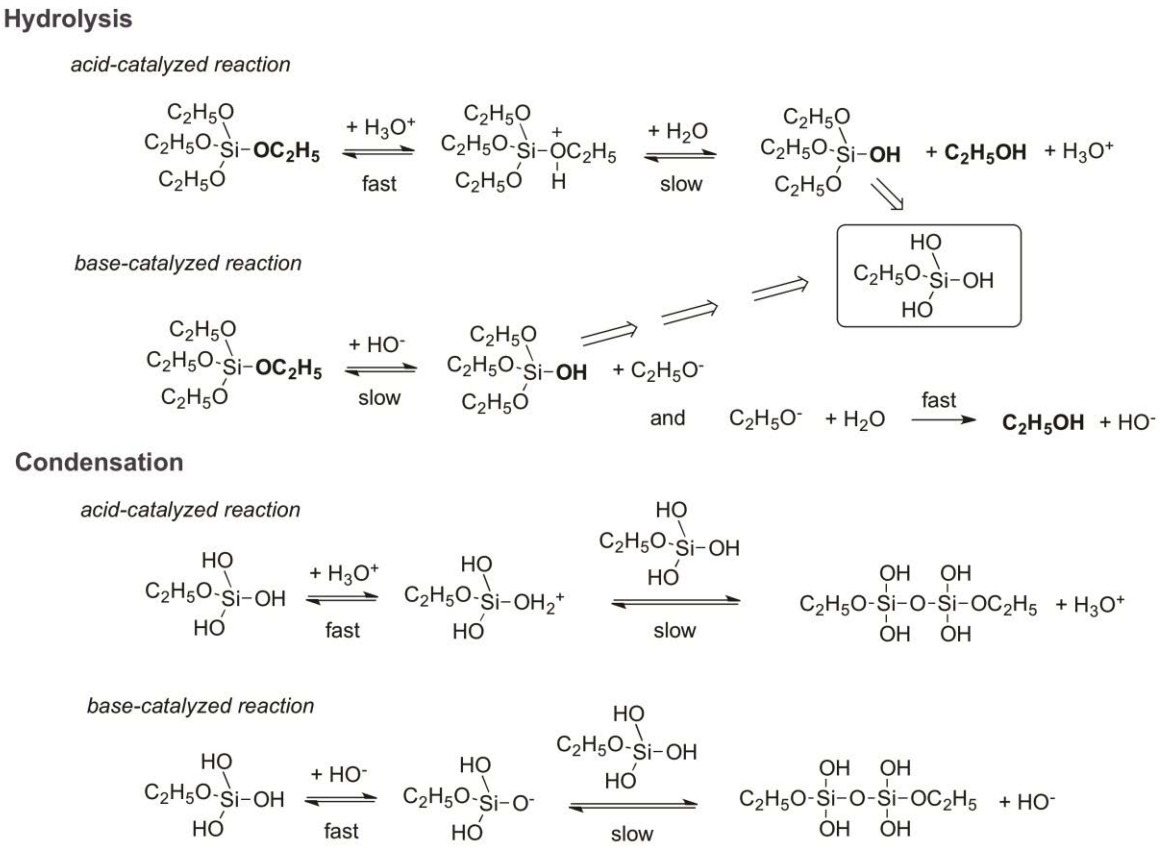

Figure 13: Hydrolysis and condensation of TEOS catalyzed by acid or base.

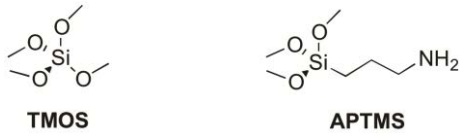

Figure 14: (left) Tetramethyl orthosilicate (TMOS), (right) (3-aminopropyl)trimethoxisilane (APTMS).

The sol-gel has been extensively studied in cell encapsulation due to its ability to form hybrid silica materials in aqueous solutions under room temperature. *Saccharomyces cerevisiae* was a pioneering study dealing with cell immobilization in silica gel.[203] It was then expanded to other types of cells ranging from bacterial to eukaryotic. Some examples are pancreatic islets for the obtention of bioartificial organs,[204] *Escherichia Coli* for the study of their enzymatic activity under confinement[205] and long-term cell viability,[206,207] anaerobic sulfate-reducing bacteria,[208] luminous recombinant *E. Coli* as a whole-cell biosensor,[209] *Serratia marcescens* for the production of prodigiosin, a red

pigment exhibiting therapeutic properties,[210] mammalian cells for transplantation,[211] the fungus *Stereum hirsutum* for remediation of polluted water[212] and *L. rhamnosus* for lactic acid production.[213]

Even though the biomineralization technique has potential for the encapsulation of a variety of cells, it cannot be seen as a generic method since the specificity of each cell must be taken into account beforehand. For instance, *S. cerevisiae* is an alcohol-tolerant yeast and therefore is able to withstand a certain level of alcohol release during the hydrolysis step of the process. On the other hand, alkoxi-based matrixes can be very often detrimental to the bacteria survival. Some approaches used in those cases are distilling the alcohol out under vacuum before adding the cells[214] or using different precursors of silica such as colloidal silica (Ludox) or sodium silicate.[215]

In the course of this study, sodium silicate, also known as waterglass, was employed as silica precursor as well. Sodium silicate is a generic name for silica compounds containing various proportions of silica and sodium oxides [$(SiO_2)_n$: Na_2O where $n<4$]. The molar ratio is defined as the ratio between the silica oxide concentration divided by the sodium oxide concentration, *i.e.* Rm = [SiO_2/Na_2O]. With the aid of ^{29}Si NMR, Harris *et al.* demonstrated that the increase of this ratio favors the polymerization of silicon species present in the solutions of sodium silicate. When Rm > 2, colloidal species were observed in the solution whereas if Rm < 2, there are predominately monomeric species.[216] The commercialized precursor used in our studies holds a Rm between 2 and 3 giving a composition of about 20 % of monomers and 80 % of oligomers in the departing sodium silicate solution.[217]

When calcium ions are added to a sodium silicate solution, the equilibrium between the monomeric and oligomeric species is destabilized and aggregates start forming. Nieto *et al.* demonstrated with the aid of ^{29}Si NMR that there is an augmentation of the connectivity degree when an initial sol reaches the gel state. Such increase implies on the formation of siloxane bonds during gelification.[217] The industry's interest on this precursor relates mainly to the fact that it is environmental-friendly and cost-effective when compared to its alkoxi counterparts.

Surfactant-induced porosity

Surfactants were briefly described in the emulsification section. Yet their use as structure-directing agents, *i.e.* for the obtainment of porous silica materials, was not described previously. First of all, in the case of the encapsulation of cells, the material porosity plays a fundamental role in the bidirectional diffusion of nutriments and metabolites in and out of the system, which allows the maintenance of cell viability under confinement.

In terms of classification, the dimension of the pores falls into three categories according to the international union of pure and applied chemistry (IUPAC): (i) microporosity with pores smaller than 2 nm, (ii) mesoporosity with pores between 2 to 50 nm, (iii) macroporosity with pores larger than 50 nm.

The synthesis of solids with controlled porosity is possible as a result of the spontaneous auto-organization of surfactant molecules in a solution. Above the critic micellar concentration (CMC) of a specific surfactant, the molecules form aggregates called micelles holding typically few nanometers in diameter. Any extra surfactant added to the system goes to the formation of these micelles. Depending on the reaction conditions (pH, temperature, addition of salts, among others) and the type of surfactant, the micelles will give rise to aggregates holding more complex geometries that will grow in size. These geometries behave as a mold once silica precursors are added to the solution and they follow their course of hydrolysis and condensation steps on the aggregates. To remove the surfactant once the silica condensation happened, a washing step or calcination is performed.

The M41S mesoporous solids exemplify the different final material structures we can obtain from surfactant arrangement. In this particular case, supramolecular aggregates of ionic surfactants (long-chain alkyltrimethylammonium halides) as structure directing agents are used in order to obtain mesoporous materials arranged hexagonally, cubically or even in lamellar layers (Figure 15).[218,219]

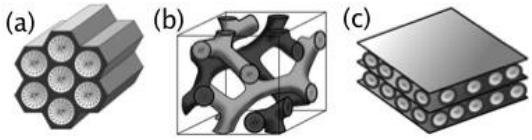

Figure 15: The three different structures of the M41S materials are: (a) MCM-41 hexagonal phase, (b) MCM-48 cubic phase, (c) MCM-50 lamellar phase. [220]

The structuring of these materials can be achieved either by the self-assembling or the templating mechanism (Figure 16).[220] The first one involves micelles of surfactants with silica (often TMOS or TEOS) that starts to condense and to finally lead to a mesostructured composite.[222] In the second approach, the silica is condensing onto a preformed liquid-crystal phase that also leads to a mesostructured composite.[221] The final mesoporous material is recovered after the removal of the surfactant by soxhlet extraction with ethanol and/or by calcination.

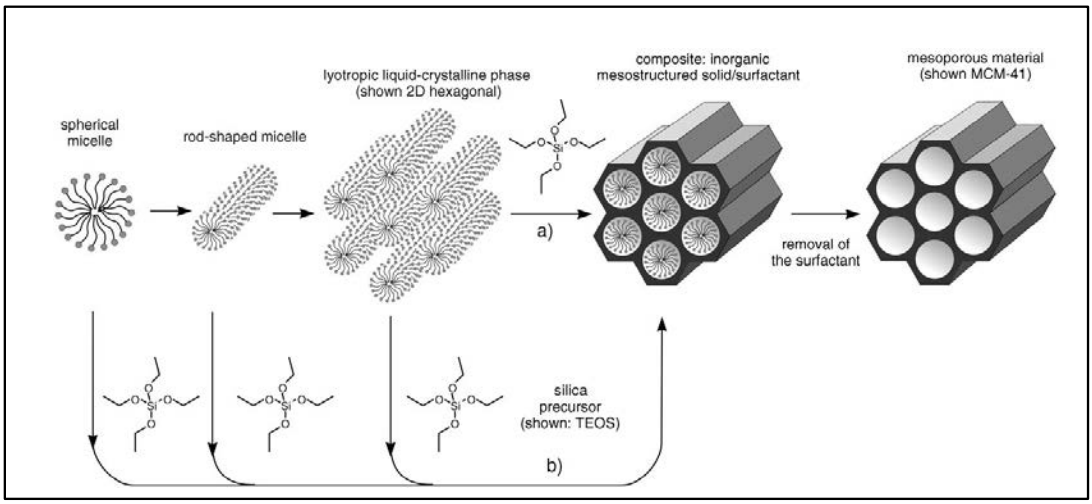

Figure 16: Formation mechanism of mesoporous silica materials through (a) self-assembling mechanism and (b) liquid-crystal templating mechanism

Chemical degradation of silica

The dissolution of amorphous silica is much faster compared to crystalline silica. Its rate increases with temperature and as a consequence of ionic corrosion, by adding salts. At near neutral pH, silica demineralization is enhanced by the presence of alkali and alkaline earth cations through weak outer-sphere type interactions between these ions and silica, and its rate is dependent upon the concentration and the type of ion.[223-225]

More recently, the work of Wallace *et al*. indicates that hydrolysis of Si-O is accelerated in presence of Ca^{2+} and Mg^{2+} via inner-sphere type interactions as well. The bridging oxygen on the silica surface is bounded to a cation and the redistribution of the electron density causes an electron depletion, which weakens the Si-O bond. The outcome is a Si-O bond more susceptible to the attack of a water molecule.[226]
The dissolution of silica is also pH-dependent. For instance, close to its isoelectric point (pI: 2 - 4) one can notice a minimum dissolution rate, probably related to its lower hydration degree.[227] Above this point, the dissolution rate increases with pH and becomes instantaneous at pH higher than 10.

The size and the porosity of the materials are also key parameters influencing silica dissolution. Mesoporous silica matrices for instance are thought to go through two steps: an erosion of the surface at first with sequential slower bulk degradation. The latter will be dictated by the physicochemical properties of the condensed material. In a time frame of 7 days, the maximum rate of dissolution was reached in the two first days with a sequential abrupt decrease ending at zero.[228] On another hand, the degradability of nanoparticles augments with an increase of their specific surface area due to increased contact of water molecules at the vicinities of the materials. The smaller these amorphous particles, the more soluble they are. Nonetheless, smaller sizes provoke cell toxicity.[229] Thus, a judicious balance between particle diameter and surface area is necessary in order to take advantage of such carriers for functional foods, where accumulation of nanoparticles within the human body must be ruled out.

2.6. Conclusions and perspectives

Currently the four main technologies used in microcapsules formation are extrusion, emulsion, spray- and freeze-drying along with ionic polysaccharides (alginate and chitosan), microbial exopolysaccharides (gellan and xanthan gums) and milk proteins as examples of most commonly used encapsulating agents. Assuming that single microbes are of about few µm in length, the final micro-cargos sizes fall in the µm range and can contain single or a consortium of strains.

In a formulation point of view alone, alginate-based materials are by far the most explored due to their biocompatibility, biodegradation, very good cytocompatibility and mucoadhesive properties. Another class of materials is the protein-based, which may combine polysaccharides and/or non-digestible fibers known as prebiotics.[105] In the interest of ameliorating the alginate or protein protection during simulated gastrointestinal passage, few recent strategies can be exemplified: (i) Alginate with polymerized whey protein coating. The protein's microstructure uniformity and enclosing structure formed after freeze-drying explain the better performance of such approach;[230] (ii) Chitosan-coated alginate containing prebiotics, herein inulin and galactooligosaccharide. Chitosan confers an extra wall protection to the encapsulated cells while the prebiotics can have a synergetic effect increasing the number of cells and/or their activity;[231] (iii) Sweet whey and skim milk encapsulating *L. acidophilus* La-5[232] and (iv) A prebiotic, fructooligosaccharides, and whey protein isolate in the case of *L. plantarum.*[233] The compartmentalization of probiotic bacteria in more sophisticated approaches such as using hydrophobized silica nanoparticles to stabilize a pickering emulsion has been reported by Wijk *et al.* and it opens up novel pathways in bacteria encapsulation.[234]

Overall a magnitude of studies lacking proper gastrointestinal experiments and/or animal testing, supposedly due to their high-cost and complexity, are reporting however relevant encapsulating systems every year. Interestingly, co-encapsulation of probiotic and drug is a promising approach envisioning a superior therapeutic effect for ulcerative colitis, Crohn's diseases and recurrent *Clostridium difficile*-associated diarrhea for example. Additionally, the encapsulation of a consortium of bacterial strains in single carriers is nowadays the latest trend in the microbiota research. The reason lies behind the fact the cells act synergistically, meaning one strain may boost the probiotic benefit of the others and vice-versa. On the top of it, leaders in probiotic research in the private sector, such as Chr. Hansen, are seeking in finding new potential probiotics strains within individual's microbiota. The challenges of this type of research escalate as a result of their fragility such as being strict anaerobes or even having unknown cultivability specifications.

Microbiome leaders in several fields gathered in the 18th Nature Café Conference on November 2016 in Tokyo. Some of the interesting discussions explored at this conference are of relevance for better understanding the impact of the microbiota research in our daily lives. Dr. Evan Elinav from the Weizmann Institute of Science (Israel) explored preliminary results on the 'Personalized Nutrition Project' launched five years ago. The initiative intends to pinpoint factors underlining blood glucose responses to food. So far responses are shown to be highly individual and therefore "one-size-fits-all diet is not appropriate. The gut microbiome is more unique than we thought" he says. Professor Kenya Honda and colleagues from the Keio University School of Medicine (Japan) begun to investigate how oral bacteria alter the intestinal immune system. He added: "every day an individual produces 1.5 liters of saliva, which contains a broad quantity of oral bacteria infiltrating the gut. The first signs of Crohn's disease can be seen by dysbiosis coming from oral-derived bacteria."

It is definitely exciting times for the microbiota/probiotics research domain since scientists are only starting to understand the diversity, dynamics nature and distribution in this microbiome. The research is on the radar of different domains as well. Recent discoveries indicate the impact of the intestine bacteria in respect to the brain functioning and its influence in disorders such as anxiety and depression. Yet the use of probiotics as a daily basis supplementation for health maintenance and nutrition is still debatable in the scientific community. Some of the reasons lie behind delicate definitions such as what is a healthy microbiome at first, or even, is it possible for an individual to become healthier? On-going and future research will unravel pathways for promising new health treatments and functional foods. Perhaps one day the microbiome will become a sort of a 'gutprint', a medical indicator of our state of health.

2.7. References

1 C. L. Maynard, C. O. Elson, R. D. Hatton and C. T. Weaver, *Nature*, 2012, **489**, 231–241.

2 T. Matsuki, K. Yahagi, H. Mori, H. Matsumoto, T. Hara, S. Tajima, E. Ogawa, H. Kodama, K. Yamamoto, T. Yamada, S. Matsumoto and K. Kurokawa, *Nat Comms*, 2016, **7**, 11939.

3 H. F. Helander and L. Fändriks, *Scandinavian Journal of Gastroenterology*, 2014, **49**, 681–689.

4 T. Yatsunenko, *et al. Nature*, 2012, **486**, 222–228.

5 P. J. Turnbaugh, R. E. Ley, M. Hamady, C. M. Fraser-Liggett, R. Knight and J. I. Gordon, *Nature*, 2007, **449**, 804–810.

6 R. M. Stilling, T. G. Dinan and J. F. Cryan, *Genes, Brain and Behavior*, 2013, **13**, 69–86.

7 W. H. Holzapfel, P. Haberer, J. Snel, U. Schillinger and J. H. J. Huis in't Veld, *International Journal of Food Microbiology*, 1998, **41**, 85–101.

8 J. A. Foster and K.-A. McVey Neufeld, *Trends in Neurosciences*, 2013, **36**, 305–312.

9 A. D. Kostic, R. J. Xavier and D. Gevers, *Gastroenterology*, 2014, **146**, 1489–1499.

10 C. Huttenhower *et. al.*, *Nature*, 2012, **486**, 207–214.

11 M. Govender, Y. E. Choonara, P. Kumar, L. C. du Toit, S. van Vuuren and V. Pillay, *AAPS PharmSciTech*, 2013, **15**, 29–43.

12 T. Iannitti and B. Palmieri, *Clinical Nutrition*, 2010, **29**, 701–725.

13 V. Tremaroli and F. Bäckhed, *Nature*, 2012, **489**, 242–249.

14 P. Hemarajata and J. Versalovic, *Therapeutic Advances in Gastroenterology*, 2013, **6**, 39–51.

15 A. Woting and M. Blaut, *Nutrients*, 2016, **8**, 202.

16 F. M. Collins and P. B. Carter, *Infection and Immunity*, 1978, **21**, 41–47.

17 L. J. Moberg and H. Sugiyama, *Infection and Immunity*, 1979, **25**, 653–657.

18 G. T. Macfarlane and S. Macfarlane, *Proceedings of the Nutrition Society*, 1993, **52**, 367–373.

19 J. L. Sonnenburg, J. Xu, D. D. Leip, C.-H. Chen, B. P. Westover, J. Weatherford, J. D. Buhler and J. I. Gordon, *Science*, 2005, **307**, 1955–1960.

20 E. A. Smith and G. T. Macfarlane, *Anaerobe*, 1997, **3**, 327–337.

21 A. Braune and M. Blaut, *Gut Microbes*, 2016, **7**, 216–234.

22 J. M. Ridlon, D. J. Kang, P. B. Hylemon and J. S. Bajaj, *Current Opinion in Gastroenterology*, 2014, **30**, 332–338.

23 R. E. Ley, P. J. Turnbaugh, S. Klein and J. I. Gordon, *Nature*, 2006, **444**, 1022–1023.

24 F. Bäckhed, H. Ding, T. Wang, L. V. Hooper, G. Y. Koh, A. Nagy, C. F. Semenkovich and J. I. Gordon, *PNAS*, 2004, **101**, 15718–15723.

25 P. J. Turnbaugh, R. E. Ley, M. A. Mahowald, V. Magrini, E. R. Mardis and J. I. Gordon, *Nature*, 2006, **444**, 1027–131.

26 E. V. Loftus Jr, *Gastroenterology*, 2004, **126**, 1504–1517.

27 M. E. V. Johansson, J. M. H. Larsson and G. C. Hansson, *Proceedings of the National Academy of Sciences*, 2011, **108**, 4659–4665.

28 S. Meconi, A. Vercellone, F. Levillain, B. Payré, T. Al Saati, F. Capilla, P. Desreumaux, A. Darfeuille-Michaud and F. Altare, *Cell Microbiol*, 2007, **9**, 1252–1261.

29 T. Ohkusa, I. Okayasu, T. Ogihara, K. Morita, M. Ogawa and N. Sato, *Gut*, 2000, **52**, 79–83.

30 M. S. Ahmad, S. Krishnan, B. S. Ramakrishna, M. Mathan, A. B. Pulimood and S. N. Murthy, *Gut*, 2000, **46**, 493–499.

31 N. Larsen, F. K. Vogensen, F. W. J. van den Berg, D. S. Nielsen, A. S. Andreasen, B. K. Pedersen, W. A. Al-Soud, S. J. Sørensen, L. H. Hansen and M. Jakobsen, *PLoS ONE*, 2010, **5**, e9085.

32 J. Qin, *et al. Nature*, 2012, **490**, 55–60.

33 P. D. Cani, S. Possemiers, T. Van de Wiele, Y. Guiot, A. Everard, O. Rottier, L. Geurts, D. Naslain, A. Neyrinck, D. M. Lambert, G. G. Muccioli and N. M. Delzenne, *Gut*, 2009, **58**, 1091–1103.

34 Z. Wang, G. Xiao, Y. Yao, S. Guo, K. Lu and Z. Sheng, *The Journal of Trauma: Injury, Infection, and Critical Care*, 2006, **61**, 650–657.

35 E. A. Griffiths, L. C. Duffy, F. L. Schanbacher, H. Qiao, D. Dryja, A. Leavens, J. Rossman, G. Rich, D. Dirienzo and P. L. Ogra, *Digestive Diseases and Sciences*, 2004, **49**, 579–589.

36 A. E. Wold, *Allergy*, 1998, **53**, 20–25.

37 Y. M. Sjögren, M. C. Jenmalm, M. F. Böttcher, B. Björkstén and E. Sverremark-Ekström, *Clinical & Experimental Allergy*, 2009, **39**, 518–526.

38 C. E. West, M. C. Jenmalm and S. L. Prescott, *Clinical & Experimental Allergy*, 2014, **45**, 43–53.

39 M. C. Jenmalm, *American Journal of Reproductive Immunology*, 2011, **66**, 75–80.

40 J. S. Bajaj, P. B. Hylemon, J. M. Ridlon, D. M. Heuman, K. Daita, M. B. White, P. Monteith, N. A. Noble, M. Sikaroodi and P. M. Gillevet, *AJP: Gastrointestinal and Liver Physiology*, 2012, **303**, G675–G685.

41 J. S. Bajaj, J. M. Ridlon, P. B. Hylemon, L. R. Thacker, D. M. Heuman, S. Smith, M. Sikaroodi and P. M. Gillevet, *AJP: Gastrointestinal and Liver Physiology*, 2011, **302**, G168–G175.

42 E. A. Mayer, K. Tillisch and A. Gupta, *J. Clin. Invest.*, 2015, **125**, 926–938.

43 M. Crumeyrolle-Arias, M. Jaglin, A. Bruneau, S. Vancassel, A. Cardona, V. Daugé, L. Naudon and S. Rabot, *Psychoneuroendocrinology*, 2014, **42**, 207–217.

44 T. Higuchi, H. Hayashi and K. Abe, *Journal of Bacteriology*, 1997, **179**, 3362–3364.

45 J. A. Bravo, P. Forsythe, M. V. Chew, E. Escaravage, H. M. Savignac, T. G. Dinan, J. Bienenstock and J. F. Cryan, *PNAS*, 2011, **108**, 16050–16055.

46 E. van Nood, A. Vrieze, M. Nieuwdorp, S. Fuentes, E. G. Zoetendal, W. M. de Vos, C. E. Visser, E. J. Kuijper, J. F. W. M. Bartelsman, J. G. P. Tijssen, P. Speelman, M. G. W. Dijkgraaf and J. J. Keller, *N Engl J Med*, 2013, **368**, 407–415.

47 R. Fuller, *Gut*, 1991, 439–442.

48 FAO/WHO, *Health and Nutritional Properties of Probiotics in Food including Powder Milk with Live Lactic Acid Bacteria*, 2001.

49 A. Schwan, S. Sjölin, U. Trottestam and B. Aronsson, *Scandinavian Journal of Infectious Diseases*, 1984, **16**, 211–215.

50 K. Kailasapathy, *Current Issues Intest. Microbiol.*, 2002, 39–48.

51 A. Passariello, P. Agricole and P. Malfertheiner, *Current Medical Research and Opinion*, 2014, **30**, 1055–1064.

52 R. Agheyisi, *The Probiotics Market: Ingredients, Supplements, Foods*, bccResearch, 2014.

53 S. Gupta and N. Abu-Ghannam, *Critical Reviews in Food Science and Nutrition*, 2012, **52**, 183–199.

54 P. Lavermicocca, F. Valerio, S. L. Lonigro, M. De Angelis, L. Morelli, M. L. Callegari, C. Rizzello and A. Visconti, *Applied and Environmental Microbiology*, 2005, **71**, 4233–4240.

55 D. Ying, S. Schwander, R. Weerakkody, L. Sanguansri, C. Gantenbein-Demarchi and M. A. Augustin, *Journal of Functional Foods*, 2013, **5**, 98–105.

56 C. S. Ranadheera, C. A. Evans, M. C. Adams and S. K. Baines, *Small Ruminant Research*, 2013, **112**, 174–180.

57 A. M. López de Lacey, E. Pérez-Santín, M. E. López-Caballero and P. Montero, *LWT - Food Science and Technology*, 2014, **55**, 314–322.

58 F. González-Sánchez, A. Azaola, G. F. Gutiérrez-López and H. Hernández-Sánchez, *International Journal of Dairy Technology*, 2010, **63**, 431–436.

59 R. Noorbakhsh, P. Yaghmaee and T. Durance, *Journal of Functional Foods*, 2013, **5**, 1049–1056.

60 V. M. Sheehan, P. Ross and G. F. Fitzgerald, *Innovative Food Science & Emerging Technologies*, 2007, **8**, 279–284.

61 S. Nualkaekul, M. T. Cook, V. V. Khutoryanskiy and D. Charalampopoulos, *Food Research International*, 2013, 304–311.

62 A. P. Mestry, A. S. Mujumdar and B. N. Thorat, *Drying Technology*, 2011, **29**, 1121–1131.

63 I. Alegre, I. Viñas, J. Usall, M. Anguera and M. Abadias, *Food Microbiology*, 2011, **28**, 59–66.

64 C. Rößle, M. A. E. Auty, N. Brunton, R. T. Gormley and F. Butler, *Innovative Food Science & Emerging Technologies*, 2010, **11**, 203–209.

65 S. Possemiers, M. Marzorati, W. Verstraete and T. Van de Wiele, *International Journal of Food Microbiology*, 2010, **141**, 97–103.

66 A. N. Roopashri and M. C. Varadaraj, *Eur Food Res Technol*, 2014, **239**, 99–115.

67 A. A. Hugo, P. F. Pérez, M. C. Añón and F. Speroni, *Food hydrocolloids*, 2014, **37**, 34–39.

68 M. K. Tripathi and S. K. Giri, *Journal of Functional Foods*, 2014, **9**, 225–241.

69 P. Tripathi, A. Beaussart, G. Andre, T. Rolain, S. Lebeer, J. Vanderleyden, P. Hols and Y. F. Dufrêne, *Micron*, 2012, **43**, 1323–1330.

70 M. Sharma and M. Devi, *Critical Reviews in Food Science and Nutrition*, 2014, **54**, 537–552.

71 P. D. Cani and M. Van Hul, *Current Opinion in Biotechnology*, 2015, **32**, 21–27.

72 J. A. Poupard, I. Husain and R. F. Norris, *Bacteriological Reviews*, 1973, **37**, 136–165.

73 N. Ishibashi, T. Yaeshima and H. Hayasawa, *Mal J Nutr*, 1997, **3**, 149–159.

74 T. Yaeshima, S. Takahashi, N. Ishibashi and S. Shimamura, *International Journal of Food Microbiology*, 1996, **30**, 303–313.

75 C. M. Slover and L. Danziger, *Clinical Microbiology Newsletter*, 2008, **30**, 23–27.

76 M. D. Collins, B. A. Phillips and P. Zanoni, *International Journal of Systematic Bacteriology*, 1989, **39**, 105–108.

77 R. Li, Y. Zhang, D. B. Polk, P. M. Tomasula, F. Yan and L. Liu, *Journal of Controlled Release*, 2016, **230**, 79–87.

78 M. Kankainen, *et al. PNAS*, 2009, 1–6.

79 M. E. Segers and S. Lebeer, *Microbial Cell Factories*, 2014, **13**, 1–16.

80 E. Larsson, V. Tremaroli, Y. S. Lee, O. Koren, I. Nookaew, A. Fricker, J. Nielsen, R. E. Ley and F. Bäckhed, *Gut*, 2012, **61**, 1124–1131.

81 R. Patel and H. L. DuPont, *Clinical Infectious Diseases*, 2015, **60**, S108–S121.

82 T. Asahara, K. Shimizu, K. Nomoto, T. Hamabata, A. Ozawa and Y. Takeda, *Infection and Immunity*, 2004, **72**, 2240–2247.

83 T. R. Klaenhammer, *Biochimie*, 1988, **70**, 337–349.

84 H. Schmitz, C. Barmeyer, M. Fromm, N. Runkel, H.-D. Foss, C. J. Bentzel, E.-O. Riecken and J.-D. Schulzke, *Gastroenterology*, 1999, **116**, 301–309.

85 J. Wyatt, H. Vogelsang, W. Hübl, T. Waldhöer and H. Lochs, *The Lancet*, 2003, **341**, 1437–1439.

86 T. Watts, I. Berti, A. Sapone, T. Gerarduzzi, T. Not, R. Zielke and A. Fasano, *PNAS*, 2005, **102**, 2916–2921.

87 A. L. Servin and M.-H. Coconnier, *Best Practice & Research Clinical Gastroenterology*, 2003, **17**, 741–754.

88 L. Ruiz, P. Ruas-Madiedo, M. Gueimonde, C. G. de los Reyes-Gavilán, A. Margolles and B. Sánchez, *Genes Nutr*, 2011, **6**, 307–318.

89 J. Koponen, K. Laakso, K. Koskenniemi, M. Kankainen, K. Savijoki, T. A. Nyman, W. M. de Vos, S. Tynkkynen, N. Kalkkinen and P. Varmanen, *Journal of Proteomics*, 2012, **75**, 1357–1374.

90 B. R. Goldin, S. L. Gorbach, M. Saxelin, S. Barakat, L. Gualtieri and S. Salminen, *Digestive Diseases and Sciences*, 1992, **37**, 121–128.

91 C. N. Jacobsen, V. R. Nielsen, A. E. Hayford, P. L. Moller, K. F. Michaelsen, A. Paerregaard, B. Sandström, M. Tvede and M. Jakobsen, *Applied and Environmental Microbiology*, 1999, **65**, 4949–4956.

92 B. M. Corcoran, C. Stanton, G. F. Fitzgerald and R. P. Ross, *Applied and Environmental Microbiology*, 2005, **71**, 3060–3067.

93 N. P. Shah, *Journal Dairy Science*, 1999, **83**, 894–907.

94 A. Gaonkar, N. Vasisht, A. Khare and R. Sobel, Eds., *Microencapsulation in the Food Industry: A pratical Implementation Guide*, Elsevier, 2014.

95 W. Sun and M. W. Griffiths, *Internationa Journal of Food Microbiology*, 2000, **61**, 17–25.

96 K. Sultana, G. Godward, N. Reynolds, R. Arumugaswamy and P. Peiris, *International Journal of Food Microbiology*, 2000, **62**, 47–55.

97 L. T. Hansen, P. M. Allan-Wojtas, Y. L. Jin and A. T. Paulson, *Food Microbiology*, 2002, **19**, 35–45.

98 C. S. Favaro-Trindade and C. R. F. Grosso, *Journal of Microencapsulation*, 2001, **19**, 485–494.

99 S. Behboudi-Jobbehdar, C. Soukoulis, L. Yonekura and I. Fisk, *Drying Technology*, 2013, **31**, 1274–1283.

100 B. M. Corcoran, R. P. Ross, G. F. Fitzgerald and C. Stanton, *J Appl Microbiol*, 2004, **96**, 1024–1039.

101 L. Yonekura, H. Sun, C. Soukoulis and I. Fisk, *Journal of Functional Foods*, 2014, **6**, 205–214.

102 F. P. De Castro-Cislaghi, C. D. R. E. Silva, C. B. Fritzen-Freire, J. G. Lorenz and E. S. Sant'Anna, *Journal of Food Engineering*, 2012, **113**, 186–193.

103 B. E. Chávez and A. M. Ledeboer, *Drying Technology*, 2007, **25**, 1193–1201.

104 M. Chavarri, I. Maranon and M. Carmen, *Encapsulation Technology to Protect Probiotic Bacteria*, InTech, 2012.

105 Q.-Y. Dong, M.-Y. Chen, Y. Xin, X.-Y. Qin, Z. Cheng, L.-E. Shi and Z.-X. Tang, *International Journal of Food Science and Technology*, 2013, **48**, 1339–1351.

106 E. Ananta, M. Volkert and D. Knorr, *International Dairy Journal*, 2005, **15**, 399–409.

107 P. de Vos, M. M. Faas, M. Spasojevic and J. Sikkema, *International Dairy Journal*, 2010, **20**, 292–302.

108 D. L. Pedroso, M. Dogenski, M. Thomazini, R. J. B. Heinemann and C. S. Favaro-Trindade, *Brazilian Journal of Microbiology*, 2013, **44**, 777–783.

109 S. Gouin, *Trends in Food Science & Technology*, 2004, **15**, 330–347.

110 P. K. Okuro, F. E. de M. Junior and C. S. Favaro-Trindade, *Food Technol. Biotechnol.*, 2013, **51**, 171–182.

111 P. K. Okuro, M. Thomazini, J. C. C. Balieiro, R. D. C. O. Liberal and C. S. Fávaro-Trindade, *FRIN*, 2013, **53**, 96–103.

112 J. K. Seo, S.-W. Kim, M. H. Kim, S. D. Upadhaya, D. K. Kam and J. K. Ha, *Asian-Aust. J. Anim.*

Sci., 2010, **23**, 1657–1667.

113 EFSA, *EFSA Journal*, 2012, **10**, 2886.

114 W. M. Rutherford, J. E. Allen, H. W. Schlameus, D. J. Mangold, W. W. Harlowe and J. R. Lebeda, *Patent*, 1994, **US5292657 A**.

115 C. P. Champagne and P. Fustier, *Current Opinion in Biotechnology*, 2007, **18**, 184–190.

116 D. Schell and C. Beermann, *Food Research International*, 2014, **62**, 308–314.

117 D. Semyonov, O. Ramon, A. Kovacs, L. Friedlander and E. Shimoni, *Drying Technology*, 2012, **30**, 1918–1930.

118 C. P. Champagne, Y. Raymond and T. A. Tompkins, *Food Microbiology*, 2010, **27**, 1104–1111.

119 H. Durand and J. Panes, *Patent*, 2003, **US 20030109025 A1**.

120 A. S. Shoji, A. C. Oliveira, J. C. C. Balieiro, O. Freitas, M. Thomazini, R. J. B. Heinemann, P. K. Okuro and C. S. Favaro-Trindade, *Food and Bioproducts Processing*, 2013, **91**, 83–88.

121 C. L. Gerez, G. Font de Valdez, M. L. Gigante and C. R. F. Grosso, *Letters in Applied Microbiology*, 2012, **54**, 552–556.

122 W. Krasaekoopt, B. Bhandari and H. Deeth, *International Dairy Journal*, 2003, 3–13.

123 S. Morelli, R. G. Holdich and M. M. Dragosavac, *Chemical Engineering Journal*, 2016, **288**, 451–460.

124 B. Kronberg, K. Holmberg and B. Lindman, *Surface chemistry of surfactants and polymers*, Wiley, 2014.

125 W. D. Bancroft, *Jounal Physical Chemsitry*, 1913, **17**, 501–519.

126 R. Wilson, B. J. van Schie and D. Howes, *Food and Chemical Toxicology*, 1998, **36**, 711–718.

127 A. L. Márquez, A. Medrano, L. A. Panizzolo and J. R. Wagner, *Journal of Colloid and Interface Science*, 2010, **341**, 101–108.

128 EFSA Panel on Food Additives and Nutrient Sources added to Food (ANS), *EFSA Journal*, 2015, **13**, 4152.

129 D. Dianawati, V. Mishra and N. P. Shah, *Food Research International*, 2013, **51**, 503–509.

130 K. M. Amine, C. P. Champagne, Y. Raymond, D. St-Gelais, M. Britten, P. Fustier, S. Salmieri and M. Lacroix, *Food Control*, 2014, **37**, 193–199.

131 F. Mantzouridou, A. Spanou and V. Kiosseoglou, *Food Research International*, 2012, **46**, 260–269.

132 N. T. L. Beck, G. Franch and D. L. I. Geneau, *Patent*, 2002, **CA 2423928 A1**.

133 S. Borges, J. Barbosa, R. Camilo, A. Carvalheira, J. Silva, S. Sousa, A. M. Gomes, M. M. Pintado, P. Costa, M. H. Amaral, P. Teixeira and A. C. Freitas, *International Journal of Food Science and Technology*, 2011, **47**, 416–421.

134 J. P. Paques, E. van der Linden, C. J. M. van Rijn and L. M. C. Sagis, *Food hydrocolloids*, 2013,

31, 428–434.

135 N. H. Khan, D. R. Korber, N. H. Low and M. T. Nickerson, *Food Research International*, 2013, **54**, 730–737.

136 N. Laelorspoen, S. Wongsasulak, T. Yoovidhya and S. Devahastin, *Journal of Functional Foods*, 2014, **7**, 342–349.

137 A. De Prisco, D. Maresca, D. Ongeng and G. Mauriello, *LWT - Food Science and Technology*, 2015, **61**, 452–462.

138 S. Graff, S. Hussain, J.-C. Chaumeil and C. Charrueau, *Pharm Res*, 2008, **25**, 1290–1296.

139 C. C. Coghetto, G. B. Brinques, N. M. Siqueira, J. Pletsch, R. M. D. Soares and M. A. Z. Ayub, *Journal of Functional Foods*, 2016, **24**, 316–326.

140 P. Pitigraisorn, K. Srichaisupakit, N. Wongpadungkiat and S. Wongsasulak, *Journal of Food Engineering*, 2017, **192**, 11–18.

141 G. Alisch, E. Brauneis, B. Pirstadt, N. Iffland and E. Brandau, *Patent*, 1995, **WO 93/02785**.

142 M. Asada, Y. Hatano, R. Kamaguchi and H. Sunohara, *Patent*, 2005, **US 20050283849 A1**.

143 L. Kearney, M. Upton and A. Mc Loughlin, *Applied and Environmental Microbiology*, 1990, **56**, 3112–3116.

144 J. R. Broadbent and C. Lin, *Cryobiology*, 1999, **39**, 88–102.

145 C. P. Champagne, N. Gardner, E. Brochu and Y. Beaulieu, *Canadian Institute of Food Science and Technology*, 1991, **24**, 118–128.

146 P. B. Conrad, D. P. Miller, P. R. Cielenski and J. J. de Pablo, *Cryobiology*, 2000, **41**, 17–24.

147 H. Tanaka, M. Matsumura and I. A. Veliky, *Biotechnology and Bioengineering*, 1984, **26**, 53–58.

148 J. L. Bergere and A. Lacourt, *Le lait*, 1968, **48**, 131.

149 G. Peter, *Acta Alimentaria*, 2001, **30**, 89–97.

150 T. F. Bozoglu, M. Özilgen and U. Bakir, *Enzyme Microb. Technol.*, 1987, **9**, 531–537.

151 K. B. P. K. Reddy, S. P. Awasthi, A. N. Madhu and S. G. Prapulla, *Food Biotechnology*, 2009, **23**, 243–265.

152 H. T. Nguyen, H. Razafindralambo, C. Blecker, C. N'Yapo, P. Thonart and F. Delvigne, *Biochemical Engineering Journal*, 2014, **88**, 85–94.

153 L. M. Crowe, J. H. Crowe, A. Rudolph, C. Womersley and L. Appel, *Archives of Biochemistry and Biophysics*, 1985, **242**, 240–247.

154 J. H. Crowe, L. M. Crowe, J. F. Carpenter, A. S. Rudolph, C. A. Wistrom, B. J. Spargo and T. J. Anchordoguy, *Biochimica et Biophysica Acta*, 1988, **947**, 367–384.

155 K. Önneby, L. Pizzul, J. Bjerketorp, D. Mahlin, S. Håkansson and P. Wessman, *World J Microbiol Biotechnol*, 2013, **29**, 1399–1408.

156 A. Siaterlis, G. Deepika and D. Charalampopoulos, *Letters in Applied Microbiology*, 2009,

48, 295–301.

157 E. Ananta, *et al. Microb Ecol Health Dis*, 2004, **16**, 113–124.

158 S. Miao, S. Mills, C. Stanton, G. F. Fitzgerald, Y. Roos and R. P. Ross, *Dairy Sci. Technol.*, 2008, **88**, 19–30.

159 L. Gasperini, J. F. Mano and R. L. Reis, *Journal of The Royal Society Interface*, 2014, **11**, 20140817–20140817.

160 W. Krasaekoopt, B. Bhandari and H. Deeth, *International Dairy Journal*, 2004, **14**, 737–743.

161 A. Heyraud and C. Leonard, *Food hydrocolloids*, 1990, **4**, 59–68.

162 F. B. Haffner, R. Diab and A. Pasc, *AIMS Materials Science*, 2016, **3**, 114–136.

163 S. S. Pinto, C. B. Fritzen-Freire, I. B. Muñoz, P. L. M. Barreto, E. S. Prudêncio and R. D. M. C. Amboni, *Journal of Food Engineering*, 2012, **111**, 563–569.

164 D. Ying, J. Sun, L. Sanguansri, R. Weerakkody and M. A. Augustin, *Journal of Food Engineering*, 2012, **109**, 597–602.

165 W. S. Cheow, T. Y. Kiew and K. Hadinoto, *Carbohydrate Polymers*, 2014, **103**, 587–595.

166 B. N. Estevinho, F. Rocha, L. Santos and A. Alves, *Trends in Food Science & Technology*, 2013, **31**, 138–155.

167 S. J. Lahtinen, A. C. Ouwehand, S. J. Salminen, P. Forssell and P. Myllärinen, *Letters in Applied Microbiology*, 2007, **44**, 500–505.

168 P. Muthukumarasamy, P. Allan-Wojtas and R. A. Holley, *Journal of Food Science*, 2006, **71**, M21–M24.

169 A. M. López de Lacey, M. E. López-Caballero, J. Gómez-Estaca, M. C. Gómez-Guillén and P. Montero, *Innovative Food Science & Emerging Technologies*, 2012, **16**, 277–282.

170 S. Sathyabama, M. Ranjith kumar, P. Bruntha devi, R. Vijayabharathi and V. Brindha priyadharisini, *LWT - Food Science and Technology*, 2014, **57**, 419–425.

171 S. B. Doherty, V. L. Gee, R. P. Ross, C. Stanton, G. F. Fitzgerald and A. Brodkorb, *Food hydrocolloids*, 2011, **25**, 1604–1617.

172 A. López-Rubio, E. Sanchez, S. Wilkanowicz, Y. Sanz and J. M. Lagaron, *Food hydrocolloids*, 2012, **28**, 159–167.

173 L. G. Gomez-Mascaraque, R. C. Morfin, R. Pérez-Masiá, G. Sanchez and A. López-Rubio, *LWT - Food Science and Technology*, 2016, **69**, 438–446.

174 M. L. Jiménez-Pranteda, D. Poncelet, M. E. Náder-Macías, A. Arcos, M. Aguilera, M. Monteoliva-Sánchez and A. Ramos-Cormenzana, *Journal of Bioscience and Bioengineering*, 2012, **113**, 179–184.

175 M. I. Brachkova, M. A. Duarte and J. F. Pinto, *European Journal of Pharmaceutical Sciences*, 2010, **41**, 589–596.

176 F. B. Haffner, M. Girardon, S. Fontanay, N. Canilho, R. E. Duval, M. Mierzwa, M. Etienne, R. Diab and A. Pasc, *J. Mater. Chem. B*, 2016, **4**, 7929–7935.

177 F. Lim and A. Sun, *Science*, 1980, **210**, 908–910.

178 M. de Jesus Raposo, A. de Morais and R. de Morais, *Marine Drugs*, 2016, **14**, 27.

179 A. Boyd and A. M. Chakrabarty, *Journal of Industrial Microbiology*, 1995, **15**, 162–168.

180 M. Glicksman, *Advances in Food Research*, 1963, **11**, 109–200.

181 T. Salomonsen, H. M. Jensen, F. H. Larsen, S. Steuernagel and S. B. Engelsen, *Food hydrocolloids*, 2009, **23**, 1579–1586.

182 D. Poncelet, V. Babak, C. Dulieu and A. Picot, *Colloids and Surfaces A: Physicochemical and Engineering Aspects*, 1999, **155**, 171–176.

183 S. K. Bajpai and S. Sharma, *Reactive and Functional Polymers*, 2004, 129–140.

184 A. Sosnik, *ISRN Pharmaceutics*, 2014, 1–17.

185 K. Kashima and M. Imai, *Advancing Desalination*, Intech, San Diego, 2012.

186 T. E. Jørgensen, M. Sletmoen, K. I. Draget and B. T. Stokke, *Biomacromolecules*, 2007, **8**, 2388–2397.

187 G. T. Grant, E. R. Morris, D. A. Rees, P. J. C. Smith and D. Thom, *FEBS Letters*, 1973, 1–4.

188 T. Matsumoto and K. Mashiko, *Biopolymers*, 1990, **29**, 1707–1713.

189 P. Sikorski, F. Mo, G. Skjak-Braek and B. T. Stokke, *Biomacromolecules*, 2007, **8**, 2098–2103.

190 Y. Fang, S. Al-Assaf, G. O. Phillips, K. Nishinari, T. Funami, P. A. Williams and L. Li, *J. Phys. Chem. B*, 2007, **111**, 2456–2462.

191 A. Haug, B. Larsen and O. Smidsröd, *Acta Chem. Scand.*, 1963, **17**, 1466–1468.

192 C. F. Meunier, P. Dandoy and B.-L. Su, *Journal of Colloid and Interface Science*, 2010, **342**, 211–224.

193 F. Aguilar, *et al. EFSA Journal*, 2009, 1–24.

194 E. Callone, R. Campostrini, G. Carturan, A. Cavazza and R. Guzzon, *J. Mater. Chem.*, 2008, **18**, 4839–4848.

195 É. Pérez-Esteve, M. Ruiz-Rico, A. Fuentes, M. D. Marcos, F. Sancenón, R. Martínez-Máñez and J. M. Barat, *LWT - Food Science and Technology*, 2016, **72**, 351–360.

196 M. Ruiz-Rico, É. Pérez-Esteve, M. J. Lerma-García, M. D. Marcos, R. Martínez-Máñez and J. M. Barat, *Food Chemistry*, 2017, **218**, 471–478.

197 A. Comas-Vives, *Physical Chemistry Chemical Physics*, 2016, **18**, 7475–7482.

198 B. A. Morrow and A. J. McFarlan, *Journal of Non-Crystalline Solids*, 1990, **120**, 61–71.

199 R. H. Glaser, G. L. Wilkes and C. E. Bronnimann, *Journal of Non-Crystalline Solids*, 1989, **113**, 73–87.

200 D. Avnir, S. Braun, O. Lev and M. Ottolenghi, *Chem. Mater.*, 1994, 1605–1614.

201 J. Livage, T. Coradin and C. Roux, *J. Phys.: Condens. Matter*, 2001, **13**, 673–691.

202 R. Diab, N. Canilho, I.-A. Pavel, F. B. Haffner, M. Girardon and A. Pasc, *Advances in Colloid and Interface Science*, 2017, 1–39.

203 G. Carturan, R. Campostrini and S. Dirè, *Journal of Molecular Catalysis*, 1989, **57**, L13–L16.

204 E. J. A. Pope, K. Braun and C. M. Peterson, *J Sol-Gel Sci Technol*, 1997, **8**, 635–639.

205 S. Fennouh, S. Guyon, C. Jourdat, C. Roux and J. Livage, *C. R. Acad. Sci. Paris*, 1999, **2**, 625–630.

206 N. Nassif, O. Bouvet, M. N. Rager, C. Roux, T. Coradin and J. Livage, *Nat Mater*, 2002, **1**, 42–44.

207 N. Nassif, C. Roux, T. Coradin, M. N. Rager, O. M. M. Bouvet and J. Livage, *J. Mater. Chem.*, 2003, **13**, 203–208.

208 K. S. Finnie, J. R. Bartlett and J. L. Woolfrey, *J. Mater. Chem.*, 2000, **10**, 1099–1101.

209 J. R. Premkumar, O. Lev, R. Rosen and S. Belkin, *Adv. Mater.*, 2001, **13**, 1773–1775.

210 N. Nassif, C. C. Roux, T. Coradin, O. M. M. Bouvet and J. Livage, *J. Mater. Chem.*, 2004, **14**, 2264.

211 A. Nieto, S. Areva, T. Wilson and M. Vallet-Regi, *Acta Biomaterialia*, 2009, **5**, 3478–3487.

212 M. Perullini, M. Jobbágy, N. Mouso, F. Forchiassin and S. A. Bilmes, *J. Mater. Chem.*, 2010, **20**, 6479.

213 Z. Zhao, X. Xie, Z. Wang, Y. Tao, X. Niu, X. Huang, L. Liu and Z. Li, *Journal of Bioscience and Bioengineering*, 2016, 1–7.

214 M. L. Ferrer, L. Yuste, F. Rojo and F. del Monte, *Chem. Mater.*, 2003, **15**, 3614–3618.

215 A. Coiffier, T. Coradin, C. Roux, O. M. M. Bouvet and J. Livage, *J. Mater. Chem.*, 2001, **11**, 2039–2044.

216 R. K. Harris, E. K. F. Bahlmann, K. Metcalfe and E. G. Smith, *Magnetic resonance in chemistry*, 1993, **31**, 743–747.

217 F. Gaboriaud, A. Nonat, D. Chaumont and A. Craievich, *Journal of Colloid and Interface Science*, 2002, **253**, 140–149.

218 C. T. Kresge, M. E. Leonowicz, W. J. Roth, J. C. Vartuli and B. J. S, *Letters to Nature*, 1992, **359**, 710–712.

219 J. S. Beck, J. C. Vartuli, W. J. Roth, M. E. Leonowicz, C. T. Kresge, K. D. Schmitt, C. T.-W. Chu, D. H. Olson, E. W. Sheppard, S. B. McCullen, J. B. Higgins and J. L. Schlenker, *J Am. Chem. Soc.*, 1992, **114**, 10834–1–843.

220 F. Hoffmann, M. Cornelius, J. Morell and M. Fröba, *Angew. Chem. Int. Ed.*, 2006, **45**, 3216–3251.

221 G. S. Attard, J. C. Glyde and C. G. Göltner, *Nature*, 1995, **378**, 366–368.

222 A. Monnier, F. Schuth, Q. Huo, D. Kumar, D. Margolese, R. S. Maxwell, S. G. D, M.

Krishnamurty, P. Petroff, F. A, M. Janicke and B. F. Chmelka, *Science*, 1993, **261**, 1299–1303.

223 W. Smit, C. L. M. Holten, H. N. Stein, J. J. M. De Goeij and H. M. J. Theelen, *Journal of Colloid and Interface Science*, 1977, **67**, 397–407.

224 P. C. Bennett, *Geochimica et Cosmochimica Acta*, 1991, **55**, 1781–1797.

225 J. P. Icenhower and P. M. Dove, *Geochimica et Cosmochimica Acta*, 2000, **64**, 4193–4203.

226 A. F. Wallace, G. V. Gibbs and P. M. Dove, *J. Phys. Chem. A*, 2010, **114**, 2534–2542.

227 S. Plettinck, L. Chou and R. Wollast, *Mineralogical Magazine*, 1994, **58A**, 728–729.

228 Q. He, J. Shi, M. Zhu, Y. Chen and F. Chen, *Microporous and Mesoporous Materials*, 2010, **131**, 314–320.

229 H. Yamada, C. Urata, Y. Aoyama, S. Osada, Y. Yamauchi and K. Kuroda, *Chem. Mater.*, 2012, **24**, 1462–1471.

230 Y. Jiang, Z. Zheng, T. Zhang, G. Hendricks and M. Guo, *International Journal of Food Sciences and Nutrition*, 2016, **67**, 670–677.

231 W. Krasaekoopt and S. Watcharapoka, *LWT - Food Science and Technology*, 2014, **57**, 761–766.

232 G. M. Maciel, K. S. Chaves, C. R. F. Grosso and M. L. Gigante, *Journal of Dairy Science*, 2014, **97**, 1991–1998.

233 R. Rajam and C. Anandharamakrishnan, *LWT - Food Science and Technology*, 2015, **60**, 773–780.

234 J. van Wijk, T. Heunis, E. Harmzen, L. M. T. Dicks, J. Meuldijk and B. Klumperman, *Chem. Commun.*, 2014, **50**, 15427–15430.

EXPERIMENTAL SECTION

3. EXPERIMENTAL SECTION

3.1. Chemicals

Silica sources	Brand
3-(Aminopropyl)-trimethoxysilane (APTMS)	Acros
Tetramethyl orthosilicate (TMOS)	Acros
Sodium silicate (26.5 wt% SiO_2, 10.6 wt% Na_2O, 62.9 wt% H_2O)	Sigma-Aldrich
Fluorescent dyes	
SYTO 9	Invitrogen
Propidium iodide	Invitrogen
SYBR Green	Invitrogen
Oil & surfactants	
Miglyol 812N	Cremer
Polyglycerol polyricinoleate (PGPR4125)	Palsgaard
Tween 40	Alfa Aesar
Sodium dodecyl sulphate	Sigma-Aldrich
Enzymes, Protein, Bacteria	
Pancreatin from porcine pancreas (P3292)	Sigma-Aldrich
TAQ-DNA polymerase	Thermo Scientific
Bovine serum albumin	Sigma-Aldrich
Lactobacillus rhamnosus GG (LMG 18243)	BCCM
Solvents	
Hexane	Sigma-Aldrich
Chloroform	Sigma-Aldrich
Phenol	Sigma-Aldrich
Isopropanol	Sigma-Aldrich
Formamide	Sigma-Aldrich
Dimethyl sulfoxide	Sigma-Aldrich
Inorganic reagents	**Brand**
Calcium chloride	Roth
Sodium chloride	Sigma-Aldrich
Disodium hydrogen phosphate	Fluka
Potassium dihydrogen phosphate	Fluka
2-amino-2-hydroxymehtyl-1,3-propanediol (Tris)	Alfa Aesar
Dehydrated fresh bile	Difco AB

Sodium citrate	Sigma-Aldrich
Sodium bicarbonate	Roth
Potassium chloride	Sigma-Aldrich
Urea	Sigma-Aldrich
Magnesium chloride	Sigma-Aldrich
Ammonium persulfate	Sigma-Aldrich
Hydrochloric acid	Sigma-Aldrich
Organic reagents	
Man, Rogosa and Sharpe broth (MRS)	Fisher
Glycerol	Alfa Aesar
Sodium alginate	Algin Texturas
Sucrose	Sigma-Aldrich
L-shime	ProDigest
Starch	Sigma-Aldrich
Ethylenediaminetetraacetic acid	Sigma-Aldrich
Polyvinylpyrrolidone (PVP40)	Sigma-Aldrich
Methylenediacrylamide	Sigma-Aldrich
1,2-Di(dimethylamino)ethane	Sigma-Aldrich
Acrylamide	Sigma-Aldrich
Others	
Glass beads (dia. 0.10/0.11 mm)	Sartorius
dNTPS	Thermo Scientific
Apple juice (100% apple juice, pasteurized)	Tropicana
Beer (5 vt% alcohol content, pasteurized)	Heineken

3.2. Syntheses methods

Preparation of hybrid microparticles via emulsification

Culture growth: A pre-inoculum was prepared adding 200 µL of the LGG stock solution into 20 mL of MRS and kept around 68 h in the hood at room temperature. In sequence, 200 µL of the pre-inoculum was added to 20 mL of MRS and incubated for 24 h at 35 °C. The bacteria pellet was harvested with 20 mL of 0.9 wt% autoclaved NaCl (4500 rpm, 5 min, 21 °C).

Emulsification: In a typical procedure ($A_2Ca_6Si_6$), the first step consisted in mixing 1 mL of miglyol with 0.3 g of PGPR, to obtain 24 wt% PGPR in miglyol. A reverse emulsion (W/O) was then prepared by adding dropwise 3.2 mL of 1.6M $CaCl_2$ under vigorous vortexing. A mixture of 3.3 g of 2 wt% sodium alginate and 1.6 mL of sodium silicate was poured over the former water-in-oil emulsion and stirred under vortexing for another 1 min. Unless otherwise specified, the alginate-silica materials were separated from the emulsion after 6 to 8 h aging at room temperature, via few water washings and centrifugation steps (4500 rpm, 3 min, 21 °C).

When the bacteria was introduced into the system, 1 mL of harvested culture was centrifuged (4500 rpm, 5 min, 21 °C), the supernatant was discarded and the alginate was added to it and vortexed for few seconds dissolving well the pellet. In sequence, the sodium silicate was added to the previous mixture, which is quickly vortexed and poured over the reverse emulsion ($CaCl_2$ in miglyol with PGPR).

Preparation of core-shell microparticles via electrospraying

Culture growth and alginate solution: A pre-inoculum was prepared adding 200 µL of the LGG stock solution into 20 mL of MRS and kept around 68 h at room temperature. In sequence, 200 µL of the pre-inoculum was added to 20 mL of MRS and incubated for 24 h at 35 °C. The bacteria pellet was harvested with 20 mL of 0.9 wt% NaCl (4500 rpm, 5 min, 21 °C). The supernatant was discarded and 20 mL of 1 wt% sodium alginate either in autoclaved distilled water or in 0.2 µm filtered 10 mM HCl-tris pH 8 was added to the pellet, which was vortexed until obtaining a homogeneous LGG alginate slurry. When sucrose was introduced to the slurry for its cryoprotectant properties, 10 wt% of sucrose was dissolved into the HCl-tris buffer and then the solution was sequentially filter with a 0.2 µm filter.

Electrospraying: The in-house assembled electrospraying device possessed a variable high-voltage with a 0 - 30 kV power supply (Figure 17). The LGG alginate slurry was contained in a sterile plastic syringe connected to a stainless steel sterile needle (23G, BD). The anode was connected to the needle and the ground electrode to the aluminum plate holding the collector dish. Negative voltage was applied to the needle and the aluminum plate holding the collector dish was connected to the ground. Solution in the

collector dish was also connected to the ground. The distance between the needle tip and the surface of the collecting solution was set at approx. 3.5 cm, the voltage 7.5 kV and the flow 13.9 mL h^{-1} or 15 mL h^{-1}(since two electrospraying setups were used during the course of this thesis). The alginate beads harden immediately once in contact with 1.5 wt% $CaCl_2$ solution, previously filtered onto a 0.2 µm sieve. They were kept in the Ca^{2+} solution for at least 1 h before further manipulation.

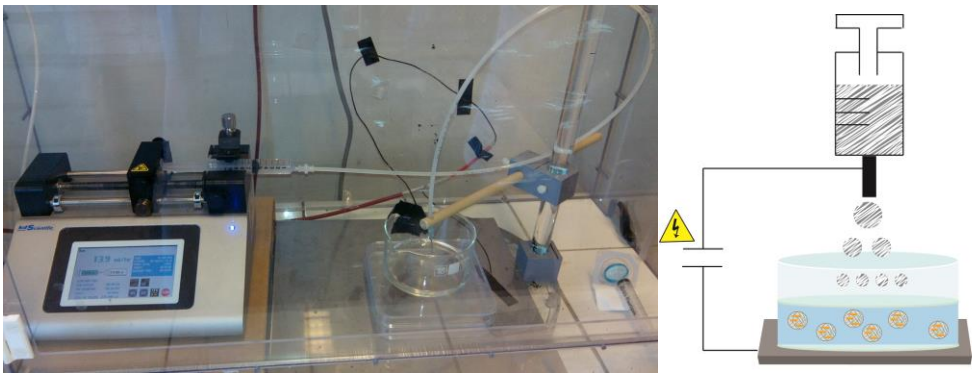

Figure 17: (left) Electrospraying setup used for the obtainment of the alginate beads, (right) alginate beads formation cartoon.

Mineralization: A volume of 2.32 mL or 2.5 mL (depending on electrospraying setup) of alginate beads dispersion was filtered through a sterile 100 µm sieve and rinsed with 50 mL of 0.9 wt% autoclaved NaCl. The beads were transferred into a sterile conical where 10 mL of 0.5 wt% PGPR in hexane or 1.5 wt% Tween 40 was dropped over while vortexing. 100 µL of APTMS was added to the solution and vortexed at 20 Hz for 1 min. In sequence, 100 µL of TMOS was added in the same way and vortexed for another 1 min. Figure 18 illustrates the coating steps for alginate beads in Tween 40. Immediately after, the supernatant was removed and the silica-coated beads were rinsed with 50 mL of 0.9 wt% autoclaved NaCl and filtered through a sterile 100 µm sieve. As a function of the alginate core media (water (w) or Tris buffer (tris)) and the mineralization media (organic (org) or aqueous (aq)) the core-shell (CS) particles are labeled C_wS_{org}, $C_{tris}S_{org}$, C_wS_{aq}, $C_{tris}S_{aq}$ respectively.

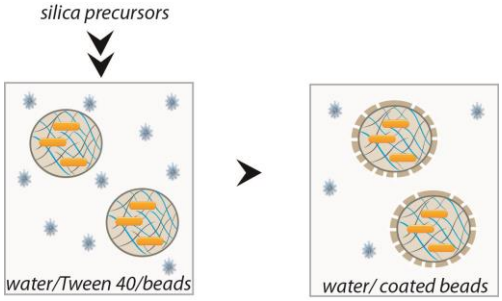

Figure 18: (left) Addition of silica precursors (APTMS and TMOS) in a 1.5 wt% Tween 40 solution containing alginate beads, (right) silica shell formed around alginate beads in 1.5 wt% Tween 40 solution prior to washing.

Freeze-drying: Alginate or silica-coated beads were transferred to fresh sterile conical tubes and plunged in liquid nitrogen for about 5 min. The tubes were place in a freeze-drier (Cryodos-80, Telstar) for about 20 h reaching -85 °C and 0.1 mbar. One batch of material represents 36 mg and 47 mg for alginate and silica-coated beads, respectively.

Study on the disintegration of alginate and silica-coated beads

Solutions assessment: While shook at 37 °C and 300 rpm, silica-coated beads of about 500 µm were put in 200 mL of the following media: 0.9 wt% NaCl, 0.01 M phosphate buffer pH 8 containing 0.9 wt% NaCl, 0.01 M tris-HCl buffer pH 8 containing 0.9 wt% NaCl, 0.01 M phosphate buffer pH 8, 0.01 M tris-HCl buffer pH 8, 0.1 M sodium citrate pH 5, 0.1 M sodium citrate pH 5 containing 0.9 wt% NaCl, 0.01M HCl pH 3 and 0.01M HCl pH 3 containing 0.9 wt% NaCl. Alginate beads were put in 200 mL of the following media: 0.9 wt% NaCl, 0.01 M phosphate buffer pH 8 containing 0.9 wt% NaCl, 0.01 M tris-HCl buffer pH 8 containing 0.9 wt% NaCl. The disintegration of all beads was followed by naked eye. Once the transparent solutions turned cloudy, it was considered as complete macroscopic disintegration of the beads.

Encapsulated bacteria proliferation within the silica-coated carrier

Sample handling: Silica-coated beads containing LGG were kept in MRS broth for 60 h to allow bacteria proliferation. The MRS was exchanged against fresh broth every 24 h. The silica-coated beads were stained with the SYTO9 and propidium iodide as described in the confocal microscopy section.

3.3. Gastrointestinal passage procedure

Preparation of fed media: 11.6 g of L-shime was mixed with 4 g of starch in 500 mL of distilled water. Once both powders were well dissolved, another 500 mL was added to the bottle. The mixture was autoclaved before further use and holds a pH of 4.8.

Preparation of pancreatic juice: 6 g of dehydrated fresh bile, 12.5 g of $NaHCO_3$ and 0.9 g of pancreatin from porcine pancreas were dissolved in 1 L of autoclaved distilled water.

Preparation of fecal inoculum: 10 g of fresh fecal sample were added to 50 mL of deoxygenated PBS and mixed with a stomacher for some seconds until all becomes liquid. It was then centrifuged for 5 min at 800 x G. The supernatant was collected and kept in a sterile conical until its use in less than 1 h after preparation.

Gastrointestinal release: The experiment was divided into 3 phases that follow in sequence: gastric, small intestine and colon. A) The gastric phase (2 h residence time): One batch of 3-weeks freeze-dried samples (either 36 mg or 47 mg) was first poured into 250 mL autoclaved penicillin bottles and 10 mL of the autoclaved fed media was added over it. In the case of the control (free LGG), a 100 µL of a 24 h LGG culture was spiked over the 10 mL autoclaved fed media. The samples had the pH gradually decreased from 4.8 to 2.0 during 2 h while they were kept at 37 °C and 120 rpm. More specifically, the samples were shook for 30 min at pH 4.8, then the pH was decreased to 4.0 (40 µL of 1 M HCl) and kept shaking for 15 min, then pH was decreased to 3.5 (40 µL of 1 M HCl) and kept shaking for 15 min, then pH was decreased to 3.0 (50 µL of 1 M HCl) and kept shaking for 15 min, then pH was decreased to 2.5 (60 µL of 1 M HCl) and kept shaking for another 15 min. Finally the pH was decreased to 2.0 (100 µL of 1 M HCl) and kept shaking for another 30 min. 200 µL aliquots in replicates were withdrawn at 1 h and 2 h for viability analysis. B) The small intestine phase (3 h residence time): 4.6 mL of pancreatic juice was added to the gastric phase where the pH reaches 6.7. The whole was shook for 3 h (37 °C, 120 rpm). 200 µL aliquots in replicates were withdrawn at 1, 2 and 3 hours for flow cytometry analysis. Additionally, 1 mL in replicate was withdrawn after 3 h for lactate measurements. C) The colon phase (24 h residence

time): 10 mL of the fecal inoculum was added over the mixture from the small intestine phase. To ensure anaerobic conditions, a mixture of N_2 and CO_2 was flushed in the previously aluminum sealed bottles. The bottles were kept at 37 °C and 120 rpm for 24 h. 300 µL aliquots in replicates were withdrawn at 2 h and 24 h for DNA characterization. Figure 19 illustrates the sealed reaction vessels after the 24 h of colon inoculation.

Figure 19: Biological triplicates of silica-coated beads after the 24 h of colon inoculation.

3.4. LGG assessment in beverages

Addition of freeze-dried carriers in beer and apple juice: 10 mL of apple juice (Tropicana Pure premium, 100 % apple juice, pasteurized) or 10 mL of beer (Heineken, 5 vt% alcohol content) were added over a batch of 1-day freeze-dried alginate beads (36 mg) or 1-day freeze-dried silica-coated beads (47 mg) and shook up and down few times. In the case of the control, a fresh LGG pellet (100 µL of LGG in 10 mL of MRS, 24 h culture at 35 °C) was harvest with 10 mL of 0.9 wt% autoclaved NaCl, centrifuged (4500 rpm, 5 min, 21 °C) and the pellet was lyophilized for about 20 h (Cryodos-80 Telstar at -85 °C and 0.1 mbar). The pellet was in sequence re-suspended in 10 mL of 0.9 wt% autoclaved NaCl. 100 µL of the re-suspended pellet was spiked over the 10 mL of apple juice or beer. The conical tubes were kept immobile at 4 °C for 3 h and 1 week before the investigations on the release of LGG into the filtrate or its maintenance in the beads. The experiment was done with two biological replicates.

LGG in filtrate: Alginate and silica-coated beads were filter with a sterile 100 µL sieve and the filtrate was serial diluted and agar plated. These values represent the released bacteria from the carriers.

LGG in the beads: The filtered beads were crushed with a sterile disposable spatula first. 5 mL of 0.9 wt% autoclaved NaCl was added to the tubes and further crushed with an Ultraturrax (3000 rpm, 1 min). The Ultraturrax probe was sterilized before every use under a flame. In sequence, another 5 mL of 0.9 wt% autoclaved NaCl was added to the tubes. The remaining material was filtered with a sterile 100 µL sieve and the filtrate was serial diluted and agar plated. These values represent the bacteria that were still confined in the carriers.

3.5. Materials characterization

Optical microscopy (OM): Images were taken with an Olympus BX51 equipped with a Toupca camera along with TouView software. The sizes of the beads correspond to an average of 300 beads for 3 individual experiments and the size distribution was analyzed with ImageJ.

Scanning electron microscopy (SEM): The morphology and structure of the beads were assessed on a Hitachi microscope (Hitachi S4800) at an accelerating voltage of 3.0 or 5.0 kV and working distance of about 8 mm. The beads coming from the electrospraying synthesis were freeze-dried for the analysis purpose. And all samples were carbon-coated under vacuum prior observation except for the material obtained via emulsification.

Transmission electron microscopy (TEM): The observations were performed with a Philips/FEI CM200 200 keV. The technique targeted the observation of local arrangement of pores in a sample and the presence of entrapped bacteria within the material hybrid matrix. To observe the arrangement of the pores from the materials obtained via electrospraying, the sample powders were dispersed in a bi-component resin (BDMA and Araldite®) that harden for 3 days at 60 °C. Ultra-thin slices of 80 nm were cut with a microtome (Leica) and were placed on a holey carbon grid coated with

copper. To observe the entrapment of bacteria within a hybrid matrix obtained via emulsification, the sample preparation was more arduous. A volume of $1mm^3$ of the powder containing the LGG alginate-silicate material was fixed for 3 h with 2 % glutaraldehyde in a sodium cacodylate buffer (pH 7.2, 4 °C). The buffer was then rinsed off during an hour followed by a post-fixation for 1 h with 1 % osmium tetraoxide (OsO_4) in the cacodylate buffer at room temperature. In the next step, a progressive dehydration with ethanol was targeted (30 % ethanol for 5 min, 50 % ethanol for 5 min, 70 % ethanol for 5 min, 80 % ethanol for 5 min, 90 % ethanol for 5 min and 100 % ethanol for 20 min, three times). A pre-impregnation was done during 1 h in a resin mixture (resin EMbed 812 with 100 % ethanol, equal volumes) and was followed by an impregnation in the pure resin overnight. Then it was added to a plastic tube with fresh resin and let it polymerase at 56 °C for 72 h. Ultra-thin slices of 80 nm were done with an ultra-microtome (Reichert-Yung) and placed over copper grids. Oolong tea extracts (OTE) and lead citrate were used for enhancement of the contrast of cell components.

Attenuated total reflectance infrared spectroscopy (ATR-FTIR): All the ATR experiments were conducted using a Shimadzu IRaffinity-1 coupled with a PIKE GladiATR accessory (PIKE Technologies, USA). The dried samples were placed on the device's window as it is. The absorbance spectra were collected within the wavenumbers of 4000 to 400 cm^{-1} averaging 32 scans at 4 cm^{-1}. The spectra collection software is LabSolutions IR (Shimadzu).

Magic-angle spinning nuclear magnetic resonance (MAS-NMR): Solid-state NMR experiments were carried out on a Bruker Biospin AVANCE III spectrometer operating at 300 MHz ^1H resonance frequency (7 T) using a 4 mm probe. Spinning frequency was set to 10 kHz. A 60 s recycle delay was used for ^{29}Si direct acquisition spectra. ^{29}Si external chemical shift reference is TMS. ^{13}C cross-polarization spectra were recorded with ^1H and ^{13}C fields of 55 kHz and 45 kHz respectively, during a 2 ms contact time. SPINAL-64[1] 80 kHz ^1H decoupling was applied during 20 ms acquisition. ^{29}Si spectra deconvolution was achieved using dmfit[2] and the results resumed in 3 peaks representing Q^2 units (at -91 ppm), Q^3 units (at -99 ppm) and Q^4 units (at -110 ppm).

Rheology measurements: The rheological measurements were carried out on a HAAKE MARS III rheometer (Thermo Fisher Scientific, Germany) set with a cone-and-plate geometry (35 mm, 1°). A Peltier unit was used to accurately control the temperature, which was fixed at 25.0 ± 0.1°C. To minimize evaporation the measuring geometry was closed with an appropriate solvent trap. In order to follow the mineralization process, different linear and non-linear experiments were performed. For each formulation, the complex viscosity (η^*) evolution was either followed continually for 12 h at 5 Pa and 1 Hz or evaluated every hour by performing a frequency sweep (from 50 to 0.1 Hz at 5 Pa) before and after running a non linear rotational test (20 s^{-1} for 1200 s). Note that while in first test the sample is kept 12h in the geometry gap, in the later test a fresh emulsion sample is loaded every hour in the rheometer.

3.6. Bacterial viability

Plate count: It was always investigated for a whole batch of beads either in a wet or a freeze-dried state. If wet, a 2.32 mL batch of electrosprayed alginate beads or coated beads were transferred to sterile flasks containing 200 mL of 0.9 wt% autoclaved NaCl. If dried, a dry mass of 36 mg of alginate beads or 47 mg silica-coated alginate beads were transferred to sterile flasks containing 200 mL of 0.9 wt% autoclaved NaCl. The flasks were shaken at 300 rpm and kept at 37°C up to 2 h until all the beads disintegrate. 100 µL of the disintegrated beads solution was spiked in 10 mL of MRS broth that was kept for 15 h at 35 °C for evaluation of the syntheses impact on LGG viability. Once the best performing synthesis was accordingly chosen, serial dilutions with 100 µL of the disintegrated beads solution was performed in sequence and seeding on MRS agar petri follows next. This latter procedure allowed us to obtain the actual LGG viability value within the carriers. The LGG colonies were read after 48 h of incubation at 35 °C under semi-anaerobic conditions, *i.e.* petri dishes were sealed with parafilm. The results were expressed as an average of 3 individual experiments of two different dilutions in duplicates. When pertinent, statistical analysis was performed using the Graphpad Prism 3.0 software package. Differences between groups were analyzed using one-way ANOVA and Bonferroni post-hoc tests. $P < 0.05$ was considered statistically significant.

Flow cytometry (FC): This technique was used to assess intact and damaged cells during the stomach and small intestine phases of the gastrointestinal experiment. It was performed using a CyAn ADP LX device (Dakocytomation, Heverlee, Belgium) equipped with a 50-mW Sapphire solid-state diode laser (488 nm). Green and red channels were collected with photo-multiplier tubes using 530/40 and 613/20 band pass filters respectively. Forward (FS) was collected with a 488/10 band pass filter. Two fluorescent dyes, SYBR Green and propidium iodide (PI), were used in combination to access the intact and damaged LGG cells. LGG samples were diluted to 1000 times in 0.2 µm filtered 0.9 % NaCl and stained with 2 µL of the staining mixture. The dyes mixture's preparation: PI (20 mM in DMSO from the Live/Dead BacLight Kit, Invitrogen) was diluted 50 times and SYBR Green (10 000 times concentrate in DMSO, Invitrogen) was diluted 100 times in 0.2 µm filtered DMSO.[3] Prior to analysis, the 96-well plate was incubated for about 15 min in the dark at room temperature.

Confocal laser scanning microscopy (CLSM): Confocal observations were carried out with a Leica TCS SPX AOBS CLSM. Images at a 315 µm side length square pixel size were obtained for each case in 1024 x 1024 matrices at 40x magnification (numerical aperture = 0.8). Fluorescence emissions were recorded within an airy disk confocal pinhole setting (Airy 1). Each channel was acquired sequentially. First channel detection was set from 492 to 525 nm with a 482 nm excitation laser line. Second channel detection was set from 597 to 716 nm with a 535 nm excitation laser line. For each sample, a z-stack containing 10 slices of the bead was recorded. The images were processed using Image J. The sample preparation followed a staining step before the CLSM assessment. Figure 20 illustrates the imagining of a mixture of damaged and intact LGG stained with propidium iodide and SYTO9, respectively.

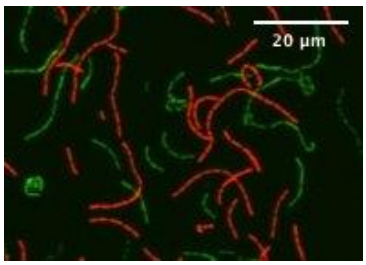

Figure 20: A mixture of damaged and intact LGG stained with propidium iodide and SYTO9, respectively.

The beads remained 15 h in a 0.2 µm filtered 1.5 wt% $CaCl_2$ prior to staining with SYTO9 and propidium iodide. A volume of 2 µL of the staining solution was added to 1 mL of beads in the $CaCl_2$ solution. The mixture was kept for 15 min in the dark and it was shaken every 5 min. Drops of this solution containing the beads were placed on microscope slides, covered with a cover glass, sealed with nail polish and wrapped in aluminum foil until observation.

3.7. LGG characterization

Ion Chromatography (IC): Lactate measurements were assessed with a 930 compact IC flex (Metrohm) with inline bicarbonate removal and an 850 IC conductivity detector. An aliquot of 100 µL was injected for each sample. The column used was a metrosep organic acids 250/7.8 column and the guard column was a metrosep organic acids guard/4.6. The results were expressed as an average of 3 individual experiments for each sample and the aliquots were sampled in duplicates in each small intestine vessel.

Denaturing gradient gel electrophoresis (DGGE): Lactobacilli and total bacteria were characterized qualitatively and quantitatively in order to study the colonization of the colon, containing a feces microbial ecosystem, by the LGG released from the microcapsules during the gastrointestinal passage. Genomic DNA was extracted in duplicates from each biological triplicate at 2 h and 24 h. The extraction was done as follows: For a 300 µL of colon aliquot, 200 mg of glass beads (dia. 0.10/0.11 mm, Sartorius) were added with 1 mL of lysis buffer (5 mL 1M Tris pH 8, 10 mL 0.5M EDTA pH 8, 1 mL 5M NaCl, 5 mL 10 wt% polyvinylpyrrolidone (PVP40), 10 mL 10 wt% sodium dodecyl sulphate (SDS) and 50 mL water). The tube was vigorously shaken with a FastPrep homogenizer (2000 rpm, 5 min) and sequentially centrifuged (14680 rpm, 5 min). The supernatant was then poured into a fresh tube containing 500 µL of phenol, vortexed and centrifuged (14680 rpm, 1 min). Once again, the supernatant was transferred to a fresh tube containing 700 µL of chloroform, vortexed and centrifuged (14680 rpm, 1 min). A volume of 450 µL of the supernatant was added to a fresh tube containing 500 µL of isopropanol and 45 µL of 3 M sodium acetate. The whole tube content was mixed by inverting it up and down and then frozen for at least 1 hour. In sequence, it was centrifuged at 4 °C and the extra liquid was dried. A purified DNA pellet

was therefore obtained. As final step, 100 µL of 1x TE buffer (10 mM Tris, 1 mM EDTA pH 8) was added to the pellet and frozen again for further processing.

DGGE was based on the protocol of Muyzer *et al.*[4] and performed using the INGENYphorU System (Ingeny International BV, The Netherlands). PCR fragments and a DNA ladder (prepared from a standard fecal sample in-house) were loaded onto 8% (w/v) polyacrylamide gel in 1x TAE buffer (20 mM Tris, 10 mM acetate, 0.5 mM EDTA pH 7.4). The polyacrylamide gel with 45-60 % denaturing agent was used to separate the PCR products obtained with a nested approach for the 16S rDNA genes of lactobacilli (primers 667R and 0159F) and total bacteria (primers 518R and 338F-GC). The first PCR amplification for lactobacilli (1:10 dilution of the DNA extracted material) was followed sequentially by a second amplification for the total bacteria (1:100 dilution on the first PCR amplification). The electrophoresis ran for 16 hours at 60 °C and 120 V. The gel was then added to 1x TAE buffer with SYBR Green ($1:10^4$ dilution; FMC BioProducts, Rockland, Maine) for 10 min and sequentially photographed on a UV transillumination table with a video camera module (Vilbert Lourmat, Marne-la Vallé, France). Sanger sequencing was used as a complimentary method to pinpoint one specific lactobacillus species observed on the DGGE gel.[5]

Quantitative PCR (qPCR): Real-time PCR (qPCR) was performed on a StepOnePlus Real-Time PCR system (Applied Biosystems, Carlsbad, CA). Triplicates of each sample with a 10-fold dilution of the DNA-extracted material were analyzed for Lactobacilli (primers 04R and 05F) and total bacteria (primers 518R and 338F). A calibration curve in triplicates was also done side by side with the samples every time a 96-well plate was read. The reaction mixture holding a volume of 25 µL was composed of 20 µL of a master mixture and 5 µL of the diluted sample. The master mixture prepared as follows: To each well of the plate, 14.18 µL of PCR water was added with 2.5 µL of TAQ Buffer (10x with KCl), 1.5 µL of $MgCl_2$ (25 mM), 0.5 µL of dNTPs (10 mM each), 0.5 µL of primer F (10µM), 0.5 µL of primer R (10µM), 0.0625 µL of BSA (20 mg/mL), 0.125 µL SYBR Green diluted in DMSO (20x) and 0.124 µL of TAQ DNA polymerase (Thermo Scientific). The qPCR program was performed in a two-step thermal cycling procedure consisting of a pre-denaturation step for 3 min at 95 °C followed by 40 cycles of 1 min at 94 °C/40 sec at 56 °C/40 sec at 72 °C (for total bacteria) and pre-denaturation step for 10 min at

95 °C followed by 40 cycles of 15 sec at 94 °C/1 min at 60 °C (for Lactobacilli). The qPCR data were represented as DNA copies per µL.

3.8. References

1 B. M. Fung, A. K. Khitrin and K. Ermolaev, *Journal of Magnetic Resonance*, 1999, **142**, 97–101.

2 D. Massiot, F. Fayon, M. Capron, I. King, S. Le Calvé, B. Alonso, J.-O. Durand, B. Bujoli, Z. Gan and G. Hoatson, *Magnetic resonance in chemistry*, 2001, **40**, 70–76.

3 K. De Roy, L. Clement, O. Thas, Y. Wang and N. Boon, *Water Research*, 2012, **46**, 907–919.

4 G. Muyzer, E. C. Waal and A. G. Uitterlinden, *Applied and Environmental Microbiology*, 1992, **59**, 695–700.

5 F. Sanger and R. Coulson, *Journal of Molecular Biology*, 1975, **94**, 441–448.

RESULTAT ET DISCUSSION/
RESULTS AND DISCUSSION

4. RESULTAT ET DISCUSSION

Les résultats obtenus à partir de deux stratégies d'encapsulation LGG sont décrits dans cette section, composées de deux parties directement liées au mode de préparation des microcapsules par émulsification (I) et électrospraying (II). En bref, dans la première partie, le matériau hybride d'alginate-silice obtenu par émulsification n'a pas permis de conserver une quantité raisonnablement importante de LGG viable sous confinement. De plus, les bactéries ne pouvaient pas être libérées des microcapsules dans les conditions de pH intestinal. Malgré le fait que cette stratégie ne semble pas appropriée pour l'encapsulation des cellules, le mécanisme de formation de ces microparticules a été étudié. Les résultats sont intéressants pour la compréhension fondamentale de la formation de matériaux composites. Nous montrons que les mesures de rhéologie *in situ* ont été particulièrement adaptées pour suivre le mécanisme de formation des microcapsules pendant le processus complexe de minéralisation et gélification de la silice et de l'alginate. Dans la deuxième partie de l'étude, les microparticules d'alginate-silice de type cœur-couronne ont été obtenues par électrospraying. Cette stratégie nous a permis d'obtenir un transporteur bactérien hautement viable aussi bien à l'état hydraté que lyophilisé. La viabilité de LGG dans les billes synthétisées a été évaluée par un modèle gastro-intestinal *in vitro* et dans deux boissons commerciales, du jus de pomme et de la bière. La bière d'un degré alcoolique de 5%, dans notre cas, peut être considérée potentiellement comme une nouvelle matrice alimentaire probiotique ciblant un public plus large ou éventuellement une nouvelle niche commerciale.

4. RESULTS AND DISCUSSION

4.1. Encapsulation of LGG via emulsification

4.1.1. Introduction

Colon-specific delivery of active biomolecules continues to challenge the oral administration route. In fact, after the intake of functional foods, dietary supplements or even pharmaceuticals, the bioavailability and chemical stability of these biomolecules may be lowered and/or altered as a result of the industrial processing followed by the physiological conditions encountered along the gastrointestinal passage. A great importance is therefore attributed to encapsulation, from probiotic cells to enzymes or molecules such as folic acid, with the aim of delivering them into the intestines.[1-4] In this context, carriers based on biodegradable polymers are of interest, especially in the case of entrapment of bacterial cells. They are known to improve not only the protection of the load enhancing the release of viable cells in the upper and lower intestines, but also allowing proliferation under confinement.[5-8] A substantial challenge however on colon delivery lies behind the need of slightly more sophisticated carriers capable of enduring the sinuous gastrointestinal passage, yet discharging the load in the lower tract with strategies resulting in changes in pH, salts concentration and/or the presence of enzymes in the environment. Thus, in order to overcome such difficulties, hybrid organic-inorganic particles are promising candidates.[9-15] Different synthesis approaches are of interest for the obtainment of hybrid materials, with water-in-oil emulsions (W/O) being a recurrent example. In our food-grade W/O systems, we emulsified a mixture of sodium alginate and *Lactobacillus rhamnosus* GG with sodium silicate in the water phase. The non-toxicity, biocompatibility, thermal and mechanical stability of silica results in very stable carriers.[16-18] Nonetheless, there is still a lack of information on materials synthesized with sodium silicate as a result of its complex gelation chemistry,[19,20] which in our scenario coexist with organic gels within the same reaction vessel. The mechanism of formation of the hybrid beads in such complex systems is therefore rather unclear. Few technics of characterization such as NMR, X-ray and light scattering are appropriate to follow *in situ* the formation of hybrid materials. Rheology is also widely used to study mechanical responses of soft matter systems such as

emulsions, hydrogels and even sol-gel processes allowing the correlation of the macroscopic behavior with physicochemical fundaments of the system.[21]

In this section, we present the synthesis of food compatible hybrid LGG-alginate-silicate microbeads whose formation has been followed by linear rheology and further correlated with NMR and SEM. The starting soft matter system is a W/O emulsion where the formation of solid microbeads is taking place exclusively in the water phase.

4.1.2. Results and discussion

Synthesis and characterization of hybrid silica materials

All water-in-oil emulsions were composed of a food grade continuous phase containing miglyol as oil and PGPR as emulsifier, and a dispersed aqueous solution of $CaCl_2$ in a first step. To this W/O emulsion is added a mixture of sodium alginate, LGG, and sodium silicate. The emulsions were stable for months and had an average droplets size distribution of about 8 ± 2 μm (Figure 21). The mineralization process evolved for 6-8 h at room temperature.

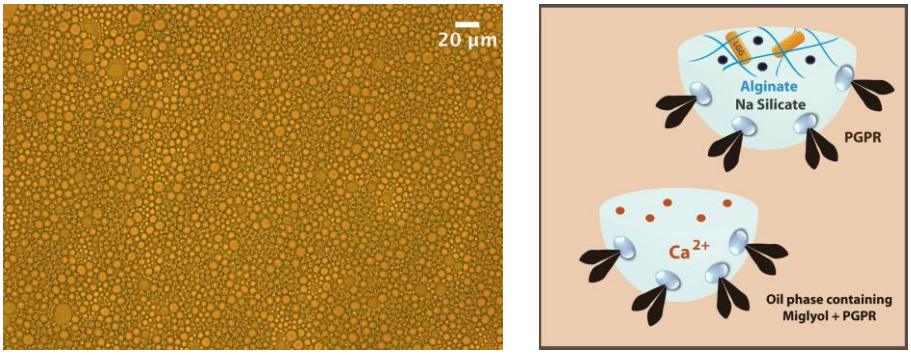

Figure 21: (left) Optical micrograph of W/O emulsion, (right) Scheme of the chemical composition of the two distinctive water droplets stabilized by polyglycerol polyricinoleate in miglyol at initial aging.

In order to investigate the role of each ingredient, the quantities of $CaCl_2$, sodium alginate and sodium silicate were varied leaving the bacterial cells out of the study in a first stage (Table 4).

Table 4: Composition of the aqueous phase of the reverse emulsions (wt%).*

	Alginate	$CaCl_2$	SiO_2	H_2O
$A_0Ca_3Si_6$	0	3.2	6.5	87.7
$A_0Ca_6Si_6$	0	5.9	6.5	85.0
$A_1Ca_3Si_6$	0.3	3.2	6.5	87.4
$A_1Ca_6Si_6$	0.3	6.0	6.4	84.6
$A_2Ca_1Si_6$	0.7	1.5	6.6	88.5
$A_2Ca_3Si_6$	0.7	3.2	6.5	87.0
$A_2Ca_6Si_6$	0.7	5.9	6.5	84.4
$A_2Ca_6Si_3$	0.7	6.0	3.0	89.1
$A_2Ca_6Si_0$	0.7	6.2	0.8	91.9

*the difference to 100% represents the wt% of Na_2O present in the solution of sodium silicate.

As it can be seen in Figure 22, spherical microparticles of 15 μm and 18 μm were obtained for the samples containing the highest amount of calcium and silica sources, namely **$A_1Ca_6Si_6$** (0.3wt% alginate, 6wt% $CaCl_2$ and 6.4wt% SiO_2) and **$A_2Ca_6Si_6$** (0.7wt% alginate, 5.9wt% $CaCl_2$ and 6.5wt% SiO_2), respectively. For both samples, SEM images revealed the presence of hollow beads with a shell of about 1-3 μm. Moreover, one can observe that the inner surface became smoother and thinner with time (from 6 to 24 h), probably due to the increased condensation of silica. This fact was confirmed by ^{29}Si solid-state NMR measurements of **$A_2Ca_6Si_6$** sample, showing that the ratio Q4/Q2 increases with time, as it can be seen on the spectra recorded at 2, 6 and 24 h (Figure 23). Figure 23a shows the mineralization kinetics. Commercial $CaSiO_3$ is solely composed of Q^2 units. The relative amount of Q^3 and Q^4 units increases with mineralization reaction time, indicating Si condensation (Table 5). On the other hand, the external surface of the beads is rather smooth, with a compact grainy morphology. A similar grainy morphology (Figure 24 B) was observed on the surface of beads prepared without sodium alginate and with the same amount of calcium chloride and sodium silicate (**$A_0Ca_6Si_6$**). However, in this case, no hollow capsules could be observed and the size of the beads was relatively smaller than the ones obtain with alginate (population centered on 4 μm).

Overall it can be concluded that when using approximately 6wt% $CaCl_2$ and 6.5wt% sodium silicate, the amount of alginate is influencing the size and the morphology of the beads. The size is increasing with the amount of sodium alginate while full beads are obtained without alginate, and mostly hollow microparticles with 0.3 or 0.7wt% of alginate.

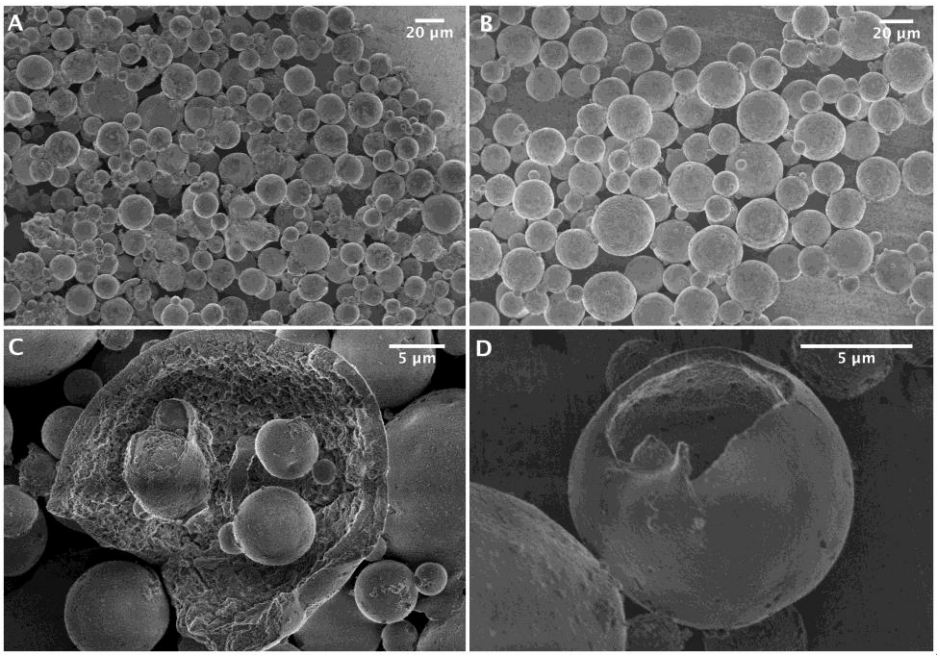

Figure 22: SEM micrographs of: A) $\mathbf{A_1Ca_6Si_6}$, B) $\mathbf{A_2Ca_6Si_6}$, hollow structures and a shell whose thickness and roughness decreases with the increase of the reaction time, from 6 h (C) to 24 h (D).

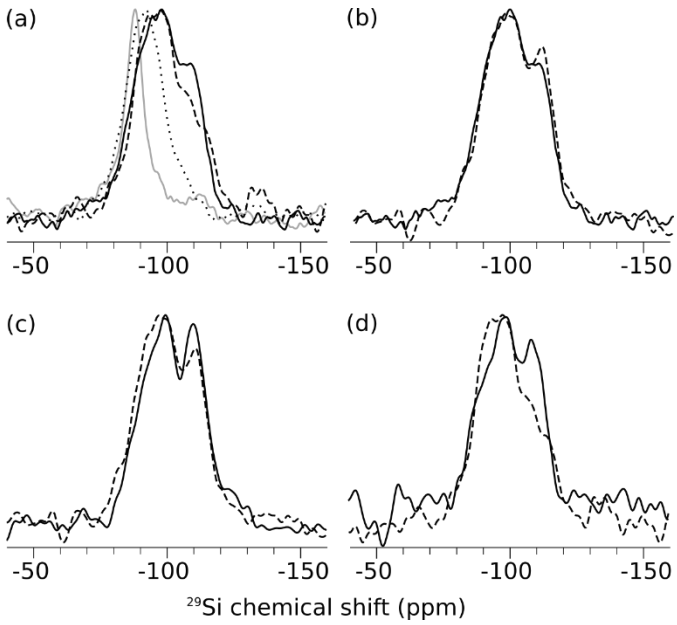

Figure 23: ^{29}Si solid-state NMR direct acquisition spectra of various samples: (a) commercial $CaSiO_3$ (grey solid line), $\mathbf{A_2Ca_6Si_6}$ after 2 h (dotted line), 6 h (dashed line) and 24 h (black solid line) mineralization reaction. (b) $\mathbf{A_0Ca_6Si_6}$ after 6 h mineralization reaction (dashed line) and $\mathbf{A_2Ca_6Si_6}$ after 24 h mineralization reaction (solid line). (c) $\mathbf{A_0Ca_3Si_6}$ (solid line) and $\mathbf{A_0Ca_6Si_6}$ (dashed line) after 6 h mineralization reaction. (d) $\mathbf{A_2Ca_3Si_6}$ (solid line) and $\mathbf{A_2Ca_6Si_6}$ (dashed line) after 6 h mineralization reaction.

Table 5: Relative proportions of Q^2 units (at -91 ppm), Q^3 units (at -99 ppm) and Q^4 units (at -110 ppm) as determined from the ^{29}Si spectra deconvolution.

	% Q^2	% Q^3	% Q^4
$A_2Ca_6Si_6$ (2h)	77	23	0
$A_2Ca_6Si_6$ (6h)	44	32	24
$A_2Ca_6Si_6$ (24h)	35	40	25
$A_0Ca_3Si_6$ (6h)	25	32	43
$A_0Ca_6Si_6$ (6h)	30	42	28
$A_2Ca_3Si_6$ (6h)	27	41	32

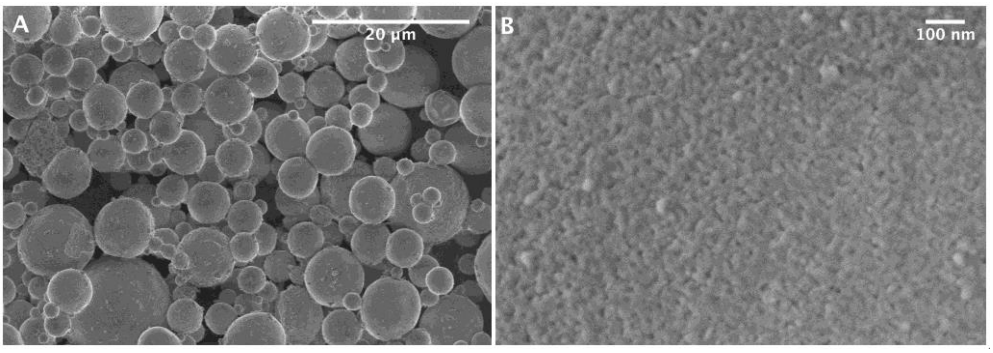

Figure 24: SEM micrographs of A) **$A_0Ca_6Si_6$** and B) its compact grainy surface.

The amount of silica source is also of paramount importance for the formation of beads. When the amount of sodium silicate is too low, of only 0.8wt% (**$A_2Ca_6Si_0$**), unshaped alginate particles were obtained (Figure 25 A) while with an intermediate value of 3wt% (**$A_2Ca_6Si_3$**) agglomerated grains of about 200 nm were formed (Figure 25 B). In both cases, the same amount of alginate and $CaCl_2$ were used, as with the **$A_2Ca_6Si_6$** sample that afforded hollow hybrid microcapsules. This clearly shows that a concentration of 6.5wt% sodium silicate is required to form round microparticles templated by the emulsion aqueous droplets. This condition is necessary but not sufficient to form beads. The amount of $CaCl_2$ has also to be controlled. In fact, $CaCl_2$ is also playing a crucial role for the beads formation since it is involved in the crosslinking of alginate to form a gel, and it acts as a catalyst in the condensation reaction of sodium silicate giving calcium silicate ($CaSiO_3$) and silica (SiO_2).

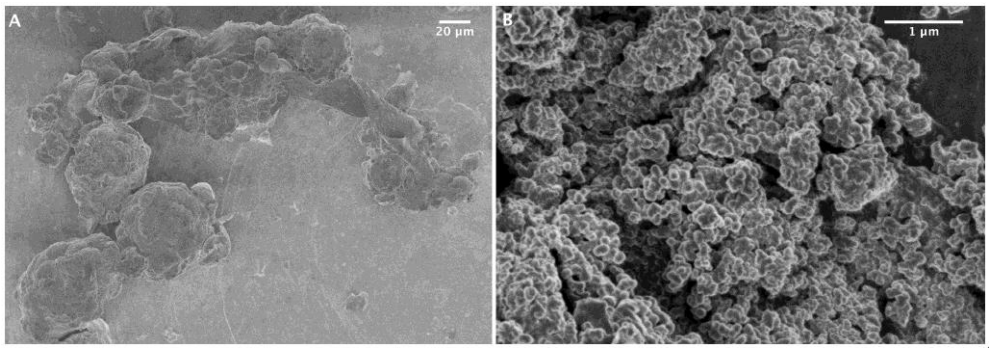

Figure 25: SEM micrographs of A) $\mathbf{A_2Ca_6Si_0}$ and B) $\mathbf{A_2Ca_6Si_3}$

Indeed, when calcium chloride is in default (1.5wt%), no material could be recovered even with the highest concentration of alginate, 0.7wt%, and sodium silicate, 6.5wt% ($\mathbf{A_2Ca_1Si_6}$). This also suggests that the alginate cannot catalyze the condensation of silica at high pH (>10), as it was previously reported in acidic conditions (1<pH<5). Or the tiny clusters formed were too small to be recovered by filtration. By increasing the amount of $CaCl_2$ to 3.2wt%, the condensation of silica/silicates can occur and materials can be recovered with the $\mathbf{A_2Ca_3Si_6}$ sample. However, only perforated beads or fragments could be observed on SEM micrographs (Figure 26), compared to perfectly smooth and round beads obtain with 6wt% $CaCl_2$ ($\mathbf{A_2Ca_6Si_6}$).

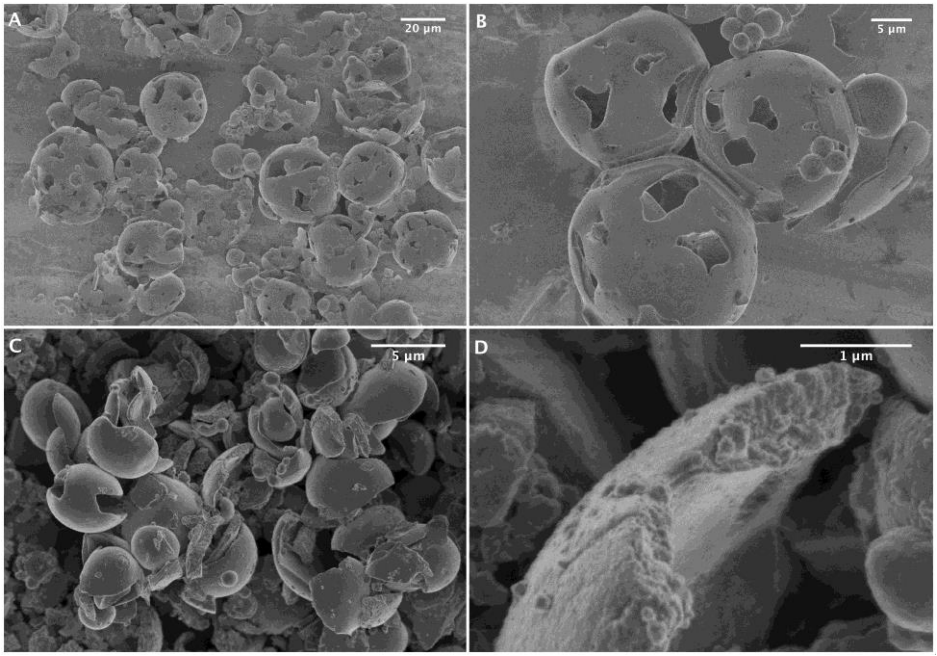

Figure 26: SEM micrographs of $\mathbf{A_2Ca_3Si_6}$ microbeads (A-D).

Similarly, even with a smaller amount of alginate, incompletely formed beads were recovered from the $\mathbf{A_1Ca_3Si_6}$ sample (Figure 27). The latter appears less fragmented

that the ones obtained in the case of **$A_2Ca_3Si_6$**. This could probably be due to the smaller amount of alginate that is crosslinked by Ca^{2+}, and thus to a highest concentration of free Ca^{2+} available to promote the condensation of silica. Again, in the absence of alginate, full microbeads were obtained (Figure 28) with the **$A_0Ca_3Si_6$** sample, as in the case of the **$A_0Ca_6Si_6$**. When using less calcium, the size of the beads was slightly larger (of about 5 µm for **$A_0Ca_3Si_6$** *vs* 4 µm for **$A_0Ca_6Si_6$**). The surface of the beads was also grainy, yet less compact compared to the material recovered with higher calcium content.

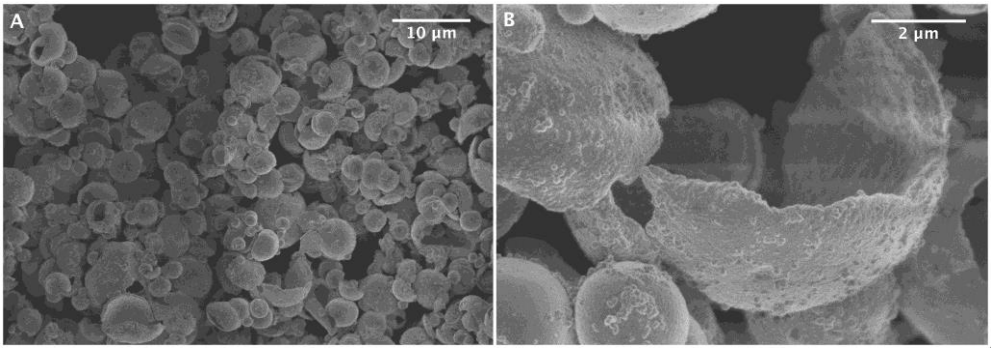

Figure 27: SEM micrographs of **$A_1Ca_3Si_6$** microbeads (A-B).

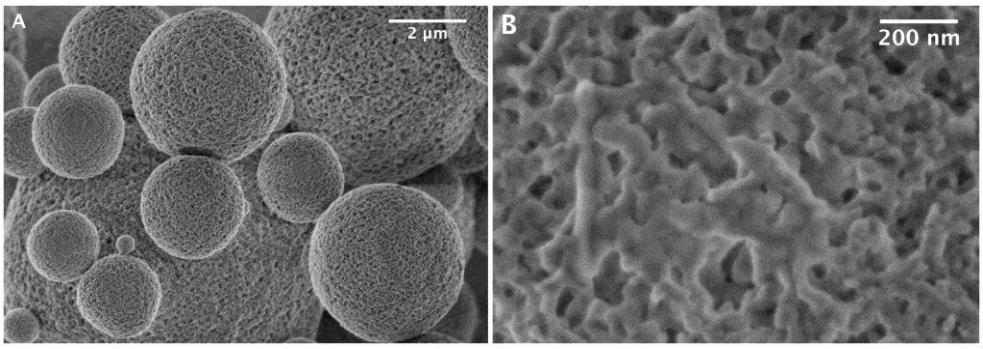

Figure 28: SEM micrographs of: A) **$A_0Ca_3Si_6$** microbeads, B) its grainy surface.

This phenomenon could be explained by the differences in the aggregation processes involved in the formation of silica and silicates as a function of the calcium content (Figure 29).[21] As a matter of fact, the addition of calcium ions to the precursor solution induces the irreversible aggregation of the colloidal silicate species. In this study, the oligomeric colloidal species ($2.6SiO_2{\cdot}Na_2O$) represent approximately 80 wt% of the sodium silicate solution while the rest are monomers.

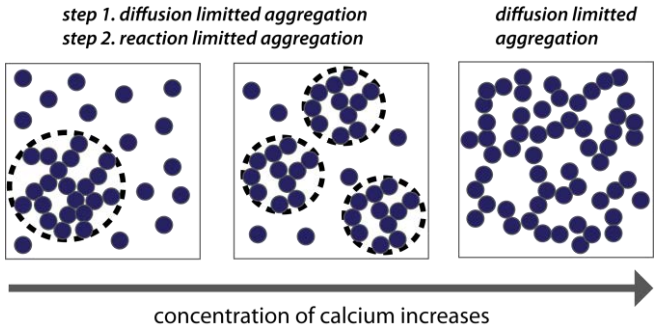

Figure 29: Schematic representation of the aggregates of primary silicate particles as a function of calcium concentration.

The reaction between calcium ions and oligomer particles are fast and limited by diffusion, but this process does not induce gelation. Only the further aggregation of initial clusters by a mechanism limited by reactivity (here the condensation of silica) leads to gel networks. As previously reported, high calcium content (molar ratio Ca/Si >1) induces the fast formation of a high number of small aggregates. This stage corresponds to the aggregation of primary particles of the initial sol and is controlled by the mechanism of cluster-cluster aggregation limited by diffusion. The formation of a very high number of aggregates prevents, in this case, their subsequent densification. Indeed, no densification is observed for $\mathbf{A_2Ca_6Si_3}$ with a molar ratio of Ca/Si of 1.4 when only agglomerated grains were observed (Figure 25 B).

If the calcium concentration is a little weaker, the aggregates start to densify and lead to beads, as in the case of $\mathbf{A_0Ca_3Si_6}$ and $\mathbf{A_0Ca_6Si_6}$, with a molar ratio of Ca/Si of 0.3 and 0.6, respectively. The process could be controlled by cluster-cluster aggregation limited by reactivity. As a matter of fact, in the presence of low concentration of calcium, the aggregation process takes place in two steps. The first one occurs through a cluster-cluster mechanism limited by diffusion. However, in this case, due to the low number of calcium ions in the sol the aggregation is only partial and some oligomer particles remain isolated. The lower is the concentration in calcium, the higher is the percentage of free oligomers. In the second step, the oligomers react with the aggregates by the action of a cluster-cluster process limited by condensation, inducing thus an increase of the size and a densification of the aggregates. Indeed, MAS-NMR measurements show that the samples with lower calcium content show a higher amount of Q^3 and Q^4 units,

thus a higher silica condensation (Figure 23 c: **$A_0Ca_3Si_6$** *vs* **$A_0Ca_6Si_6$** and Figure 23 d: **$A_2Ca_3Si_6$** *vs* **$A_2Ca_6Si_6$**).

In situ rheometry: continuous time evolution of viscoelastic properties during the mineralization and crosslinking processes

The rheological properties of the emulsions, in particular the complex viscosity (η^*) were studied in order to rationalize the role of each of the main components, *i.e.* sodium alginate, calcium chloride and sodium silicate, during the mineralization process. Understanding the evolution of such rheological properties, their interdependence on the composition and their impact on the final morphology of the systems is crucial for the design of new materials with desired features. Thus, an *in-situ* linear analysis was recorded during a 12 h reaction and the evolution η^* is given in Figure 30.

As a general trend, the overall complex viscosity exhibits a slight variation in the early stage of the process, then is increasing with time until reaching a maximum and is finally slightly decreasing to attend a steady state. However, the samples giving the smooth round beads, such as **$A_1Ca_6Si_6$** and **$A_2Ca_6Si_6$**, also exhibit a shoulder before reaching the maximum complex viscosity value. Indeed, as shown in Figure 30 a, the complex viscosity increases continuously up to 225 Pa·s at 150 min and 160 Pa·s at 170 min, respectively for **$A_1Ca_6Si_6$** and **$A_2Ca_6Si_6$**. After this regime (II), η^* continues to increase but with a lower rate before reaching a maximum at 250 Pa·s after about 325 min and 275 Pa·s after about 450 min, respectively for **$A_1Ca_6Si_6$** and **$A_2Ca_6Si_6$**.

In the early stage of the process (t<75 min) the crosslinking of alginate might take place, and the complex viscosity of the formed network is comparable to the one of the emulsion **$A_2Ca_6Si_0$** (η^* approx 100 Pa·s, as determined from the plateau, see Figure 30 b). Interestingly, when comparing to the template (**$A_2Ca_6Si_6$**), the sample having half of the alginate amount (**$A_1Ca_6Si_6$**) has a higher initial viscosity (Figure 30 a). This fact may be explained by a facilitated mobility of the Ca^{2+} ions within the bulk composed of alginate and sodium silicate at time zero, translating into a faster formation of the network and therefore a rapid increase in viscosity. Alternatively, the higher viscosity might be related to the fact that the concentration of alginate used for the **$A_1Ca_6Si_6$**

system is still below the critical entanglement concentration, and thus the polymer is capable to diffuse more freely within the droplet and "react" with Ca^{2+} to form the gel.

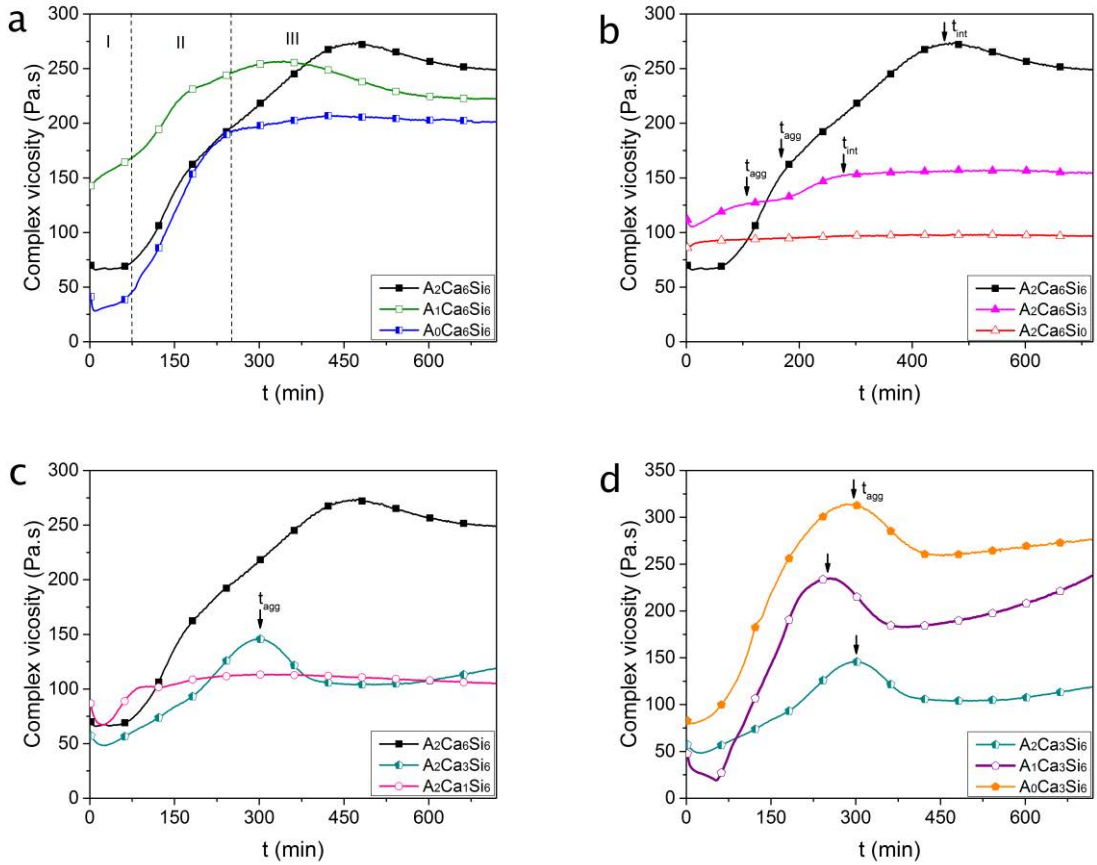

Figure 30: *In situ* complex viscosity (η*) profile recorded over 12 h according to variable content of: Alginate ($A_xCa_6Si_6$ and $A_xCa_3Si_6$) (a, d), Silica ($A_2Ca_6Si_x$) (b) and Calcium ($A_2Ca_xSi_6$).

In the intermediate stage of the process (75 min<t<300 min), one can observe the increase of the complex viscosity with time. This could be due to the formation of silicate aggregates that can further grow due to silica condensation. Certainly, as previously explained, Ca^{2+} is promoting the aggregation of primary particles of silicate and catalyzes the condensation of remaining sodium silicate into silica. This phenomenon is clearly seen in Figure 30 c, where the profile of viscosity over time is given at different calcium ion contents. With the lowest content in Ca^{2+} (**$A_2Ca_1Si_6$**), η^* remains constant. At an intermediate value content in Ca^{2+} (**$A_2Ca_3Si_6$**) a maximum η^* is observed at t_{agg} =300 min, corresponding to the end of the aggregation time. This value is shifted to a lower reaction time (of about 170 min), when the concentration of

Ca^{2+} increases (**$A_2Ca_6Si_6$**). In conclusion, one can observe that the increase of the concentration of calcium ions is accelerating the condensation of silica and silicate. Moreover, when the amount of calcium is too low compared to silica precursor (3.2wt% $CaCl_2$ vs 6wt%SiO_2), as in the case of samples **$A_0Ca_3Si_6$**, **$A_1Ca_3Si_6$** and **$A_2Ca_3Si_6$** (Figure 30 d), the maximum viscosity values are decreasing with the increase of alginate content. Interestingly, a maximum in viscosity for all three samples was observed at around ca. 4 hours of reaction. Despite the obvious differences in the structure morphology (grainy full beads for **$A_0Ca_3Si_6$** and perforated beads or fragments for **$A_1Ca_3Si_6$** and **$A_2Ca_3Si_6$**) with different alginate concentrations, the systems enriched in alginate suggest to slow the silica mobility, and therefore the kinetics of beads formation. On opposite direction, the lower the alginate content, the faster is the increase in viscosity.

In the late stage of the process (t>400 min on Figure 30 a), an increase of the complex viscosity over time is observed only for the two samples giving smooth and round beads, **$A_1Ca_6Si_6$** and **$A_2Ca_6Si_6$**. This was related to the interactions between the alginate network and calcium silicate particles formed in the previous step. No increase of η^* is recorded for **$A_0Ca_6Si_6$** sample, exempt of alginate. The overall viscosity augments with the amount of alginate and it delays the processes related to the aggregation of silica and silicate particles. This is in agreement with MAS-NMR measurements, indicating how the presence of alginate delays silica condensation by slowing down calcium diffusion (Figure 23 b). Indeed, the relative proportions of Q^2, Q^3 and Q^4 units of **$A_0Ca_6Si_6$** after 6h reaction time and **$A_2Ca_6Si_6$** after 24h reaction time are very close (Table 5). At the end of the synthesis process, the final viscosity plateaus are observed to increase with the alginate content (Figure 30 a), which might be related to a more robust alginate-silica matrix. Similarly, the viscosity is increasing with the amount of sodium silicate (Figure 30 b). While with almost no silica precursor (**$A_2Ca_6Si_0$**), the viscosity remains constant, and with intermediate silica value (**$A_2Ca_6Si_3$**) a change of slope between the second (II) and the third (III) regimes is observed at t=200min, suggesting again some interactions between alginate network and calcium silicate aggregates. This behavior is clearly enhanced when further increasing the silica precursor content (**$A_2Ca_6Si_6$**).

To summarize, the main reactions taking place at the different stages of the process are schematized in Figure 31.

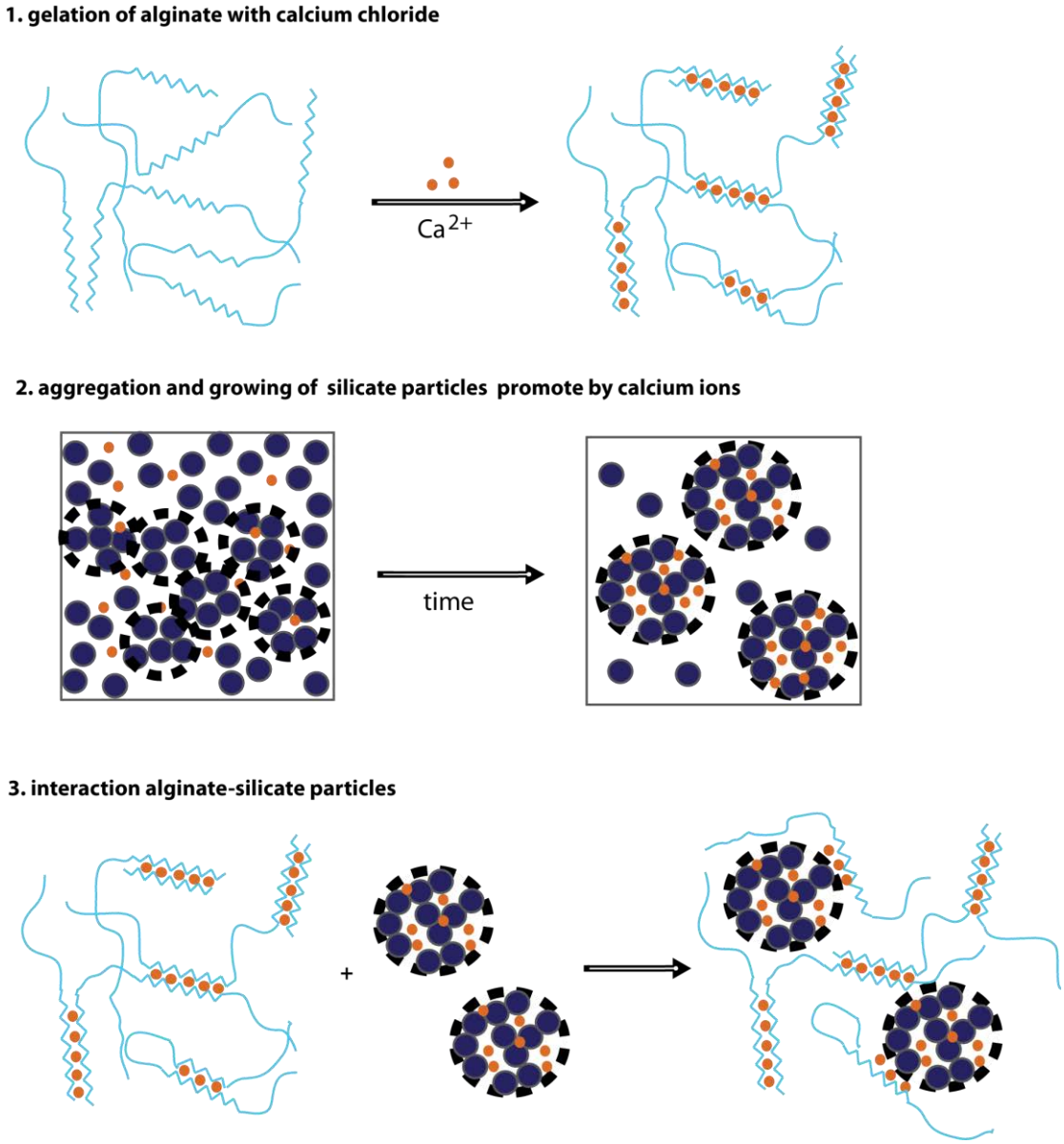

Figure 31: Schematic representation of the 3 steps involved in the mechanism of formation of beads.

An additional rheological shear test at 1Hz has been made on a time-point experiment (Figure 32). Every 1 h during 6 h, a fresh scoop from the emulsion reacting in a conical tube was loaded on the rheometer. The shear viscosity signals obtained for the sample **$A_2Ca_6Si_6$** indicate that during the synthesis, the global viscosity of the emulsion is decreasing until 3 h of reaction (Figure 32 a). At this point, the shear viscosity profile

remained constant. Once again, such fact could indicate the orientation of the beads on the device's surface once they were formed. Nonetheless, for the sample **$A_0Ca_6Si_6$**, after an instantaneous shear viscosity increase; it decreases with a similar profile meaning that no different structuration is occurring in the sample during the reaction (Figure 32 b). Furthermore, the elastic modulus (G') recorded at 1Hz for each time point experiment (Figure 32 c, d) is of about 15000 Pa for **$A_2Ca_6Si_6$** and 45 000 Pa for **$A_0Ca_6Si_6$**, probably due to the presence of the alginate. The organic polymer might indeed play the role of binder not only in the early stage of the reaction (during the alginate crosslinking with Ca^{2+}), but also at later stage, during the formation of the beads (by the interaction with the aggregates of calcium silicate). However, the solid core of **$A_0Ca_6Si_6$** appears to be harder compared to the core in **$A_2Ca_6Si_6$** sample.

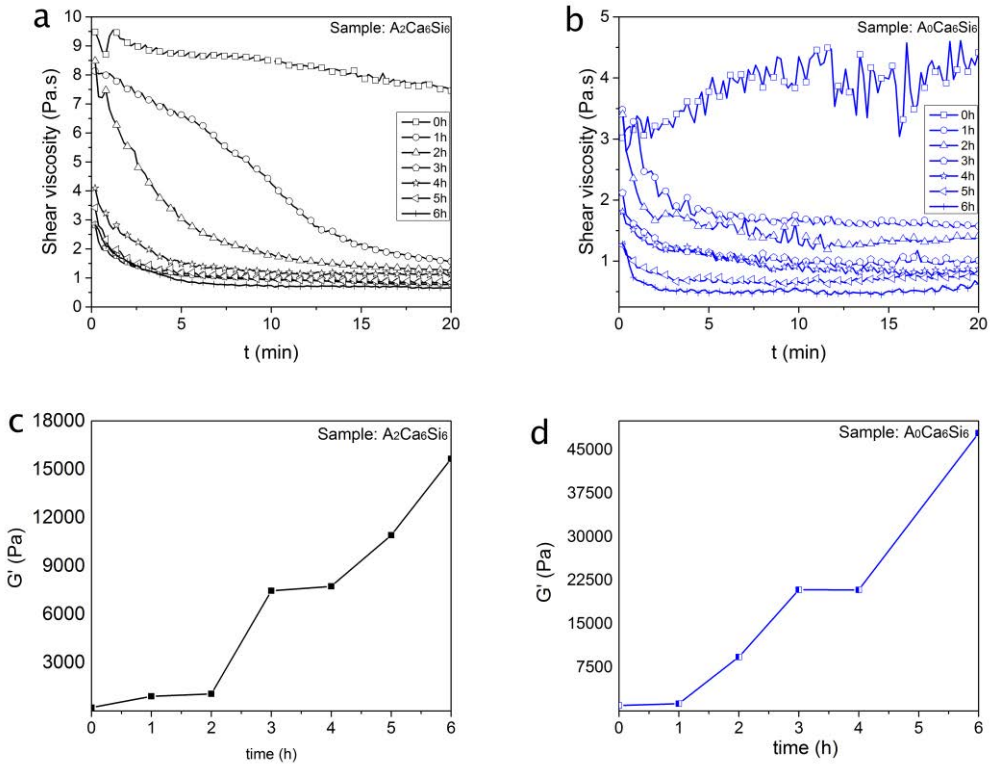

Figure 32: Shear viscosity follow-up during 20 min of 6 time-points corresponding to the six first hours of reaction for: (a) $A_2Ca_6Si_6$ and (b) $A_0Ca_6Si_6$; and G' of (c) $A_2Ca_6Si_6$ and (d) $A_0Ca_6Si_6$.

In conclusion, smooth and round beads were obtained only with **$A_1Ca_6Si_6$** and **$A_2Ca_6Si_6$**, which shown a unique profile, with three regimes. According to the rheological profiles these regimes were hypothesized to be due to: (I) the ionic crosslinking of alginate with

Ca^{2+}, followed mainly (II) by the condensation of silica and silicates aggregates (t_{agg}) and finally to (III) the strengthening of the alginate network through ionic interactions with the silicate aggregates (t_{int}).

Characterization of LGG in the W/O emulsion

The hybrid alginate-silicate material was elaborated with the ultimate goal of delivering LGG to the lower section of the intestines. The synthesis **$A_2Ca_6Si_6$** served as cargo of bacteria mainly as a result of their larger microparticles sizes, of about 18 μm, when compared to the other syntheses. Consequently, a higher density of cells fits in the volume of those carriers. Three major microscopy techniques, SEM, TEM and CLSM, were utilized not only to evaluate the presence of the cells in the interior but also on the exterior of the microbeads. On the surface of the material, we observed indeed imprints of LGG (Figure 33 A) as well as a solitary cell followed by couple of imprints (Figure 33 B).

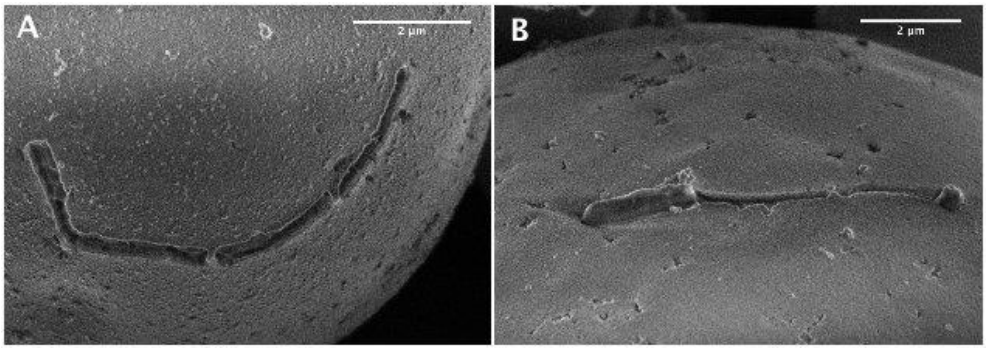

Figure 33: SEM micrographs show the surface of two beads contaning: A) imprints of LGG and B) a solitary LGG with imprints right next to it.

TEM allowed us to go deeper in the alginate-silicate matrix in order to confirm the entrapment of a larger quantity of cells (Figure 34 A, B). White spots are observed embedded within the thin bead slice and with the aid of sequential zooms, a white matter area appeared as a rod-shape, reinforcing the hypothesis of the successful encapsulation of LGG. (Figure 34 C) This bead is clearly full whereas without the addition of LGG, we often observed hollow spheres for the same bead composition.

Nonetheless, keeping a substantial amount of cells viable inside the carriers until their release in the target site is a key prerequisite for considering the developed system a

success. For such, first the disintegration of the beads was investigated in 0.01 M PBS pH 8 and 0.1 M sodium citrate pH 4.4 during 3 h and 24 h. These buffers were chosen for their potential in dissolving the alginate-silicate matrix while being gentle to the living microbeads load.

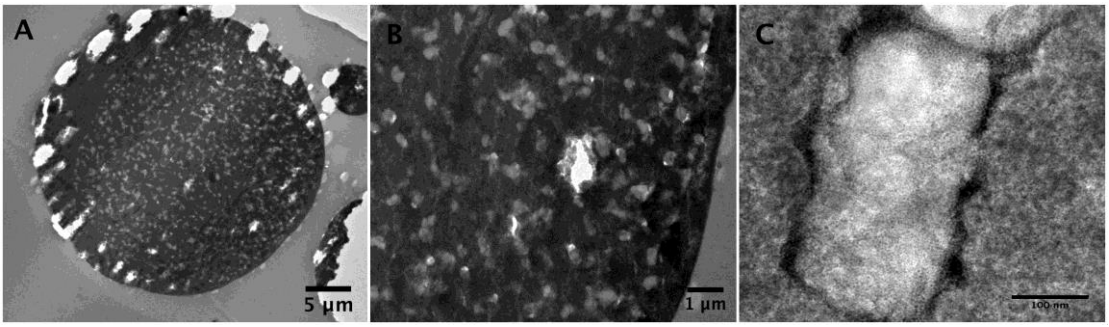

Figure 34: TEM micrographs displaying a thin-cut section of a bead: A) spherical slice of the bead, B) zoom on the slice where white spots can be noticed, C) further zoom on the slice showing a LGG surrounded by the alginate-silicate matrix.

The complete dissolution attempt failed even for a 24 h period of time stirring at 250 rpm and 37 °C as shown on Figure 35. Some fragments can be seen on Figure 35 B, yet overall the larger beads remained intact. Obtaining monodisperse materials is of importance at the degradation stage for a steady release in the intestines. Smaller beads will therefore degrade faster due to their higher surface areas.

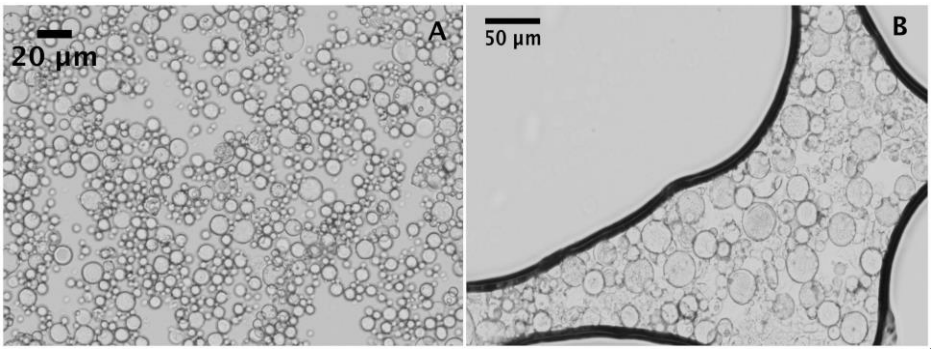

Figure 35: Optical microscopy of beads: A) before PBS or citrate treatment and B) after 24 h treatment of PBS or citrate.

Even though the beads turned out to be extremely robust, we still investigated in a second step the viability of the encapsulated LGG in the alginate-silicate matrix with the confocal technique and two fluorescent dyes, namely SYTO 9 and propidium iodide.

While SYTO 9 stains both, intact and damaged bacteria, propidium iodide can only penetrate when the bacterial cell wall is compromised, which is indicative of non-viability. Once the green, red and transmission channels are overlaid, green represents live and orange or red represent dead LGG. The encapsulation seems to be heterogeneous in these carriers with several spheres lacking any entrapment and with the propidium iodide dye marking the alginate-silicate matrix as well. Only few live bacteria are observed green-labeled on Figure 36. The arrows indicate an area where we clearly observe viable cells in distinct planes depths in the same sample area.

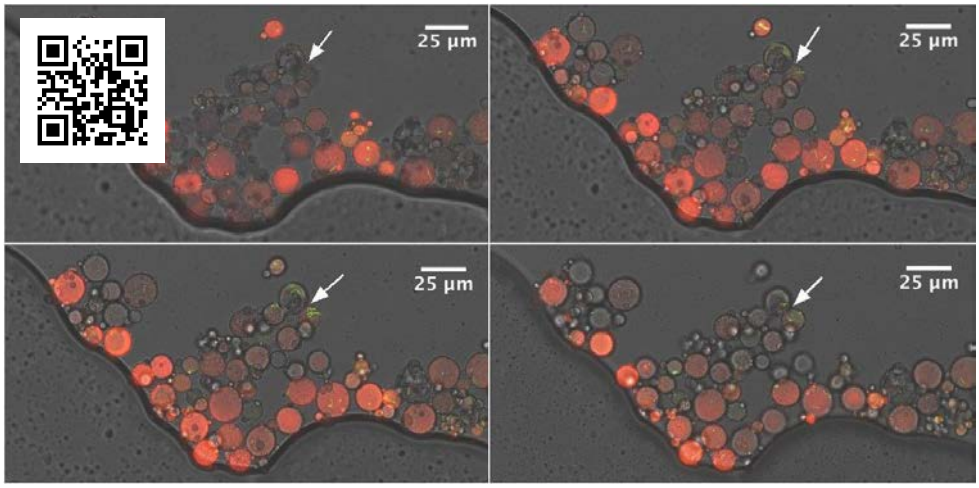

Figure 36: CLSM micrographs of four different depths of the same sample area (clockwise observation starting on barcode image). The arrows indicate green-labeled LGG. (Check the entire video online for a better examination https://www.youtube.com/watch?v=Q96WzI1t9r8 or read with a good resolution smartphone the barcode on the upper left of the above image with the 'Barcode Scanner' App).

The main reason behind the poor cell viability lies behind the incompatible basic pH of the mixture alginate/sodium silicate with this specific bacterial strain. Trials on decreasing the pH of the mixture with an ion-exchange resin were attempted in a third step. The sol-gel process happened too quickly once the pH was brought to 8.5, leaving little room for the emulsion preparation. As we had encountered obstacles in disintegrating these beads on the top of the basicity of the pH, we decided to drop the emulsion strategy.

4.1.3. Conclusions

New food compatible alginate-silicate microbeads were synthesized with a one pot simple approach. In the majority of the cases, the systems obtained are typically well-defined hybrid particles round and monodisperse. However, tuning the ratio between the different aqueous components may induce some relevant structural changes (i.e. bigger structures or broken microbeads) and definitely affect the kinetics of mineralization (inorganic silica shell) and the sol-gel process (alginate 3D matrix). Remarkably, linear rheological experiments are observed to be sensitive to the different formulations. Generally, alginate increases the viscosity of the initial reverse emulsion and apparently delays the gelification of the system (i.e. lower diffusion rate of alginate and silica precursor). On the other hand, calcium is observed to drive not only the formation of the alginate network but also tunes the final morphology of the calcium silicate shell (i.e. smooth *vs* perforated shell). Last but not least, the concentration of the silica precursor will drive the formation of robust round beads.

The evolution of the rheological properties during the sol-gel process and the final material microstructure are important features for the design of new materials. Indeed, the fairly simple reverse emulsion route presented in this study constitutes an innovative approach with potential application in different areas such as the encapsulation of, for instance, water-soluble biomolecules.

Nonetheless, the strain *L. rhamnosus* GG did not cope with the basicity of the water phases of the reserve emulsion. Using confocal microscopy and fluorescent DNA intercalating dyes, only few viable LGG were spotted in the carriers. Additionally, we were not able to disintegrate these beads under gastrointestinal pH in order to release the encapsulated load, and assess their viability with the standard plate count technique. At this stage of the study, we concluded that the material synthesized was not suitable for the encapsulation of LGG.

4.2. Encapsulation of LGG via electrospraying

4.2.1. Introduction

Core-shell electrospraying approach

The poor viability outcome of the LGG entrapped within the emulsion section drove us to a core-shell strategy utilizing the electrospraying technique. This approach minimizes the direct contact of silica with the probiotic bacteria. In this case, the LGG is encapsulated in alginate in a first step via electrospraying with further synthesis of silica onto the beads holding a mesoporous shell (Figure 37).

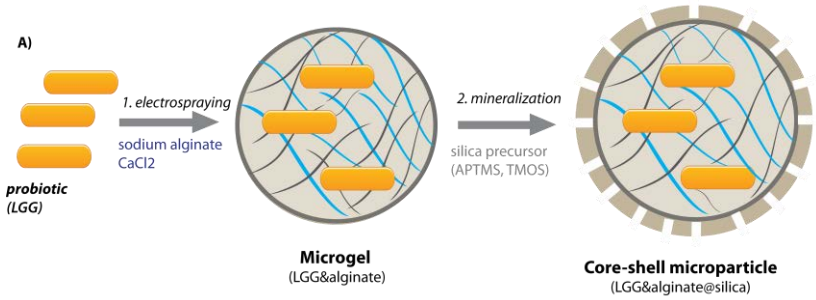

Figure 37: Schematic representation of the general procedure leading to core-shell microgels.

Alginate alone does not provide an excellent protection barrier to bacterial cells for oral delivery since it is highly porous.[22] Thus, the stomach's hydrochloric acid diffuses into the beads resulting in significant loss of the bacterial viability. The diffusion of the cells to the bead media is also a valid scenario. To overcome such flaws, silica is brought to the system due to its non-toxicity, thermal and mechanical matrix stabilities, with good biocompatibility and biodegradability already previously mentioned. The inorganic barrier limits bead swelling and, therefore active material leakage as well as water uptake. The possibility of tuning the porosity of the alginate-silica beads is another advantage of this strategy.

Electrospraying technique

Due to its straightforward feasibility, this extrusion technique has been often accessed in the encapsulation of biologically active ingredients in food systems including probiotic bacteria.[23-30] Electrospraying has been recently emerging as novel technique

in virtues of its utilization at room temperature, application of food-grade solvents and obtainment of fine monodisperse particles.[31,32] The technique relies on the application of a high potential electrical field to obtain spheres. The polymer solution containing the bacteria is extruded from a capillary where two major electrostatic forces are acting, the repulsion of like charges and the Coulombic forces of the external electrical field. At the tip of the needle, the droplet is distorted in a conical shape, and once the electrostatic forces counteract the surface tension of the bead, a charged droplet is ejected from the tip of the cone in a form of a spray.[33,34] The beads are formed once this spray touches the receiving solution containing the crosslinking agent. The Figure 38 exemplifies the setup in question.

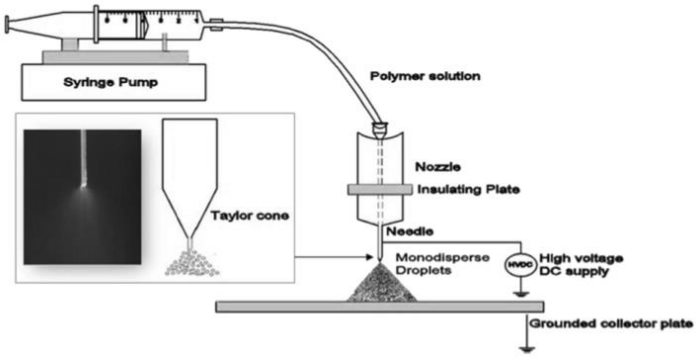

Figure 38: Electrospraying setup showing a digital image of a spray and an illustration of the Taylor cone on the insert. [33]

It is of importance to note that the ambient humidity, temperature and air velocity in the electrospraying chamber should be kept constant in order to obtain equal solvent evaporation and therefore experiment reproducibility.[33]

The optimization of the system accounts for several inter-dependent parameters and their combination influence the obtainment of a consistent spray during a desired period of time. This spray will guide the spherical formation of the particles with a narrow size distribution. The consistency in sizes is important on loading and release of the bacteria into the target site.[35-37] The distance to the collecting dish, needle diameter, voltage, flow rate, polymer molecular weight are some of the parameters influencing the final material size (Table 6).[38]

Table 6: The influence of main parameters on final bead sizes.[38]

Parameters	Increasing
Voltage	Smaller beads
Distance needle – spray collector	Larger beads
Flow rate	Larger beads
Polymer molecular weight	Larger beads
Needle diameter	Larger beads

In order to obtain potential mechanically stable porous probiotic carriers that ensure bacteria viability all the way until the intestines, we designed micrometric alginate-silica particles through this mild conditions synthesis.

Storage: cryoprotectant role

Up-to-date drying is one of the best options to keep a high cell viability in a product for a longer shelf-life, accounting for spray-, freeze-, vacuum- and fluidized bed-drying as the most common techniques used.[39] Indeed maintaining high cell viability in the carrier during storage before ingestion provides better chances of larger quantities surviving the harsh conditions of the gastrointestinal passage followed by their proliferation in the target site.

In the case of freeze-drying, the success during the dehydration process is often associated with the use of cryoprotectants. These molecules are thought to stabilize the lipid membrane and proteins by hydrogen bonds preventing denaturation and cell wall disruption.[40] Additionally, the formation of an amorphous matrix translates into lower molecular motility and therefore less chemical deterioration along with serving as a shielding barrier around the cells.[41] Ideal cryoprotectants should be food grade, permeate through the cell wall and contain non-toxic solutes. The efficacy of several chemicals as protectants has been investigated over the years. Often the outcome of these studies highlights the fact that each specific strain behaves differently in the presence of the same chemical.[42] The most common in the literature are milk proteins,[23] polyols such as glycerol[23] or sorbitol,[43] disaccharides such as lactose,[44,45] trehalose,[43-47] and sucrose.[43,45,46,48,49]

We have taken the microparticles of our best performing synthesis and we studied the impact of freeze-drying on the LGG viability. The cryoprotectant sucrose was added to alginate/LGG/HCl-tris slurry in order to enhance bacterial protection during the freeze-drying step.

Gastrointestinal assessment

A large variety of experimental protocols assessing the impact of the gastrointestinal passage exist. They can be categorized according to their representativeness for the *in vivo* gut environment and different stringency levels: gastric residence time, bile salt concentrations, fasted or fed conditions and others. Minekus *et al.* proposed a consensus batch protocol for fasted conditions[50] whereas Mainville *et al.* proposed a batch process in fed conditions.[51] A more sophisticated strategy utilizing a continuous process that simulates not only the upper gastrointestinal passage, but also the colon with a microbial community is of possibility as well. The simulator of the human intestinal microbial ecosystem (SHIME®, co-registered by Ghent University and ProDigest) is a scientifically validated dynamic model. The set-up allows an accurate control of the reactor's environmental parameters, which translates into a stable microbial community. The technology was of interest in different domains such as in nutrition studies,[52,53] in toxin production and survival of the food-born pathogen *Bacillus cereus,*[54] and in oral delivery of probiotics in chocolate.[55]

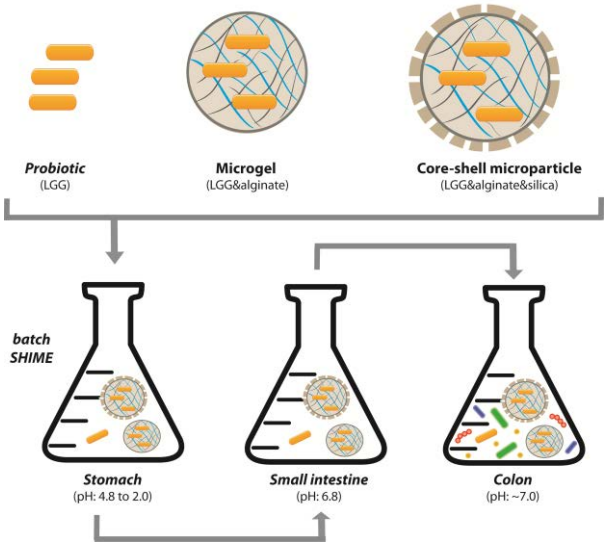

Figure 39: *In vitro* simulation of a human gastrointestinal passage considering the stomach, the small intestine and the colon containing a fecal inoculum (SHIME).

In our experiments we considered a fed batch SHIME that simulated the stomach, small intestine and colon. We investigate the behavior of 3-week freeze-dried alginate and silica-coated microcapsules in such *in vitro* model as human gut simulator (Figure 39). The main aim was to evaluate the viability of the released bacteria in the different segments of the gastrointestinal tract.

Addition of LGG carriers to beverages

Food matrices containing beneficial bacteria as probiotic delivery systems belong to one of the fastest growing markets in the world.[56] Dairy products containing these bacteria are known to dominate the market still up to date. However, the global population reality when it comes to cholesterol restricted diets, the rise of vegetarianism or more strikingly, the increase of lactose intolerance,[57,58] incites the development of non-dairy novelties. In recent times, beverages made of fruits, vegetables and cereals have been investigated for such purpose.[59]

As a proof of their potential, Tropicana®, GoodBelly®, and ProViva® are examples of companies leading the concept on the American and Swedish markets (Figure 40).

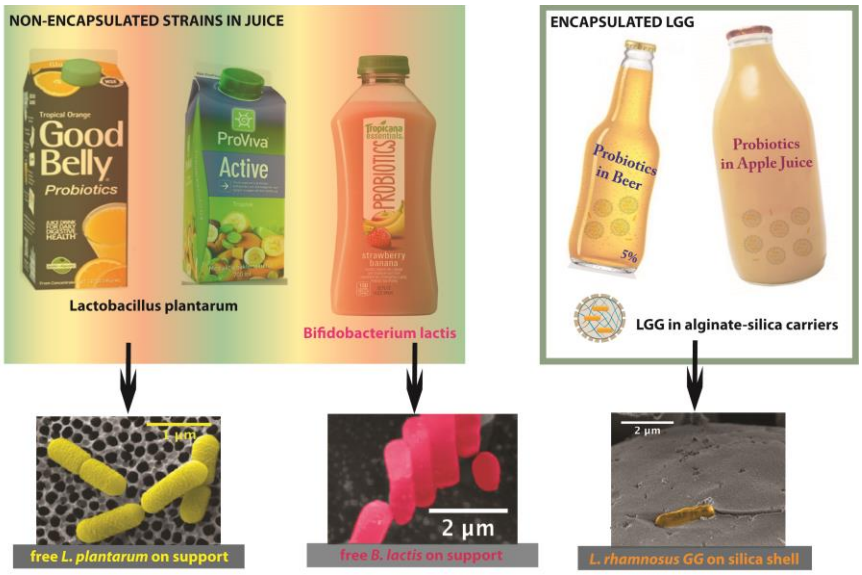

Figure 40: (left) Non-encapsulated strains (*L. plantarum and B. lactis*) present in juices sold currently on the American and Swedish markets; (right) the concept of encapsulated LGG in beer and apple juice. *L. plantarum and B. lactis* SEM micrographs were adapted.[60,61]

Fruit and vegetable juices are promising probiotic carriers due to their essential nutrients content along with their appeal to a niche of consumers who already care about healthier habits.[62] Additionally, the correlation of fruits extracts with benefits for certain health conditions reinforces their positive interest. For instance, aqueous extracts of kiwifruit and avocado have shown high anti-inflammatory activity in Crohn's disease assays. The non-aqueous extracts of both fruits along with blueberry and broccoli have shown a certain potentiality as well.[56] Another study investigated the intake of nine micronutrients, *i.e.* vitamin E, calcium, folate, retinol, β-carotene, riboflavin, pantothenic acid, biotin and nicotin acid, on genome damage and repair.[63] These compounds are often present in fruits and vegetables, fact that emphasizes the idea of coupling juices with probiotics. The challenge can be still considerable since bacteriocins and low pH are main factors affecting bacteria survivability in the case of fruits or vegetables.

On a rather unusual tone, beer could also be a food matrix of interest for probiotic delivery. As a popular beverage consumed worldwide, it opens up the probiotic consumption to a wider public. The studies on beer as a probiotic carrier are scarce however, with the main reason lying on the eventual detrimental effects of the alcohol on the bacterial strains.[64]

The ultimate focus of this section of our studies was to investigate the viability of free and encapsulated LGG in alginate and silica-coated carriers after 3 h and one-week in apple juice and beer with a 5 vt% of alcohol content.

4.2.2. Results and discussion

Electrospraying parameters *vs* bead sizes

As a first screening assessment, we changed specific parameters on the electrospraying setup and we observed how the alginate beads behaved in terms of size and shape. The increase in voltage allows a decrease in the beads diameters in about 200 μm when working with a non-autoclaved 1 wt% alginate solution (Figure 41 A *vs* B). The decrease in concentration of the same non-autoclaved alginate solution from 1 wt% to 0.5 wt% while keeping the voltage constant decreases abruptly the beads sizes in around 400

µm (Figure 41 A *vs* C). The sterilization of the alginate solution is however mandatory in our case since beads will be loaded next with bacteria and contamination must be avoided. Therefore we tested 1 wt% and 0.5 wt% of alginate solutions containing the polymer autoclaved at a voltage of 7.5 kV. The concentration of 1 wt% formed beads of about 220 µm whereas 0.5 wt% did not form round beads, instead the polymer agglomerated on the surface of the crosslinking solution. Figure 41 D shows the size outcomes when the 1 wt% alginate solution is autoclaved and bacterial cells are present in the slurry.

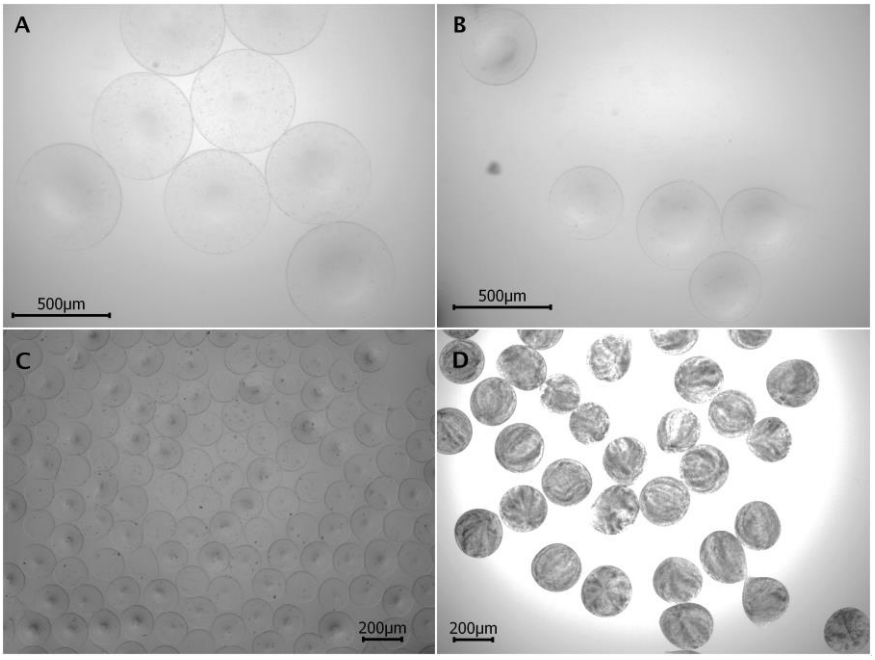

Figure 41: Changing electrospraying parameters. A) 1 wt% alginate non-autoclaved & 7.5 kV voltage, B) 1 wt% alginate non-autoclaved & 12 kV, C) 0.5 wt% alginate non-autoclaved & 7.5 kV voltage, D) 1 wt% alginate autoclaved, 7.5 kV voltage & beads containing LGG.

The autoclave step may affect the length of the alginate polymer due to the temperature treatment (121 °C, 15 min). Both, shorter polymer chains and the introduction of the bacteria load, affect the final viscosity of the solution before electrospraying. We fixed its concentration at 1 wt% with prior sterilization of the polymer powder, and the voltage at 7.5 kV for all the experiments conducted along this thesis work.

Synthesis of core-shell microparticles encapsulating LGG

In a typical procedure, core-shell microparticles were obtained in a two steps synthesis (Figure 42). In the first step, the LGG/sodium alginate slurry was electrosprayed over a calcium bath leading to alginate microgels (Figure 42 B and Figure 43 A). In a second step, the microgels were dispersed in an organic or an aqueous solution containing a surfactant, PGPR or Tween 40, respectively (Figure 42 C). As a function of the alginate core media (water (w) or Tris buffer (tris)) and the mineralization media (organic (org) or aqueous (aq)) the core-shell (CS) particles were labeled C_wS_{org}, $C_{tris}S_{org}$, C_wS_{aq}, $C_{tris}S_{aq}$ respectively.

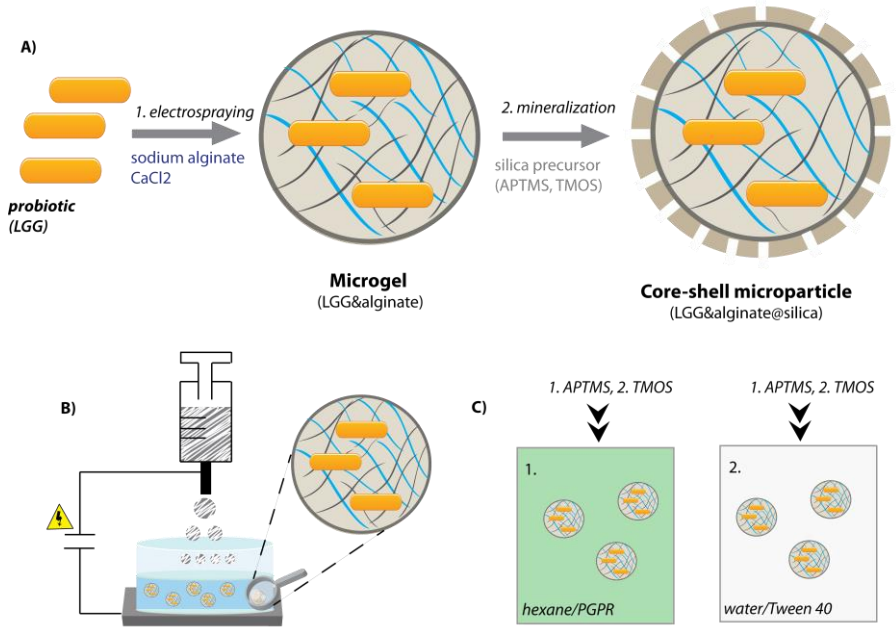

Figure 42: Schematic representation of the general procedure leading to core-shell microgels (A); cartoon of electrospray setup leading to ionogels (B) and organic (C1) and aqueous (C2) mineralization media of microgels.

The silica precursors were added to those dispersions sequentially. First, the APTMS was added under vortex stirring and it was allowed to react for 1 min in order to form a first layer around the microgel through electrostatic interactions between ammonium groups of APTMS and carboxylate groups of the alginate. To complete the coating of the beads, TMOS was added in sequence, and it was allowed to react for another 1 min. The hydrolysis of both precursors and their co-condensation resulted in core-shell microparticles (Figure 43 B)

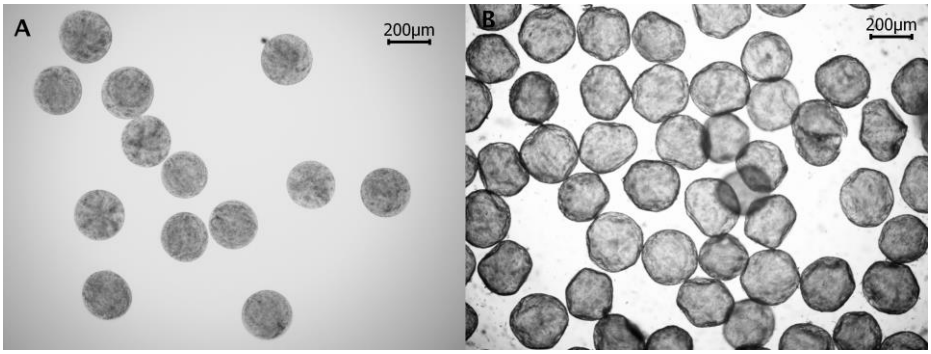

Figure 43: A) Optical microscopy micrograph of wet LGG&alginate beads recovered by ionogelation of the electrosprayed polymeric solution containing the bacteria and, B) of wet core-shell LGG&alginate@silica microparticles.

The sizes of the resulting beads did not significantly depend on the reaction media, aqueous or organic (C_wS_{org}-$C_{tris}S_{org}$ *vs* C_wS_{aq}-$C_{tris}S_{aq}$, Figure 44), or on the presence of the HCl-tris buffer ($C_{tris}S_{org}$, $C_{tris}S_{aq}$) or water (C_wS_{org}, C_wS_{aq}) in the alginate microgels. The size of the wet alginate beads is of about 220 ± 15 µm whereas wet core-shell beads is of about 230 ± 10 µm, as it was determined from the imageJ analysis of the optical microscopy micrographs (Table 7). The shell thickness of about 8 µm is slightly thinner when the mineralization takes place in aqueous media compared to organic media, when the silica is of about 13 µm thick, considering the alginate prepared with water. This effect was expected since the mineralization happens only around the hydrated alginate beads in the organic media, but all over the bulk of the aqueous media.

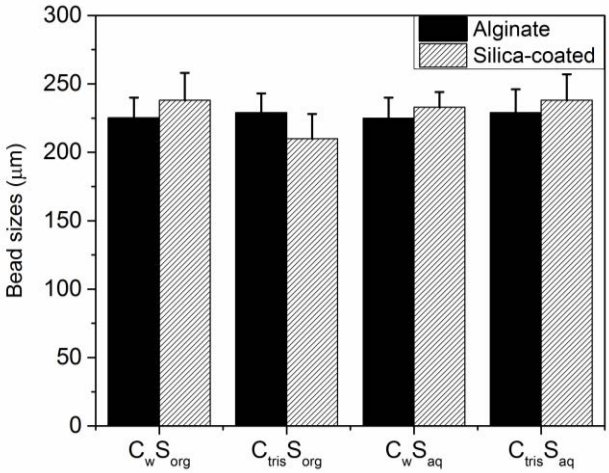

Figure 44: Size distribution of the alginate beads and silica-coated alginate beads for the samples C_wS_{org}/$C_{tris}S_{org}$ (in organic media) and C_wS_{aq}/$C_{tris}S_{aq}$ (in aqueous media).

Table 7: Sizes of alginate before and after coating for organic and aqueous medias. The sizes of the beads correspond to an average of 300 beads for 3 individual experiments.

SYSTEMS	Alginate (H_2O)	Alginate (HCl-tris)	C_wS_{org}	$C_{tris}S_{org}$	C_wS_{aq}	$C_{tris}S_{aq}$
Average sizes (µm)	225 ± 15	229 ± 14	238 ± 20	210 ± 18	233 ± 11	238 ± 19

To gather further insights in the morphology and the structure of the materials, SEM measurements were performed onto lyophilized, dried beads. Uncoated alginate beads completely lose their round shape after freeze-drying (Figure 45 A). In the meantime, the bacterial cells are observed underneath the alginate network confirming their entrapment (Figure 45 B). All silica-coated alginate beads are monodisperse and maintain well better their round shape than the uncoated polymer beads, as it can be seen on Figures 45 C and 45 D for C_wS_{org} sample. Moreover, on Figures 45 E and 45 F, one can clearly see the core-shell structure of the microparticle and the porous network of the inner polymeric core (insert in Figure 45 E). On image 45 G, one can observe the shell thickness of about 3.5 µm for the synthesis C_wS_{aq}. It is relevant to observe that the shell size of about 8 µm represents an average of 300 beads whereas this image illustrates a shell part of a single bead only. We can therefore expect different thicknesses within beads. Interestingly, on image 45 H, one can observe the grainy and porous structure of the silica shell of the C_wS_{aq}. SEM analysis also allowed the observation of two types of bacterial encapsulation, in the inner alginate core and encrusted in the silica shell (Figure 45 I, J).

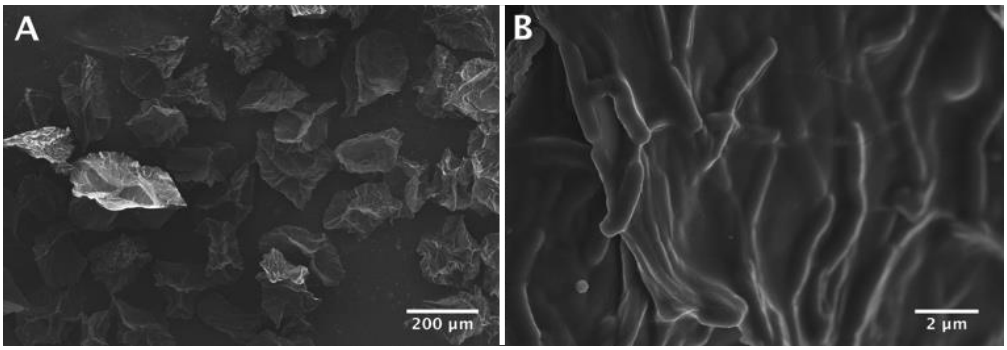

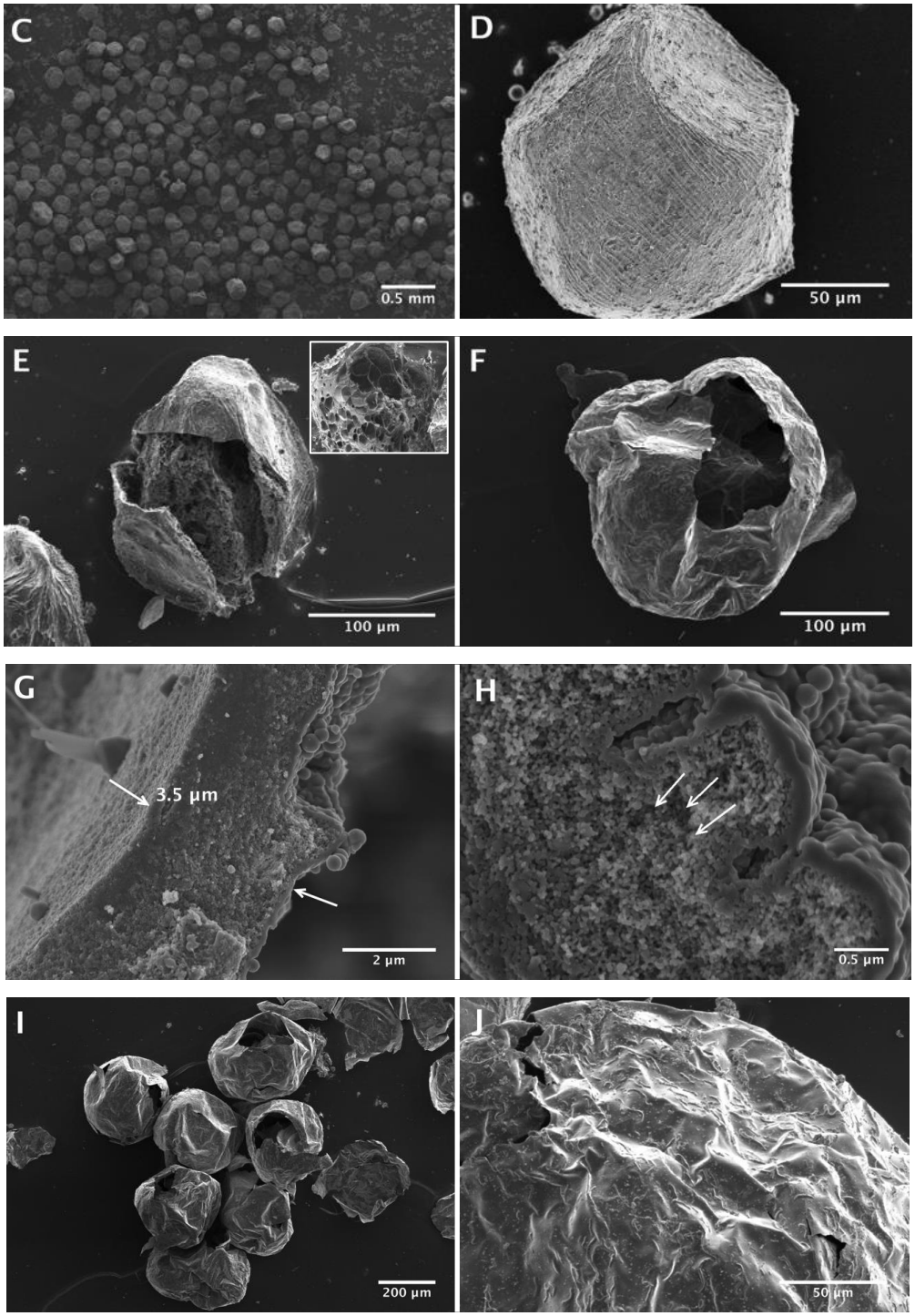

Figure 45: SEM micrographs of freeze dried LGG&alginate beads (A, B) and of wet core-shell LGG&alginate@silica microparticles C_wS_{org} (C, D), $C_{tris}S_{org}$ (E), $C_{tris}S_{aq}$ (F), C_wS_{aq} (G, H); $C_{tris}S_{aq}$ (I, J).

The silica shell is formed through the hydrolysis/condensation of APTMS and TMOS precursors, following a mechanism already described in the literature.[65] The positively charged amino group of APTMS will interact electrostatically with the carboxylates of

the outer part of the alginate bead (Figure 46). Locally the pH will rise due to amino groups bearing a pKa of about 9 favoring the condensation process. Once TMOS is added to the system, hydrolysis of this precursor will follow with co-condensation of APTMS and TMOS at the locally higher pH.

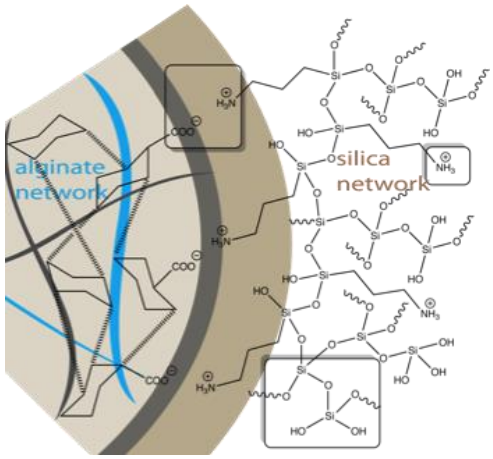

Figure 46: Scheme of the condensed silica shell on the alginate bead.

The presence of silica was also confirmed by FT-IR measurements. All core-shell microparticles present the characteristics peaks at 1612 and 1410 cm^{-1} (COO^- asymmetric and symmetric stretching) of alginate along with 1090 cm^{-1} (Si-O-Si bond) and 950 cm^{-1} (Si-OH) (Figure 47).[66-68]

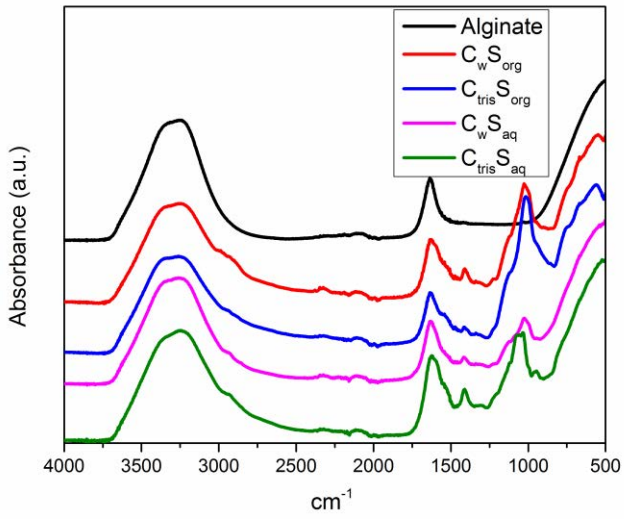

Figure 47: FT-IR spectra of alginate beads and of silica coated alginate beads confirming both the presence of alginate in the core-shell beads (ν_{COO^-} = 1410, 1612 cm^{-1}) and of silica (δ_{Si-O} 990-1100 cm^{-1}).

Beads disintegration media

The silica coating of the alginate beads should provide an extra protection to the bacterial cells reducing cell leakage. Yet, the coating needs to disintegrate at intestinal pH in order to release the encapsulated cells that will further colonize the gut. Nine and four different disintegration media were tested with silica-coated beads and alginate beads of about 500 μm, respectively. Their fragmentation was followed by naked eye (Table 8).

Table 8: The observation of fragmentation of silica-coated alginate beads and alginate beads of around 500 μm.

Media	Silica coated?	Disintegration time	Overall observations
0.9 wt% NaCl	YES	< 2h	No swelling.
Phosphate Buffer pH 8 containing 0.9 wt% NaCl	YES	4h	Beads swell in a short period after in contact with buffer
Tris-HCl Buffer pH 8 containing 0.9 wt% NaCl	YES	5h	No swelling
Tris-HCl Buffer pH 8	YES	>24h	No swelling
Phosphate Buffer pH 8	YES	>6h	Eventually it disintegrates completely
Citrate Buffer pH 5	YES	-	It never disintegrates totally since only the alginate dismantles and the coating remains
Citrate Buffer pH 5 containing 0.9 wt% NaCl	YES	>72h	Beads disintegrate over few days
HCl pH 3	YES	-	Beads shrink in size but never disintegrate completely
HCl pH 3 containing 0.9 wt% NaCl	YES	>72h	Beads shrink at first, but did disintegrate
0.9 wt% NaCl	NO	<15min	No swelling
Phosphate Buffer pH:8 containing 0.9 wt% NaCl	NO	<15min	Some swelling
Tris-HCl Buffer pH:8 containing 0.9 wt% NaCl	NO	<15min	No swelling
Citrate Buffer pH:5	NO	<15min	No swelling

The uncoated alginate beads disintegrated in all four media in less than 15 min. Alginate holds a carboxyl group on every sugar unit of its linear polymer chain, which are linked electrostatically one to another once di- or trivalent cations are present in the solution. The network is dismantled once, for instance, alkali metals are present in the same solution. The Ca^{2+} ions of the network undergo ion exchange with the Na^{+} cations present in the disintegration media. Bajpai *et al.* observed as well the swelling of alginate beads in phosphate buffer pH 7.4 and not in tris-HCl buffer pH 7.4 [69]. When the Ca^{2+} ions are replaced by the Na^{+} ions, the network relaxes and water uptake happens. It is plausible to assume that due to steric effects, the phosphate from the buffer media will occupy a larger space within the alginate bead than the Cl^{-} from the NaCl media, and therefore, swelling occurs in presence of phosphate buffers.

The most efficient disintegration media for silica-coated alginate beads is 0.9 wt% NaCl, a so-called isotonic solution for cells. As previously discussed in the state-of-the-art, the presence of alkali and alkaline earth cations enhance silica demineralization, which is attributed to outer- and inner-sphere type interactions between these ions and silica. The latter interaction reflects on a redistribution of the electron density caused by the binding of a Na^{+} or Ca^{2+} to the bridging oxygen on the silica surface leading to local electron depletion. The weaker Si-O bond becomes more susceptible to the attack of a water molecule.[70] In our experiments, an autoclaved 0.9 wt% NaCl solution was thus chosen to disintegrate the alginate or silica-coated beads when assessment of bacteria viability via plate counting was necessary.

Viability of encapsulated LGG in wet carriers

A major goal of the present study is to develop a method to encapsulate viable LGG cells and to ensure viability throughout and after encapsulation. Two techniques were at this stage used to evaluate the cell viability: (i) by count plating the released bacteria from the disintegrated beads and (ii) by staining with confocal fluorescence microscopy.

The viability dramatically decreased upon coating in organic media (6.0×10^{1} CFU mL^{-1} for C_wS_{org} and 3.0×10^{5} CFU mL^{-1} for $C_{tris}S_{org}$). This fact could be due to detrimental effects of the hexane and/or the methanol release causing cell death (Figure 48). Note that methanol is hydrophilic and it will preferentially diffuse to the core of the bead.

Additionally, organic solvents can be very toxic to microbial cells even in very low concentrations such as 0.1 vt% since they cause changes to the cell membrane affecting not only its structure but also its functionality.[10,71-74] To avoid both phenomena, mineralization of the alginate beads was undertaken in an aqueous solution. The viability of LGG increased to reach the values of the control LGG&alginate beads in the case of $C_{tris}S_{aq}$ (4.1×10^8 CFU mL^{-1}). It is noteworthy to mention that the number of cultivable bacteria cells in silica-coated beads (sample $C_{tris}S_{aq}$) was found to be not significantly different from that in alginate beads, which means we were able to keep an excellent bacteria viability during the coating step.

It should be also observed that the presence of the buffer (HCl-tris, pH 8) had a positive effect on the survivability of the microbial cells. Less of a log cycle improvement in the LGG viability was observed for the materials synthesized in aqueous media (Figure 48, C_wS_{aq} *vs* $C_{tris}S_{aq}$) compared to a 4-log cycles improvement on the bacteria viability for the materials synthesized in organic media (Figure 48, C_wS_{org} *vs* $C_{tris}S_{org}$).

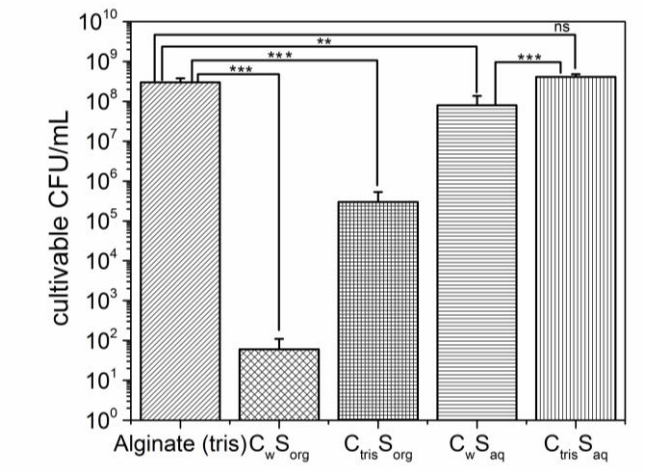

Figure 48: LGG viability studies in different synthesis conditions. The results are expressed as the average of three independent experiments. Error bars indicate standard deviations. Error bars indicate standard deviations. Comparisons were done between all pairs of columns. **p<0.01, *** p<0.001 and ns stands for not significant difference.

Indeed, by buffering the aqueous core of the alginate beads, one might counteract the increase of the local pH otherwise caused by the formation of aminopropylsilane during

the synthesis of the silica shell, which is detrimental to the cells. When abrupt changes in pH happen within the bacteria surroundings, they use community strategies to keep thriving, *e.g. L. bulgaricus* forms clumps when the pH goes beyond 8.5 due to the failing out of certain enzymes that chop off the rod shaped chains.[75] Besides, the buffering capacity of the alginate core balances out its pH when the viable entrapped bacteria secrete lactic acid.

The classical microbiological plate count technique allows us to determine the colony-forming units (CFU) and thus, to quantitatively access the number remained cultivable. The disintegration time and conditions might have a detrimental effect on the viability of the cells. Therefore, the confocal laser scanning microscopy (CLSM) technique along with a staining technique previously mentioned based on fluorescent dyes, SYTO 9 (green) and propidium iodide (red) was used to confirm qualitatively the plate count results (Figure 49 A, B, C, D).

The positive impact on the viability of LGG after the addition of Tris-HCl at pH 8 to the alginate slurry is clear when observing the images 49 A and 49 B. More than 90 % of the bacteria remained viable in the electrosprayed alginate bead with the buffer (Figure 49 B). We can affirm at this stage that the voltage applied during the electrospraying process imposes a negligible detrimental effect on the cells. However, when we access the viability after synthesizing the silica coating, then the impact of such step turns out to be of great importance. For instance, less than 10 % survived in organic conditions after coating (Figure 49 D). Interestingly, in aqueous mineralization conditions, the encapsulation rate of the bacteria appears lower than in pure alginate beads or in coated alginate beads in organic media. Nevertheless, a large fraction of the bacteria keeps its integrity and appears green (Figure 49 C). The cracks in the inorganic shell may afford an escape route for the cells before imaging. A detailed discussion on beads defects takes place in following pages.

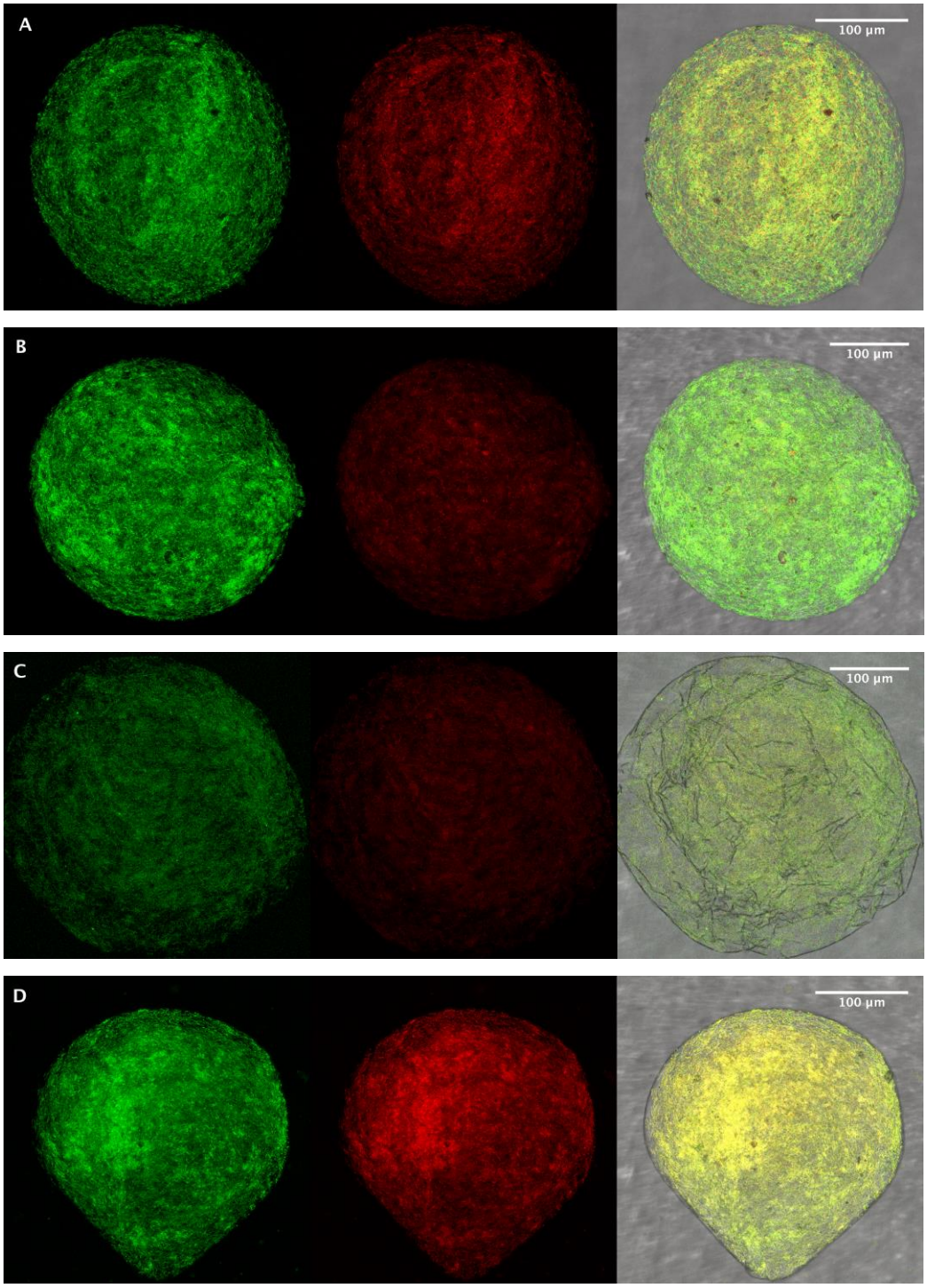

Figure 49: CLSM micrographs of A) Alginate bead in water; B) Alginate bead in HCl-tris buffer pH 8; C) Coated alginate bead in aqueous solution containing Tween 40; D) Coated alginate bead in organic solution containing PGPR.

Proliferation of encapsulated LGG in wet carriers

One challenging topic in bacterial growth is to control the proliferation in a restricted area or compartment. This is advantageous in avoiding contamination by other

biological agents or in ensuring the presence of an adequate concentration of confined microorganisms for a defined application. In the latter case, the silica shell was designed to be mesoporous allowing nutrient-metabolite diffusion in and out of the polymeric core containing the probiotics. Mesoporous silica materials are often prepared through the cooperative templating mechanism of a micellar phase of a surfactant along with a silica precursor. Our group already synthesized mesoporous silica capsules through a dual templating mechanism combining a Tween type surfactant and solid lipid nanoparticles as macrocavities templates.[11,76,77] In the case of Tween 40, the mesopores size is of about 5 nm and the material has a wormlike structure. In the present study, we used two biocompatible porogens, PGPR for the mineralization in organic media and Tween 40 for the mineralization in aqueous solution. Combined scanning and transmission electron microscopy analysis of the core-shell materials synthesized in the presence of Tween 40 showed that the surface have an inter-particular and an intra-particular mesoporosity (Figure 50).

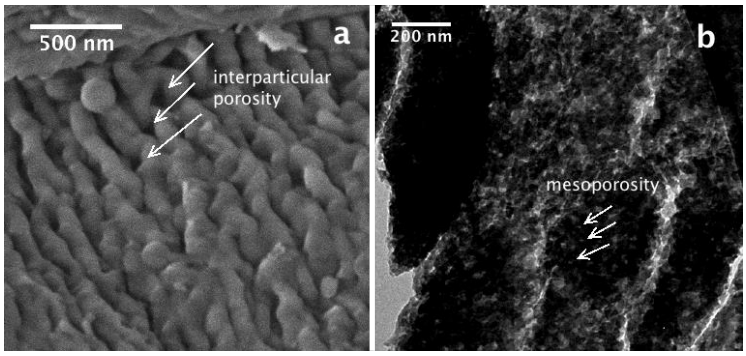

Figure 50: a) SEM and b) TEM micrographs of the silica-coated alginate beads obtained in aqueous media with Tween 40 as porogens ($C_{tris}S_{aq}$).

The inter-particular porosity (less than 50 nm) is associated with the voids between the silica grains and is dramatically decreased in the absence of the surfactant. It should also be noted that the grains have disordered mesopores of about 10 nm, when Tween 40 is used. No mesopores were observed within the silica grains in the absence of surfactants (Figure 51). The inter- and intra-particular porosity is small enough to prevent probiotic leakage, and to allow nutriments and metabolites diffusion through the shell capsule, insuring thus bacteria proliferation inside beads. To observe such fact, coated and uncoated alginate beads were left for 60 h in MRS broth.

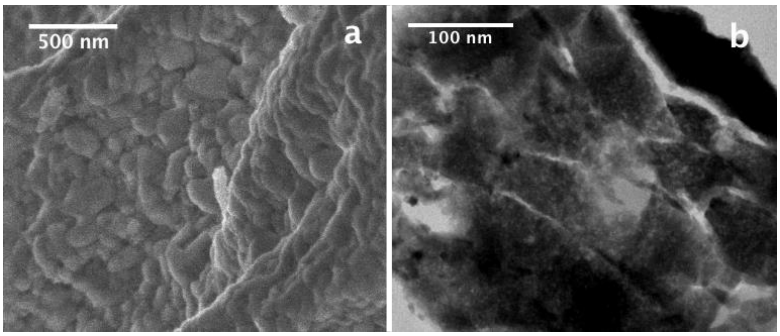

Figure 51: a) SEM and b) TEM micrographs of the coated alginate beads obtained in aqueous media in the absence of surfactants.

The bacterial growth proliferation was not observed in the uncoated alginate beads due to their completely disintegration in less than 1 h. This effect is most likely due to the presence of the salts in the broth that are competing with the complexation of the Ca^{2+}/carboxylate couple. Interestingly, MRS was not able of dismantling the silica-coated alginate beads and the confocal images confirmed the successful proliferation of the cells under confinement (Figure 52 A, B). For example, when comparing the CLSM micrographs of the core-shell capsules $C_{tris}S_{aq}$ before and after exposure to the MRS broth for 60 h (Figure 52 A), it can be clearly seen an increase on the density of the living bacteria. Only restricted areas within the polymeric core remained similar to the one of the untreated beads, indicating that some dead bacteria were still present inside capsules.

Additionally, the MRS broth pH dropped from 6.0 to 4.4 and ended with 3.9 at time zero (silica-coated beads freshly added to broth), time 24 h (first MRS broth replacement) and time 48 h (second MRS broth replacement), respectively. Indeed the metabolism of these bacteria was functional. The presence of dead bacteria is even more pronounced within the edge of the silica shell, where the red-labeled bacteria are predominant (Figure 52 A, B right). This differentiation between dead and live bacteria on the shell and in the core is accentuated in the case of materials obtained by mineralization in organic media when compared to aqueous solution containing Tween as porogen (Figure 52 B right). By keeping an appropriate addition of nutrients, the number of green-labeled bacteria dramatically increased. On the contrary, the bacteria entrapped within the silica shell were all dead, and appear red in the CLSM micrographs.

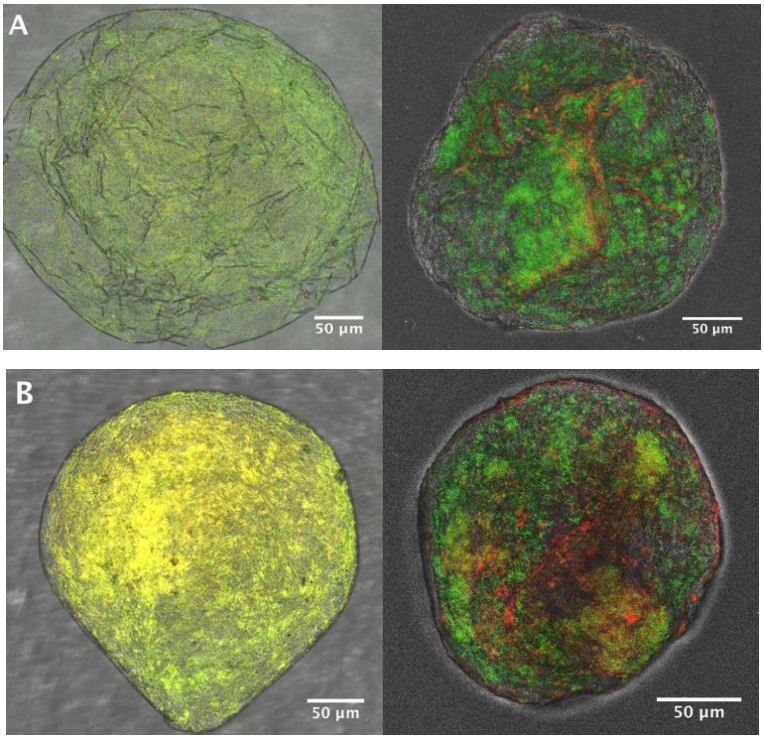

Figure 52: CLSM micrographs of A) left: Coated alginate bead in aqueous media, right: Coated alginate bead in aqueous media after 60 h in MRS broth. B) left: Coated alginate bead in organic media, right: coated alginate bead in organic media after 60 h in MRS broth.

The strategy of encapsulating bacterial cells in hybrid core-shell systems enhances the variety of strains possible of being kept under confinement since these microorganisms remain in a near-natural environment with nutriments-metabolites diffusion through mesopores while entrapped. To the best of our knowledge, probiotic bacteria embedded in mesoporous silica particles, as food delivery systems, were not previously reported. Growth of cells in these conditions was assessed for eukaryotic cells,[78] fungi,[79] *Bacillus subtilis* spores[80] and *Bacillus coagulans*.

Cryoprotectant role on freeze-dried alginate-silica carriers

Core-shell microparticles were prepared in a second step with an addition of 10 wt% sucrose into the alginate/HCl-tris electrospraying slurry. The beads were recovered in the same way from a calcium chloride bath. The resulting microgels, of about 500 µm, were about twice as big as without sucrose, probably due to the increased viscosity of

the electrosprayed mixture in the presence of the cryoprotectant (Figure 53). Indeed, the electrospraying technique is very much sensitive to viscosity and surface tension.[33] In the second step of the synthesis, the microgels were dispersed only in an aqueous solution containing Tween 40 followed by the sequential addition of APTMS and TMOS.

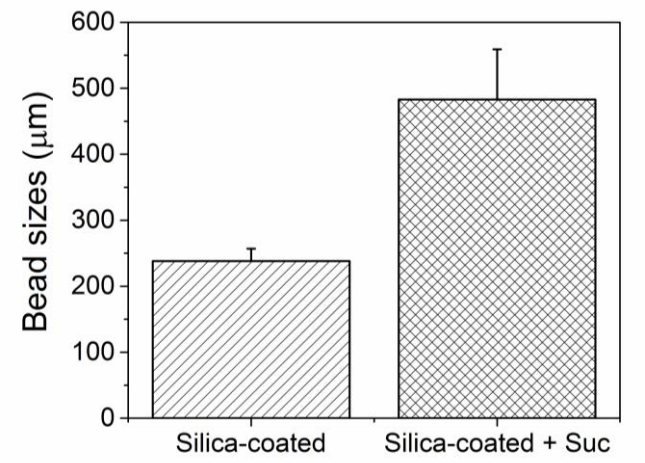

Figure 53: Wet silica-coated beads sizes comparison without and with sucrose. The average accounts for of 300 beads for 3 individual experiments. Labels: Suc: sucrose.

In terms of the morphology, as in the previous section, a rather shrunk and rough surface is observed for the alginate bead (Figure 54 A, C) and smoother surface for the silica-coated bead (Figure 54 B, D). Additionally, a large amount of LGG was spotted entrapped in the alginate/sucrose network (Figure 54 E) while only few LGG were on the silica shell (Figure 54 F). Sucrose did not affect the overall morphology of the alginate beads (Figure 55 A, B) whereas more rounded silica-coated alginate beads are obtained when the cryoprotectant is present (Figure 55 C, D).

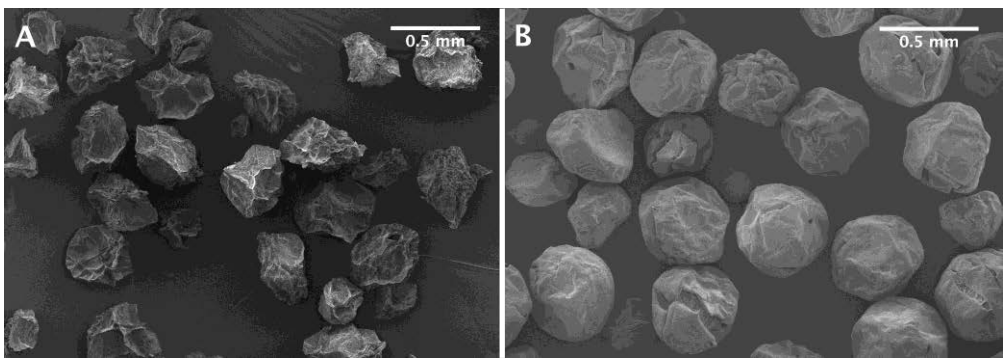

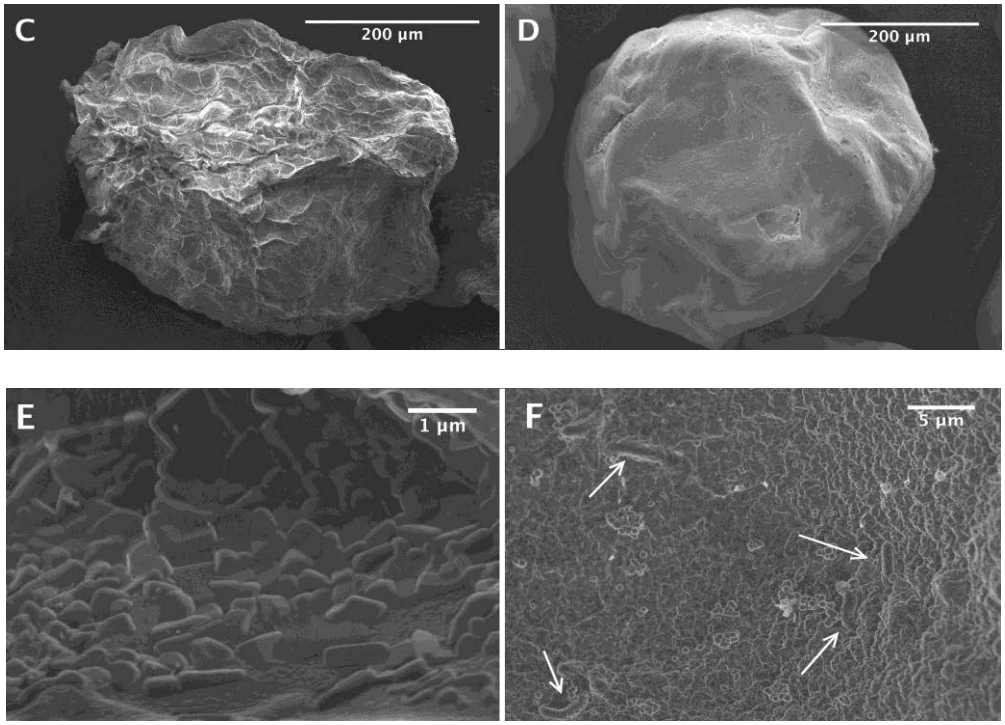

Figure 54: SEM micrographs of: Alginate bead (A, C, E), Silica-coated alginate beads (B, D, F), LGG entrapped within alginate/sucrose network (E) and on the surface of the silica shell (F).

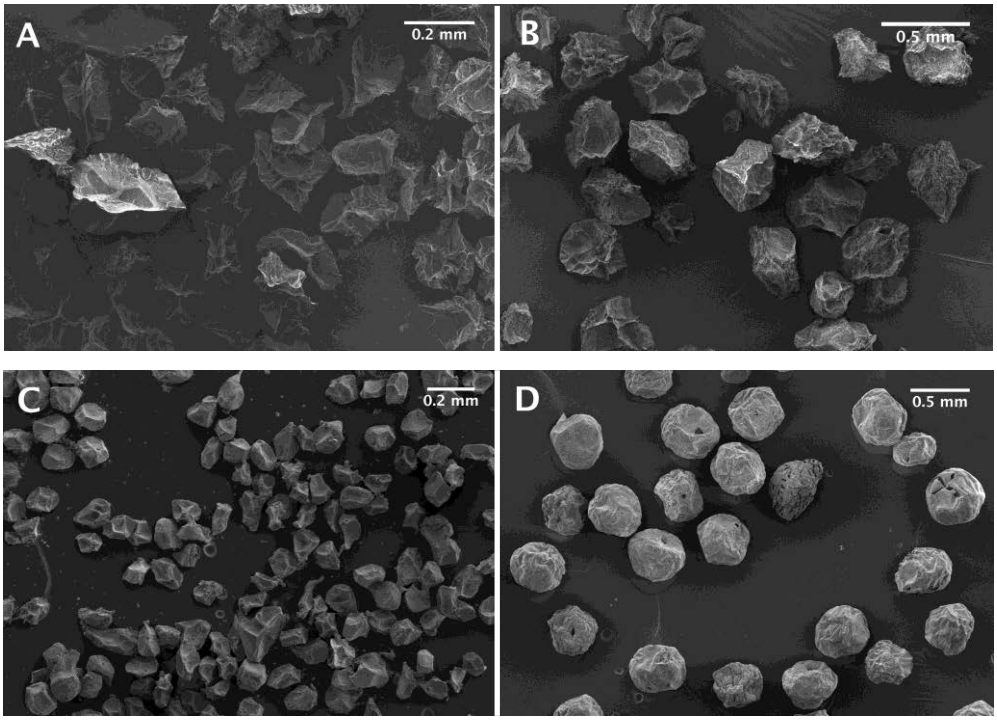

Figure 55: SEM micrographs showing the morphology of the materials: Alginate beads without sucrose (A) and with sucrose (B); silica-coated beads without sucrose (C) and with sucrose (D).

The presence of defects on the silica-coated beads was investigated as well. We observed fractures of few µm in size on the coating (Figure 56 A, B). When zooming on the fractures, bacteria were spotted as well as NaCl and/or $CaCl_2$ crystals (Figure 56 C, D). The fractures may well come from the impact of freeze-drying on weak points of the coating. Before loading the beads into the freeze-drying device, they are plunged in liquid nitrogen at a temperature of – 196°C, where they remain for at least 5 min. The temperature shock can undoubtedly lead to abrupt ruptures in the inorganic network. The presence of salt crystals within the fractures was not a surprise. Calcium chloride is used to form the alginate beads themselves while sodium chloride is used to rinse off the beads from extra calcium chloride after the formation of the alginate beads, or from extra silica precursors and Tween 40 after the silica synthesis. One of the hypotheses on the release of the LGG from these carriers is drawn around the fractures, additionally to the inner- and outer-sphere types of interactions between certain ions and silica, previously discussed.

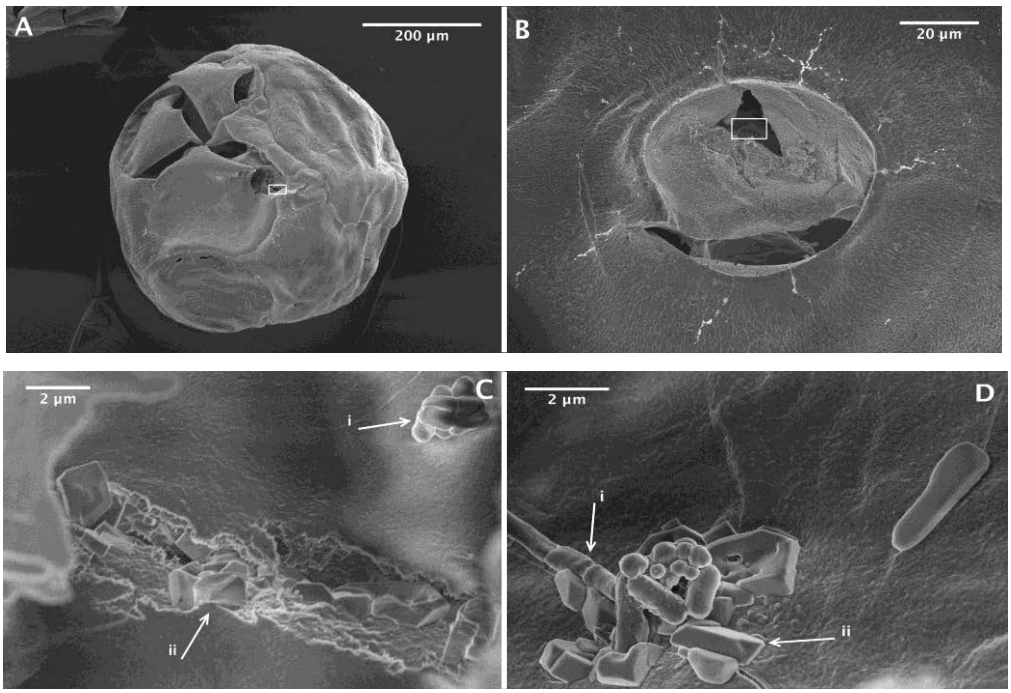

Figure 56: SEM micrographs showing defects of a silica-coated bead (A, B, C, D). C is a zoom on the square of image A, and D is a zoom on the square of image B. Bacteria (i) and salt crystals (ii) were spotted in the splits.

Viability of encapsulated and freeze-dried LGG

The viability of LGG was assessed by the standard plate count and aliquots of the disintegrated beads containing LGG were kept overnight at 35 °C before serial dilutions and plating. In a first step we investigated essentially the influence of the sucrose in keeping a high viability in the carriers after freeze-drying since a loss of about 10^5 CFU mL^{-1}, from 4.1×10^8 CFU mL^{-1} to 3.1×10^3 CFU mL^{-1}, after performing the freeze-dying step was observed (silica-coated *vs* silica-coated FD, Figure 57). The addition of sucrose as cryoprotectant bounced the viability of the synthesis back to 3.2×10^8 CFU mL^{-1} (silica-coated FD + Suc, Figure 57). This disaccharide was already reported in the literature as a good LGG cryoprotectant candidate. Siaterlis *et al.* obtained 80% survivability when adding 10 wt% sucrose[43] while Ananta *et al.* observed one log reduction.[81]

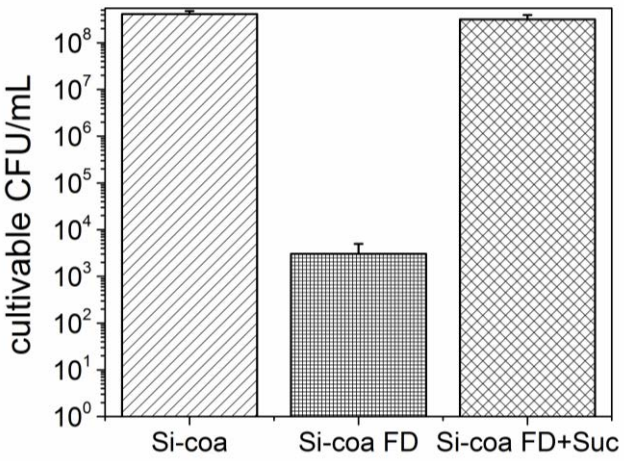

Figure 57: Freeze-drying impact on the viability of LGG in the silica-coated alginate beads without and with sucrose. The results are expressed as an average of 3 individual experiments. Labels: Si-coa: Silica-coated, FD: freeze-dried, Suc: sucrose.

In a second step, we assessed the actual viability of cultivable bacterial cells within these carriers. For such, LGG was released and subsequently plated. A clear maintance of the bacteria viability in the alginate and silica-coated carriers from t=0 to t=3 weeks was therefore followed (Figure 58). Before the drying process, alginate and silica-coated retained the same concetration of viable LGG, *i.e.* 1.0×10^7 CFU mL^{-1} (4.8×10^{10} CFU g^{-1}). Once dried, silica-coated lost one log of cultivability, 1.0×10^6 CFU mL^{-1} (5.8×10^9 CFU g^{-1}) while the cultivability of bacteria embedded in alginate beads remained intact.

After 3 weeks of lyophilization and keeping the powders at room temperature, alginate ended up with 6.2×10^6 CFU mL^{-1} (3.4×10^{10} CFU g^{-1}) and silica-coated 7.4×10^4 CFU mL^{-1} (4.1×10^8 CFU g^{-1}). Even with such decrease, the viability of encapsulated bacteria into the silica-coated carrier is in line with total cell count of products momentarily in the market ($\geq 1.0 \times 10^9$ CFU g^{-1}, Winclove 505 Adult).

The loss in viability from the LGG encapsulated in the silica-coated is also related to the fact that non-cultivable bacteria are not accessed with the plate counting technique. It is important to note that non-cultivable bacteria may become cultivable again since this trait is not only a characteristic of a damaged strain. In other words, our viability values are underestimated. Indeed, on the gastrointestinal release section of the manuscript, more details on the metabolism activity of the LGG after being released from alginate beads and silica-coated are discussed, and LGG coming from the silica-coated material is mostly inactive at this stage.

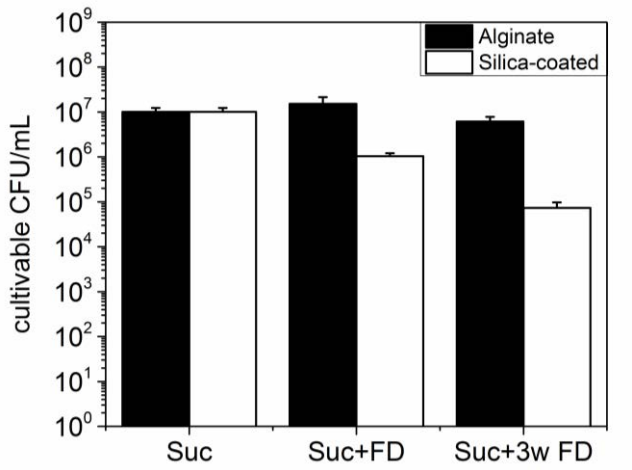

Figure 58: Effective viability of LGG in the carriers before, right after and after 3-weeks of freeze-drying. Labels: Suc: sucrose, FD: freeze-dried, 3w: 3 weeks.

LGG viability and metabolism activity during gastrointestinal passage

The release of 3-week freeze-dried carriers was monitored every hour during the gastric and small intestine phases. Silica-coated beads were more efficient in protecting the bacteria during the gastric phase, keeping the viability as high as 3.5×10^6 and 2.0×10^6 CFU mL^{-1} in the first (pH 3.5) and second hours (pH 2.0), respectively (Figure 59, left). In the case of alginate beads, in the first hour of gastric digestion, we observed

more damaged cells than intact cells, *i.e.* 2.1×10^6 CFU mL^{-1} vs 7.3×10^4 CFU mL^{-1}, respectively (Figure 59, right and left). On the other hand, free cells performed well in the first hour, but an abrupt drop in viability from 8.3×10^6 to 3.3×10^4 CFU mL^{-1} followed when pH reached 2.0 whereas the coated carriers protected LGG viability during the first two hours (Figure 59, left). In the case of our better performing system, the silica shell may not only decrease HCl diffusion to the interior of the beads, but we can also consider that the cells are less impacted by the low pH since they have their metabolism excessively slowed down at the stomach and small intestine stages. This hypothesis was confirmed with the observation of LGG proliferation during the residence time in the small intestine, but not for silica-coated (Figure 60, left).

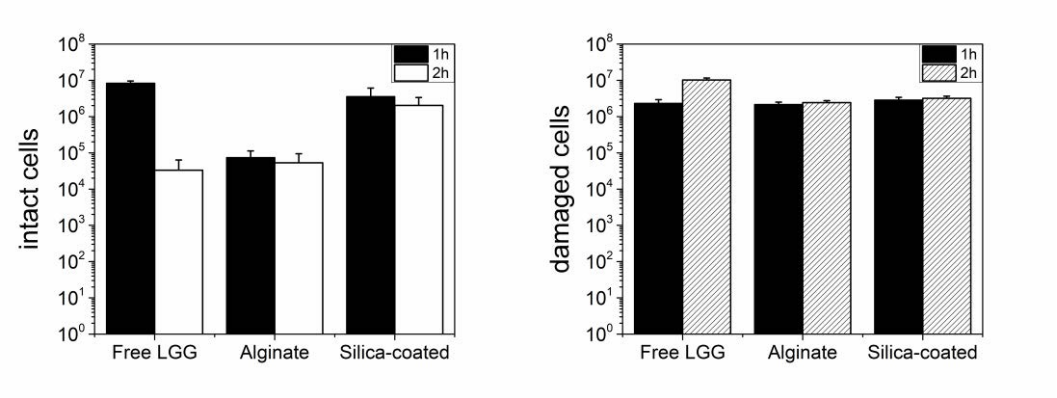

Figure 59: LGG viability during the 2 h of gastric passage: (left) intact LGG, (right) damaged LGG. All error bars represent an average of 3 individual experiments.

In order to assess information on the metabolism of the encapsulated cells, lactate measurements were performed after the 3 h of residence time in the small intestine. We observed that the LGG encapsulated in the silica-coated material produced a minor quantity of lactate, 12 mg L^{-1}, while free LGG and alginate beads produced 80 and 87 mg L^{-1} respectively (Figure 60, right). We therefore conclude that the majority of the bacteria are dormant and their metabolism is mostly inactive in the inorganic carrier. The LGG may shut down its metabolism due to the release of methanol and increase of the pH during the silica shell synthesis. The cells need a longer time and an optimal media to become active again when compared to the LGG encapsulated in alginate only. Indeed we observed LGG proliferation in the silica-coated beads after adding them to MRS for 60 h at room temperature as already discussed.

As a matter of fact, it is of importance to highlight the possibility of obtaining the total viable cells with flow cytometry and not only the cultivable cells as obtained with plate counts. Using the latter technique, we obtained an initial concentration count of 7.4×10^4 CFU mL^{-1} for the 3-weeks freeze-dried silica-coated material. Nevertheless, a release of at least a 100-fold was observed in the 1 h hour of stomach residence time for the same carrier (Figure 59, left).

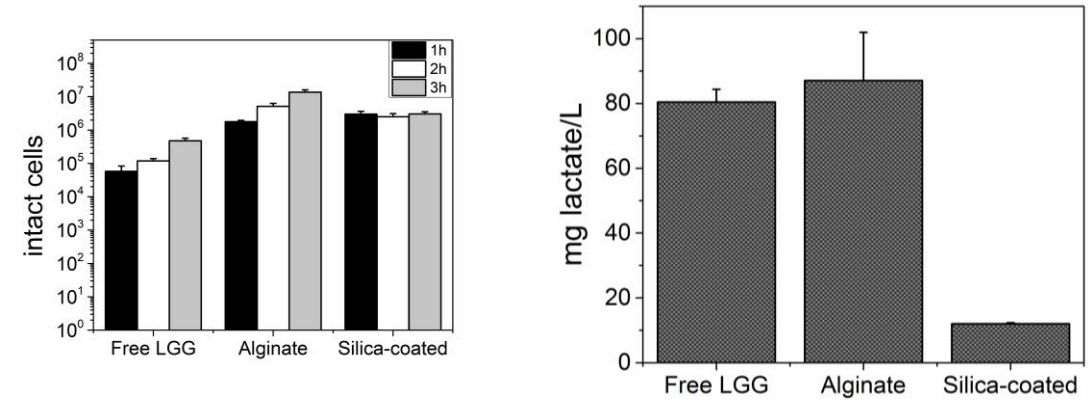

Figure 60: LGG viability during the 3 h of small intestine passage and its metabolism response: (left) intact LGG during the passage, (right) Lactate measurements after the 3 h of residence time. All error bars represent an average of 3 individual experiments.

Capacity of LGG to colonize the colon

The capacity of the LGG to get released from the carriers, keep its functionality and perpetuate in a fecal ecosystem are key factors for considering a successful encapsulation process. A fingerprint on the presence of Lactobacilli in the colon was evaluated with a *Lactobacillus*-specific DGGE and followed by its quantification with qPCR. A DGGE profile typically leaves a signature with each DNA band corresponding to a separate bacterial species. An upper and a lower bright band appear on the DGGE gel for all three samples (Figure 61). Sanger sequencing revealed the lower band to correspond with the LGG strain. Interestingly, the upper band disappeared from the 24 h timepoint in the case of the silica-coated carrier while the lower DNA band corresponding with LGG maintained its intensity (Figure 61, arrows). This fact indicates that LGG increases its abundance compared to other *Lactobacillus* species in the community and that it was able to thrive within the ecosystem in a 24 h time period. LGG is indeed known to be able to adhere to epithelial cells due to their hair-like

appendages known as pili that favors gut colonization,[82,83] yet mucus or epithelial surfaces were not incorporated in our setup. In our case, the colonization was due to a successful competition with the fecal microbiota.

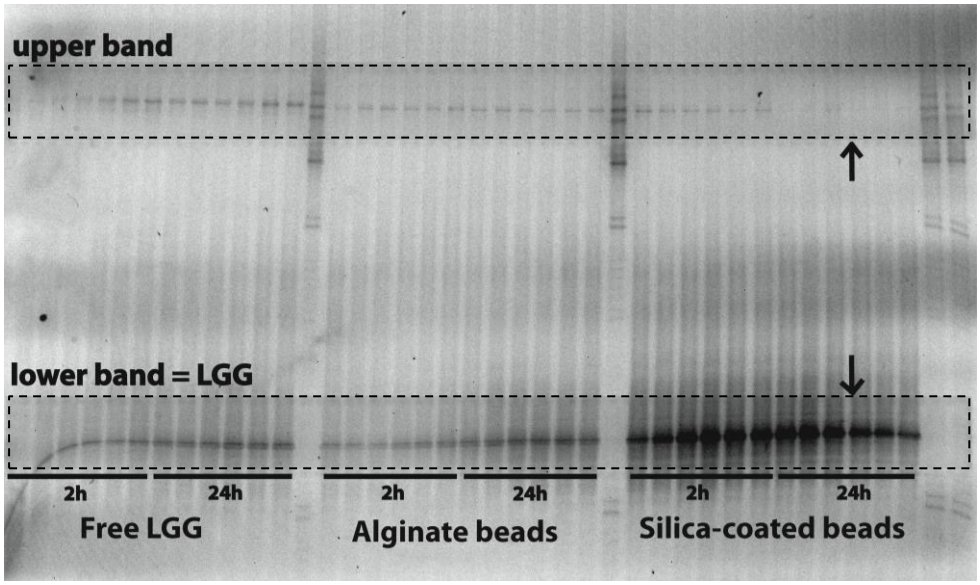

Figure 61: DGGE fingerprint of Lactobacilli.

Additionally, qPCR confirms the increase of Lactobacilli from point 2 h to 24 h and the increment is larger for both encapsulated systems (Figure 62). At timepoint 2 h, Lactobacilli represented 0.15 % and 0.08 % in the whole community of bacteria in the case of alginate and silica-coated, respectively. These values rose to 0.69 % and 0.42 % after 24 h, respectively.

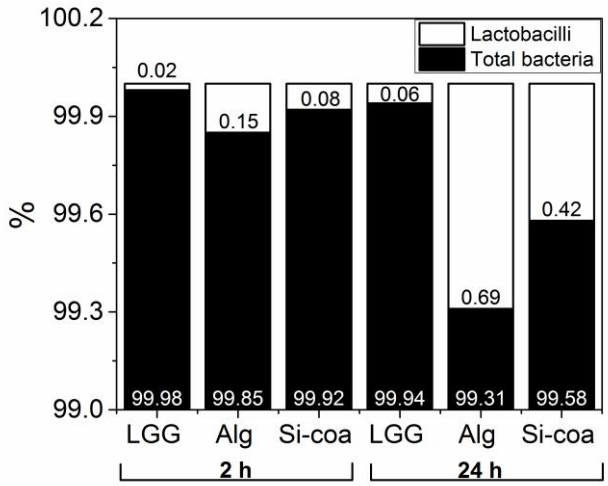

Figure 62: qPCR % evolution of Lactobacilli at 2 h and 24 h in the colon. Labels represent: LGG: free LGG, Alg: Alginate and Si-coa: Silica-coated.

In resume, total bacteria decreased from 6.3×10^7 to 3.2×10^7 whereas Lactobacilli increased from 9.4×10^4 to 2.2×10^5 DNA copies/µL for the alginate carriers. The total bacteria decreased from 1.1×10^8 to 6.0×10^7 whereas Lactobacilli increased from 8.4×10^4 to 2.5×10^5 DNA copies/µL for the silica-coated carriers. The total bacteria and Lactobacilli of the control (Free LGG) decrease however from 7.5×10^7 to 2.4×10^7 DNA copies/µL and 1.8×10^4 to 1.4×10^4 DNA copies/µL, respectively (Table 9).

Table 9: DNA copies/µL for all timepoints of total bacteria and lactobacilli. Legend represents LGG: free LGG, Alg: Alginate bead and Si-Coa: Silica-coated bead, Std error: Standard error (the replicates considered are 6 in all cases expect for the Lactobacilli Alg 2 h and Alg 24 h with only 5).

	Total Bacteria*	Std error*	Lactobacilli*	Std error*
LGG a	7.5×10^7	3.7×10^6	1.8×10^4	1.2×10^3
LGG b	2.4×10^7	8.2×10^5	1.4×10^4	1.2×10^3
Alg a	6.3×10^7	4.5×10^6	9.4×10^4	1.4×10^4
Alg b	3.2×10^7	1.7×10^6	2.2×10^5	2.2×10^4
Si-Coa a	1.1×10^8	6.6×10^6	8.4×10^4	9.7×10^3
Si-Coa b	6.0×10^7	1.1×10^6	2.5×10^5	2.9×10^4

a: 2h, b: 24h, *DNA copies/µL

LGG release in apple juice and beer

Keeping the cells viable during the storage of food matrices will enhance the acceptance of these products holding a probiotic label by the regulating organizations, likewise will be their commercialization. In our study, we chose to get insights on the behaviour of our both carriers, alginate and silica-coated, once in apple juice or in beer. Remarkably, free freeze-dried LGG (the control) maintained high viability after one week in apple juice (pH: 3.6). As it was observed via plate counting, less than one-log viability loss was observed after one-week storage in apple juice (5.2×10^6 to 1.7×10^6 CFU mL^{-1}) The viability of free LGG in beer (pH: 4.6) has resulted in a slightly greater loss, from 5.2×10^6 to 7.3×10^5 CFU mL^{-1} after one week storage (Figure 63). It was not a surprise that the acid-tolerant LGG thrived within one-week in apple juice and to some extent in beer. It is known that sub-lethal stresses such as temperature shocks induce the adaptation of strains to changing environments via induction of specific genes synthesis and stress-responsive proteins.[84,85] In our case, a cell pellet containing no cryoprotectant was

plunged in liquid nitrogen for around 5 min before a 20 h freeze-drying cycle. In the following stage, the carbon sources present in the matrix of apple juice and beer allow the more resistant LGG to readily harvest energy for their metabolism re-launching step.

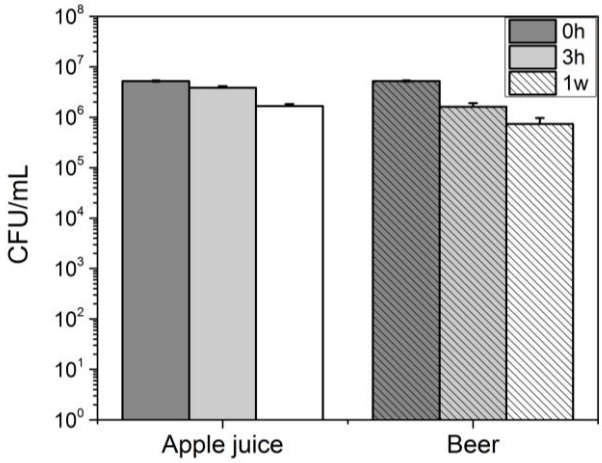

Figure 63: Viability of free freeze-dried LGG in 3 h and one-week in apple juice and beer with a 5 vt% alcohol content.

On another important tone, our investigations showed that free LGG lost 100-fold in cultivability after a 2 h of gastric passage whereas it maintained its viability, *i.e.* 10^6 CFU mL^{-1}, when encapsulated in alginate-silica beads. Coghetto *et al.* obtained similar results with a decrease of 5-logs and 2 logs for free and encapsulated *L. plantarum* BL011 respectively.[86] Overall significant differences between free state and encapsulated bacteria for a variety of strains are often described in the literature.[2,87-94]

Microencapsulation has potential to boost the survivability of the cells during storage in beverage matrices in like manner. Ying *et al.* microencapsulated LGG in matrices of whey protein and resistant starch.[95] The carriers containing LGG were added to apple juice and citrate buffer and the cells viability was investigated in a 5-weeks period. One-log was the loss in LGG viability after one-week in apple juice at 4 °C whereas bacteria proliferation was observed under storage at 25 °C. It is noteworthy to highlight that the studies of these researchers and ours started with the same freeze-dried LGG strain, which were however obtained from different suppliers (Valio Ltd *vs* BCCM culture bank). Additionally, the bacteria culture was not handled in the same way and different juice brands were selected in both studies, and spray-drying encapsulation was utilized

in their case. Both studies confirm however that free freeze-dried LGG is a robust acid-tolerant strain when it comes to delivery apple juice. In the case of the investigations of Sheehan *et al.*, free LGG was supplemented in orange (pH: 3.6) and pineapple (pH: 3.4) juices. The acid robustness of the LGG strain in both beverages was reconfirmed where no loss was observed in orange juice and a narrow loss in pineapple juice during one-week at 4 °C.[96] Another very large study enclosing fourteen encapsulation systems for *Lactobacillus plantarum* and *Bifidobacterium longum* was investigated by Nualkaekul *et al.* during a 6-week period at 4 °C in pomegranate (pH: 3.1) and cranberry (pH: 2.7) juices.[97] The strain-dependency on media acidity is elegantly detected in this work. In pomegranate juice, free *L. plantarum* lost one-log and *B. longum* four-logs during one-week of refrigerated storage. On the contrary, both strains vanished completely in the same one-week in cranberry juice, in which the pH decreased only in 0.4 pH units, *i.e.* 3.1 to 2.7. The importance of encapsulation was also investigated in the same study. When the strains were confined in alginate, *L. plantarum* decreased in viability, but four-logs were still viable after the 6-weeks storage while *B. longum* disappeared after five weeks in pomegranate juice. The harsher pH condition of cranberry juice imposed a colossal impact in viability for both strains. Overall *L. plantarum* coped better in pomegranate juice for all encapsulating systems.

In the case of beer, to the best of our knowledge, no study was done with LGG to date. Sohrabvandi *et al.* studied the viability of *Lactobacillus acidophilus* La-5 and *Bifidobacterium lactis* Bb-12 in freshly brewed beer holding 2.5 vt% and less than 0.5 vt% of alcohol content for a period of 20 days at 5°C. The work pointed out two-logs loss in viability in only 5-days of storage for La-5 in beer with 2.5 vt%. Bb-12 also lost more than one-log in the same period of time and conditions. The viability losses for both bacterial strains during the 20-days storage were more gradual in beer containing 0.5 vt% of alcohol in comparison to 2.5 vt%, but results were still declared insufficient in terms of final viability. La-5 maintained 6.0 log CFU mL^{-1} in 0.5 vt% beer whereas only 3.6 log CFU mL^{-1} of viable counts were observed in 2.5 vt% beer after 20 days of refrigerated storage.[64] The authors concluded therefore that beer is not a suitable food matrix to delivery probiotics. We believe such statement needs further examination since results are fiercely dependent on strain type, prior bacteria handling or even the use or not of bacterial cells under confinement.

Along these lines, we added alginate and silica-coated beads to apple juice and 5 vt% beer and we followed the release of LGG from the carriers after 3 h and one-week of residence time in each beverage. Additionally, we investigated the amount of bacteria that remained confined inside the carriers. Silica-coated beads diminish the leak of bacteria into the filtrate when compared to alginate beads (Figure 64). After one-week residence time of silica-coated beads in apple juice and beer, the filtrate contained only 1.0×10^2 and 2.7×10^2 CFU mL^{-1} cells respectively. In the case of alginate beads, the values in the filtrate increased a 100-fold in apple juice and a 10-fold in beer after the same one-week.

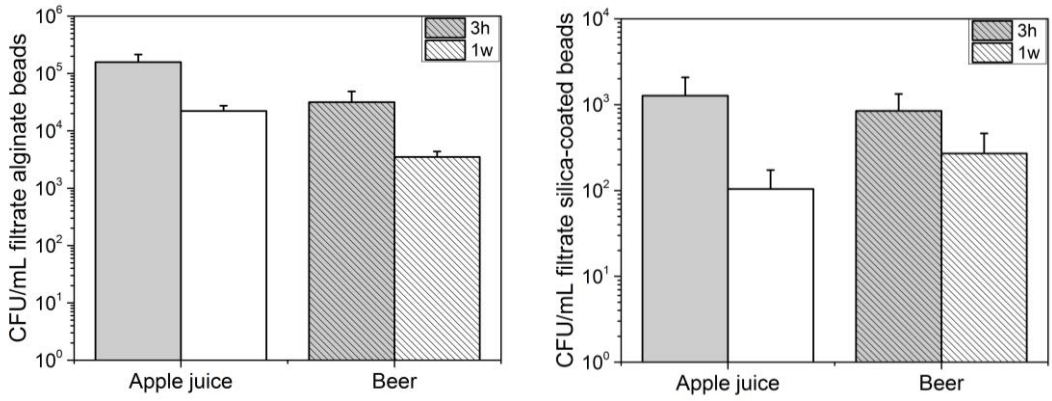

Figure 64: Viability of LGG released in the filtrate after 3 h and one-week in apple juice and beer (5 vt% alcohol): (left) in alginate beads, (right) silica-coated beads.

The viability of the bacteria inside the carriers was investigated as well after 3 h and one-week of residence time. Indeed, the bacteria in alginate beads had an abrupt decrease in viability after only 3 h in beer with almost two-logs loss whereas less than one-log was impacted in apple juice (Figure 65, left). The porosity of the alginate matrix may explain the higher diffusion of ethanol within the beads. In the case of silica-coated beads, although there was one-log loss in beer from 3 h to one-week, there was in contrast two-logs loss in apple juice (Figure 65, right). In this case, it seems that silica-coated protects better the bacterial cells in beer than in apple juice. This could be due to the fact that as these cells were in contact with methanol during the silica synthesis, they adapted to a harsh alcoholic environment and consequently could better perform when ethanol was present in the system.

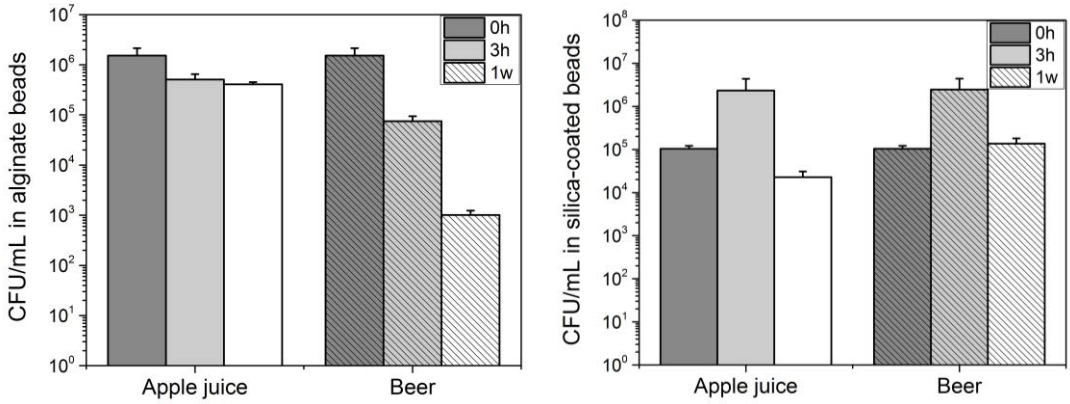

Figure 65: Viability of LGG remained in the beads after 3 h and one-week in apple juice and beer (5 vt% alcohol): (left) in alginate beads, (right) silica-coated beads.

4.2.3. Conclusions

Wet synthesis of LGG alginate-silica carriers

Core-shell alginate-silica microcapsules embedding LGG were synthesized by coating the electrosprayed ionogel with a silica shell via hydrolysis/condensation of alkoxysilane precursors APTMS and TMOS. The viability of encapsulated LGG was enhanced when the inner core was buffered (HCl-tris, pH 8) compared to water. The viability of LGG was also higher in the microparticles mineralized in aqueous solution *vs* organic phase containing hexane. Notably, the mesoporosity (<50 nm) of the silica shell prevents cell leakage and allows nutriment-metabolite diffusion to additionally insure bacterial growth inside the microcapsules. In conclusion, these wet alginate and silica-coated beads show potential as carriers of probiotics.

Dry storage of LGG alginate-silica carriers

LGG was encapsulated into both alginate and alginate-silica microbeads of about 500 µm using electrospraying and sol-gel coating, respectively. Formulating microparticles with sucrose as cryoprotectant allowed maintaining bacteria viability and cultivability upon freeze-drying for weeks, as determined by plate counting. The standard technique of plate counting underestimates the counts of viable bacteria however. Such assessment only accounts for cultivable bacteria although viable bacteria could be non-cultivable, yet become cultivable again in a next stage when the media or environment conditions allow them to do so. After the freeze-drying, round and smooth beads were

observed for the beads with the silica coating whereas rough and shrunk beads were observed for the alginate beads. Additionally, fractures in the range of μm were observed on the silica coating most likely due to a freezing temperature shock during the freeze-drying step.

Overall our freeze-dried carriers are promising when having them compared to current products on the market. The product Winclove 505 Adult holds at least 1.0×10^9 CFU g^{-1} in a sachet containing 3 g. Our alginate and silica-coated carriers contain at least 8.4×10^{10} CFU g^{-1} and 5.8×10^9 CFU g^{-1}, respectively.

LGG release in the SHIME gut model

Our study elegantly points out the possibility of using silica to reinforce the protection of encapsulated LGG in alginate. The viability of released bacteria was evaluated in an *in vitro* batch SHIME model (simulator of the human intestinal microbial ecosystem) by denaturing gradient gel electrophoresis (DGGE) and quantitative PCR (qPCR). It was revealed that microencapsulation efficiently protect LGG from the low gastric pH, especially in the case of silica-coated beads. Both encapsulation systems (alginate and alginate-silica) allowed for a better colonization of the colon compared with free LGG. Interestingly, metabolically inactive in GIT, LGG released from silica coated beads boost their metabolism once in colon, where they out compete the community of other *Lactobacillus*. In view of these results, we show that silica, usually used as anti-caking agent in food powders, can play an active role in probiotics delivery and colon colonization. However, the LGG functionality once in the colon should be still investigated in order to confirm its probiotic benefit at the target site.

LGG release in apple juice and beer

Maintaining probiotic viability in food matrices before consumption is key, and it remains a challenge for the successful delivery of the cells into the intestines. Food carriers such as fruit juices and beer increase the challenge imposed to the cells as a result of their acidity and alcohol content. Interestingly our study shows that free freeze-dried LGG is able to maintain a high viability, from 5.2×10^6 to 1.7×10^6 CFU mL^{-1}, in apple juice for an entire week at 4 °C. In the case of beer, the loss was slightly

greater, from 5.2×10^6 to 7.3×10^5 CFU mL^{-1}, yet surprising that the 5 vt% alcohol content of the beer did not impose a harder poisoning on the bacterial cells. Globally, encapsulation boosts the protection of the cells during storage and in a second step during the gastrointestinal passage. Opposing prior allegation, we conclude that beer could be a suitable matrix for probiotics delivery. In silica-coated beads, a cultivability of 2.5×10^6 CFU mL^{-1} and 1.4×10^5 CFU mL^{-1} after 3 h and one-week was observed in 5 vt% beer, respectively. A 300-fold load could reach the target site when drinking a single 30 cl glass of beer. In like manner is apple juice considered a suitable food matrix.

4.3. REFERENCES

1 S. Pandey, K. Senthilguru, K. Uvanesh, S. S. Sagiri, B. Behera, N. Babu, M. K. Bhattacharyya, K. Pal and I. Banerjee, *International Journal of Biological Macromolecules*, 2016, **92**, 504–514.

2 A. C. Anselmo, K. J. McHugh, J. Webster, R. Langer and A. Jaklenec, *Adv. Mater.*, 2016, 1–5.

3 É. Pérez-Esteve, M. Ruiz-Rico, A. Fuentes, M. D. Marcos, F. Sancenón, R. Martínez-Máñez and J. M. Barat, *LWT - Food Science and Technology*, 2016, **72**, 351–360.

4 M. Ruiz-Rico, É. Pérez-Esteve, M. J. Lerma-García, M. D. Marcos, R. Martínez-Máñez and J. M. Barat, *Food Chemistry*, 2017, **218**, 471–478.

5 F. Lim and A. Sun, *Science*, 1980, **210**, 908–910.

6 S. Sakai, T. Ono, H. Ijima and K. Kawakami, *J Sol-Gel Sci Technol*, 2003, **28**, 267–272.

7 A. Sosnik, *ISRN Pharmaceutics*, 2014, 1–17.

8 F. B. Haffner, M. Girardon, S. Fontanay, N. Canilho, R. E. Duval, M. Mierzwa, M. Etienne, R. Diab and A. Pasc, *J. Mater. Chem. B*, 2016, **4**, 7929–7935.

9 R. F. Fakhrullin and R. T. Minullina, *Langmuir*, 2009, **25**, 6617–6621.

10 J. van Wijk, T. Heunis, E. Harmzen, L. M. T. Dicks, J. Meuldijk and B. Klumperman, *Chem. Commun.*, 2014, **50**, 15427–15430.

11 S. Kim, M.-J. Stébé, J.-L. Blin and A. Pasc, *J. Mater. Chem.*, 2014, **2**, 7910–7917.

12 Y.-T. Liao, K. C. W. Wu and J. Yu, *J Biomed Mater Res Part B*, 2014, **102**, 293–302.

13 I.-A. Pavel, S. F. Prazeres, G. Montalvo, C. García Ruiz, V. Nicolas, A. Celzard, F. Dehez, L. Canabady-Rochelle, N. Canilho and A. Pasc, *Langmuir*, 2017, **33**, 3333–3340.

14 Z. Cao, L. Yang, Q. Ye, Q. Cui, D. Qi and U. Ziener, *Langmuir*, 2013, **29**, 6509–6518.

15 A. Assifaoui, F. Bouyer, O. Chambin and P. Cayot, *Acta Biomater.*, 2013, **9**, 6218–6225.

16 C. Spedalieri, C. Sicard, M. Perullini, R. Brayner, T. Coradin, J. Livage, S. A. Bilmes and M. Jobbágy, *J. Mater. Chem. B*, 2015, **3**, 3189–3194.

17 C. F. Meunier, P. Dandoy and B.-L. Su, *Journal of Colloid and Interface Science*, 2010, **342**,

211–224.

18 M. Perullini, M. Calcabrini, M. Jobbágy and S. A. Bilmes, *Mesoporous Biomater*, 2015, **2**, 3–12.

19 A. A. Hamouda and H. A. A. Amiri, *Energies*, 2014, **7**, 568–590.

20 M. Fujiwara, K. Shiokawa and T. Kubota, *Materials Science and Engineering: C*, 2012, **32**, 2484–2490.

21 F. Gaboriaud, A. Nonat, D. Chaumont and A. Craievich, *Journal of Colloid and Interface Science*, 2002, **253**, 140–149.

22 T. Coradin, N. Nassif and J. Livage, *Appl Microbiol Biotechnol*, 2003, **61**, 429–434.

23 L. Kearney, M. Upton and A. Mc Loughlin, *Applied and Environmental Microbiology*, 1990, **56**, 3112–3116.

24 T. Y. Sheu and R. T. Marshall, *Journal of Food Science*, 1993, **54**, 557–561.

25 D. Poncelet, V. Babak, C. Dulieu and A. Picot, *Colloids and Surfaces A: Physicochemical and Engineering Aspects*, 1999, **155**, 171–176.

26 E. Selmer-Olsen, T. Sorhaug, S.-E. Birkeland and R. Pehrson, *Journal of Industrial Microbiology & Biotechnology*, 1999, **23**, 79–85.

27 P. Allan-Wojtas, L. Truelstrup Hansen and A. T. Paulson, *LWT - Food Science and Technology*, 2008, **41**, 101–108.

28 C. Zohar-Perez, I. Chet and A. Nussinovitch, *Biotechnology and Bioengineering*, 2004, **88**, 671–674.

29 M. R. Corbo, A. Bevilacqua and M. Sinigaglia, *International Journal of Food Science and Technology*, 2011, **46**, 2212–2217.

30 M. I. Brachkova, M. A. Duarte and J. F. Pinto, *European Journal of Pharmaceutical Sciences*, 2010, **41**, 589–596.

31 N. Bock, M. A. Woodruff, D. W. Hutmacher and T. R. Dargaville, *Polymers*, 2011, **3**, 131–149.

32 L. G. Gomez-Mascaraque, R. C. Morfin, R. Pérez-Masiá, G. Sanchez and A. López-Rubio, *LWT - Food Science and Technology*, 2016, **69**, 438–446.

33 J. A. Bhushani and C. Anandharamakrishnan, *Trends in Food Science & Technology*, 2014, **38**, 21–33.

34 A. Jaworek and A. T. Sobczyk, *Journal of Electrostatics*, 2008, **66**, 197–219.

35 H. Valo, L. Peltonen, S. Vehviläinen, M. Karjalainen, R. Kostiainen, T. Laaksonen and J. Hirvonen, *Small*, 2009, **5**, 1791–1798.

36 N. Arya, S. Chakraborty, N. Dube and D. S. Katti, *J. Biomed. Mater. Res.*, 2009, **88B**, 17–31.

37 B. G. Amsden and M. F. A. Goosen, *Journal of Controlled Release*, 1997, **43**, 183–196.

38 D. Poncelet, B. Bugarski, B. G. Amsden, J. Zhu, R. Neufeld and M. F. A. Goosen, *Appl Microbiol Biotechnol*, 1994, 251–255.

39 G. Broeckx, D. Vandenheuvel, I. J. J. Claes, S. Lebeer and F. Kiekens, *International Journal of Pharmaceutics*, 2016, **505**, 303–318.

40 J. H. Crowe, L. M. Crowe, J. F. Carpenter, A. S. Rudolph, C. A. Wistrom, B. J. Spargo and T. J. Anchordoguy, *Biochimica et Biophysica Acta*, 1988, **947**, 367–384.

41 K. Önneby, L. Pizzul, J. Bjerketorp, D. Mahlin, S. Håkansson and P. Wessman, *World J Microbiol Biotechnol*, 2013, **29**, 1399–1408.

42 C. P. Champagne, N. Gardner, E. Brochu and Y. Beaulieu, *Canadian Institute of Food Science and Technology*, 1991, **24**, 118–128.

43 A. Siaterlis, G. Deepika and D. Charalampopoulos, *Letters in Applied Microbiology*, 2009, **48**, 295–301.

44 A. Nag and S. Das, *International Journal of Dairy Technology*, 2013, **66**, 162–169.

45 M. Basholli-Salihu, M. Mueller, S. Salar-Behzadi, F. M. Unger and H. Viernstein, *LWT - Food Science and Technology*, 2014, **57**, 276–282.

46 B. Li, F. Tian, X. Liu, J. Zhao, H. Zhang and W. Chen, *Appl Microbiol Biotechnol*, 2011, **92**, 609–616.

47 P. B. Conrad, D. P. Miller, P. R. Cielenski and J. J. de Pablo, *Cryobiology*, 2000, **41**, 17–24.

48 A. S. Carvalho, J. Silva, P. Ho, P. Teixeira, F. X. Malcata and P. Gibbs, *Journal of Food Science*, 2003, **68**, 2538–2541.

49 T. F. Bozoglu, M. Özilgen and U. Bakir, *Enzyme Microb. Technol.*, 1987, **9**, 531–537.

50 M. Minekus *et al*, *Food Funct.*, 2014, **5**, 1113.

51 I. Mainville, Y. Arcand and E. R. Farnworth, *International Journal of Food Microbiology*, 2005, **99**, 287–296.

52 T. Wiele, N. Boon, S. Possemiers, H. Jacobs and W. Verstraete, *FEMS Microbiology Ecology*, 2004, **51**, 143–153.

53 P. De Boever, B. Deplancke and W. Verstraete, *Journal of Nutrition*, 2000, 2599–2606.

54 S. Ceuppens, M. Uyttendaele, K. Drieskens, M. Heyndrickx, A. Rajkovic, N. Boon and T. Van de Wiele, *Applied and Environmental Microbiology*, 2012, **78**, 7698–7705.

55 S. Possemiers, M. Marzorati, W. Verstraete and T. Van de Wiele, *International Journal of Food Microbiology*, 2010, **141**, 97–103.

56 K. H. Sutton, *Mutation Research/Fundamental and Molecular Mechanisms of Mutagenesis*, 2007, **622**, 117–121.

57 D. Granato, G. Branco, F. Nazzaro, A. G. Cruz and J. A. F. Faria, *Comprehensive Reviews in Food Science and Food Safety*, 2010, **9**, 292–302.

58 J. Suez, T. Korem, D. Zeevi, G. Zilberman-Schapira, C. A. Thaiss, O. Maza, D. Israeli, N. Zmora, S. Gilad, A. Weinberger, Y. Kuperman, A. Harmelin, I. Kolodkin-Gal, H. Shapiro, Z. Halpern, E. Segal and E. Elinav, *Nature*, 2014, 1–6.

59 M. Perricone, A. Bevilacqua, C. Altieri, M. Sinigaglia and M. Corbo, *Beverages*, 2015, **1**, 95–103.

60 C. J. Ingham, M. Beerthuyzen and J. van Hylckama Vlieg, *Applied and Environmental Microbiology*, 2008, **74**, 7750–7758.

61 P. Ruas-Madiedo, M. Gueimonde, F. Arigoni, C. G. de los Reyes-Gavilan and A. Margolles, *Applied and Environmental Microbiology*, 2009, **75**, 1204–1207.

62 J. Barbosa and P. Teixeira, *Food Reviews International*, 2016, **33**, 335–358.

63 M. Fenech, *Carcinogenesis*, 2004, **26**, 991–999.

64 S. Sohrabvandi, S. H. Razavi, S. M. Mousavi and A. M. Mortazavian, *The Philippine Agricultural Scientist*, 2010, **93**, 24–28.

65 S. Sakai, T. Ono, H. Ijima and K. Kawakami, *J. Biomater. Sci.*, 2003, **14**, 643–652.

66 Z. Zhao, X. Xie, Z. Wang, Y. Tao, X. Niu, X. Huang, L. Liu and Z. Li, *Journal of Bioscience and Bioengineering*, 2016, 1–7.

67 S.-W. Xu, Y. Lu, J. Li, Y.-F. Zhang and Z.-Y. Jiang, *J. Biomater. Sci.*, 2007, **18**, 71–80.

68 P. S. Anbinder, L. Deladino, A. S. Navarro, J. I. Amalvy and M. N. Martino, *JEAS*, 2011, **01**, 80–87.

69 S. K. Bajpai and S. Sharma, *Reactive and Functional Polymers*, 2004, 129–140.

70 A. F. Wallace, G. V. Gibbs and P. M. Dove, *J. Phys. Chem. A*, 2010, **114**, 2534–2542.

71 H. Yamada, C. Urata, Y. Aoyama, S. Osada, Y. Yamauchi and K. Kuroda, *Chem. Mater.*, 2012, **24**, 1462–1471.

72 S. Plettinck, L. Chou and R. Wollast, *Mineralogical Magazine*, 1994, **58A**, 728–729.

73 Y. Sardessai and S. Bhosle, *Research in Microbiology*, 2002, 263–268.

74 Q. He, J. Shi, M. Zhu, Y. Chen and F. Chen, *Microporous and Mesoporous Materials*, 2010, **131**, 314–320.

75 S. K. Rhee and M. Y. Pack, *Journal of Bacteriology*, 1980, **144**, 865–868.

76 R. Ravetti-Duran, J.-L. Blin, M.-J. Stébé, C. Castel and A. Pasc, *J. Mater. Chem.*, 2012, **22**, 21540–21548.

77 A. Pasc, J.-L. Blin, M.-J. Stébé and J. Ghanbaja, *RSC Adv.*, 2011, **1**, 1204–1206.

78 S. Boninsegna, R. Dal Toso and R. Dal Monte, *J Sol-Gel Sci Technol*, 2003, **26**, 1151–1157.

79 K. R. Duarte, C. Justino, T. Panteleitchouk, A. Zrineh, A. C. Freitas, A. C. Duarte and T. A. P. Rocha-Santos, *Int. J. Environ. Sci. Technol.*, 2013, **11**, 589–596.

80 M. Perullini, M. Jobbágy, G. J. A. A. Soler-Illia and S. A. Bilmes, *Chem. Mater.*, 2005, **17**, 3806–3808.

81 E. Ananta *et al.*, *Microb Ecol Health Dis*, 2004, **16**, 113–124.

82 M. Alander, R. Korpela, M. Saxelin, T. Vilpponen-Salmela, T. Mattila-Sandholm and A. von Wright, *Letters in Applied Microbiology*, 1997, **24**, 361–364.

83 M. E. Segers and S. Lebeer, *Microbial Cell Factories*, 2014, **13**, 1–16.

84 C. Lacroix and S. Yildirim, *Current Opinion in Biotechnology*, 2007, **18**, 176–183.

85 H. T. Nguyen, H. Razafindralambo, C. Blecker, C. N'Yapo, P. Thonart and F. Delvigne, *Biochemical Engineering Journal*, 2014, **88**, 85–94.

86 C. C. Coghetto, G. B. Brinques, N. M. Siqueira, J. Pletsch, R. M. D. Soares and M. A. Z. Ayub, *Journal of Functional Foods*, 2016, **24**, 316–326.

87 S. Sathyabama, M. Ranjith kumar, P. Bruntha devi, R. Vijayabharathi and V. Brindha priyadharisini, *LWT - Food Science and Technology*, 2014, **57**, 419–425.

88 W. Sun and M. W. Griffiths, *Internationa Journal of Food Microbiology*, 2000, **61**, 17–25.

89 C. S. Favaro-Trindade and C. R. F. Grosso, *Journal of Microencapsulation*, 2001, **19**, 485–494.

90 A. De Prisco, D. Maresca, D. Ongeng and G. Mauriello, *LWT - Food Science and Technology*, 2015, **61**, 452–462.

91 R. Rajam and C. Anandharamakrishnan, *LWT - Food Science and Technology*, 2015, **60**, 773–780.

92 D. Schell and C. Beermann, *Food Research International*, 2014, **62**, 308–314.

93 J. Wang, D. R. Korber, N. H. Low and M. T. Nickerson, *Food Research International*, 2014, **55**, 20–27.

94 P. K. Okuro, M. Thomazini, J. C. C. Balieiro, R. D. C. O. Liberal and C. S. Fávaro-Trindade, *FRIN*, 2013, **53**, 96–103.

95 D. Ying, S. Schwander, R. Weerakkody, L. Sanguansri, C. Gantenbein-Demarchi and M. A. Augustin, *Journal of Functional Foods*, 2013, **5**, 98–105.

96 V. M. Sheehan, P. Ross and G. F. Fitzgerald, *Innovative Food Science & Emerging Technologies*, 2007, **8**, 279–284.

97 S. Nualkaekul, M. T. Cook, V. V. Khutoryanskiy and D. Charalampopoulos, *Food Research International*, 2013, 304–311.

CONCLUSIONS GÉNÉRALES ET PERSPECTIVES / GENERAL CONCLUSIONS AND PERSPECTIVES

5. CONCLUSIONS GÉNÉRALES ET PERSPECTIVES

Ce travail a été réalisé dans le cadre du réseau européen BIBAFOODS, consortium international réunissant des chercheurs et des institutions reconnus de plusieurs pays européens: le Portugal, l'Espagne, la France, l'Allemagne, la Belgique, le Danemark et la Suède. L'objectif principal du réseau BIBAFOODS est le développement et la compréhension des systèmes polymériques pour l'encapsulation et la libération de bactéries probiotiques et d'enzymes, pour enfin proposer de nouveaux systèmes cargos pour des aliments fonctionnels. Dans l'ensemble, les collaborations ont été très productives en raison de l'expertise complémentaire et spécifique disponible au sein des partenaires. Par exemple, nous avons bénéficié dans ce travail des compétences particulières en rhéologie, grâce à notre partenaire de l'Université d'Algarve (Bruno Medronho) et de la connaissance particulière d'un modèle d'intestin *in vitro* à travers notre partenaire de l'Université de Gand (Tom van de Wiele).

Dans ce même contexte, le but de ce travail de recherche était en développer des microparticules potentiellement compatibles avec des aliments et contenant une bactérie modèle : la *Lactobacillus rhamnosus* GG. Pour mener à bien cet objective, un polymère organique, l'alginate et une matrice inorganique, la silice, ont été choisis. Deux stratégies de microencapsulation ont donc été investies afin d'obtenir les particules hybrides d'alginate et de silice: (1) émulsification et (2) électrospraying couplé à une étape d'enrobage par une couche de silice.

Dans la première stratégie, utilisant l'**émulsification**, des microparticules hybrides d'environ 10 à 20 µm ont été obtenues à température ambiante. Pour ce faire, une émulsion eau-dans-huile (W/O) d'alginate de sodium et de silicate de sodium dans le miglyol a été préparée en utilisant le PGPR comme émulsifiant. L'ajout d'une solution de $CaCl_2$ a conduit à la formation de microparticules, pleines, creuses ou perforées selon la quantité de chaque constituant (alginate, source de silice et de calcium). Le mécanisme de formation de ces matériaux a été étudié en combinat des analyses de RMN, de microscopie électronique à balayage et des mesures de rhéologie. Il est notamment à remarquer que les expériences *in situ* de rhéologique linéaire ont été sensibles aux

différentes formulations et ont nous ont permis d'obtenir des informations importantes quant au mécanisme de formation. On observe ainsi que le calcium entraîne non seulement la formation du réseau d'alginate, mais influence également la morphologie finale de la couche de silicate, conduisant à des billes lisses ou perforées, tandis que la concentration du précurseur de silice entraîne la formation de billes rondes et robustes. Il est intéressant de noter que le réseau d'alginate a pu être renforcé de par son interaction avec des agrégats de silicate, pour des valeurs supérieures à la concentration critique en calcium.

Cependant, malgré le taux important de bactéries encapsulées (conformément aux analyses par microscopie électronique à transmission et confocal), les LGG ne possèdent qu'une faible viabilité lorsqu'elles sont évaluées avec des colorants intercalants d'ADN. En outre, la désintégration du matériau dans les conditions gastro-intestinales n'a pas été possible. Par conséquent, ces résultats nous ont permis de conclure qu'un tel matériau composite pourrait être utilisé dans l'encapsulation d'autres molécules d'intérêt, mais il ne semble pas convenir aux cellules, et plus particulièrement aux LGG.

Les principaux atouts de cette synthèse sont liés au coût réduit et au label « vert » de la source de silice, à la monodispersité du matériau final ainsi qu'à la stabilité des émulsions W/O. En outre, comme les humains ne sont pas capables de détecter des particules inférieures à 25 µm et comme la sensation en bouche est un paramètre décisif dans le développement de matrices alimentaires, ces particules auraient un réel intérêt. Néanmoins, pour des applications futures, il est encore nécessaire d'optimiser la méthode de séparation des particules alginate-silice de l'émulsion concentrée et le scalling-up de la méthode de synthèse devrait être étudié. En résumé, cette voie de synthèse, par émulsification, constitue une approche innovante avec une application potentielle dans l'encapsulation de biomolécules hydrosolubles compatibles avec un pH basique.

La deuxième stratégie de synthèse consiste à obtenir de microparticules cœur-couronne constituées donc d'un cœur d'alginate entouré d'une couche de silice. D'abord, la synthèse des particules monodisperses d'alginate été mise au point en utilisant l'électrospraying. Des particules d'alginate d'environ 220 µm ont été obtenues avec seulement les LGG et des particules d'environ 600 µm en ajoutant également un

cryoprotecteur, le saccharose. Par ailleurs, la présence du cryoprotecteur n'est avérée aussi indispensable pour maintenir la viabilité cellulaire lors de la lyophilisation des billes. Ensuite, les microionogels ont été couverts d'une couche de silice poreuse en utilisant le tetramethoxysilane (TMOS) et l'aminopropyltrimethoxysilane (APTMS) comme source de silice, et le Tween 40 comme porogène. L'effet du milieu réactionnel, organique ou aqueux, sur la viabilité des bactéries a été testé. Seul le milieu aqueux a permis de maintenir une viabilité suffisante des bactéries, qui ont pu, de plus, se multiplier à l'intérieur de la capsule grâce à la pénétration des nutriments à travers la couche silicatée poreuse.

Il est important de noter qu'une viabilité élevée de LGG a été maintenue à la fois dans l'alginate et l'alginate-silice pendant 3 semaines à la température ambiante ($3{,}4\ 10^{10}$ CFU g^{-1} et $4{,}1\ 10^{8}$ CFU g^{-1}, respectivement). Ces valeurs correspondent au nombre total de cellules existant dans les produits actuels du marché européen ($\geq 1{,}0 \times 10^{9}$ CFU g^{-1}, Winclove 505 Adulte).

Afin d'explorer la potentialité de ces prototypes cargo pour l'administration de probiotiques par la voie orale, leur comportement lors du passage à travers le tractus gastro-intestinal a été étudié. Pour ce faire, le modèle *in vitro* SHIME (simulator of the human intestinal microbial ecosystem) a été utilisé. Cette étude a été réalisée en collaboration avec Tom van de Wiele à l'Université de Gand en Belgique. Il s'est avéré que la microencapsulation a en effet permis de protéger la bactérie du pH acide du milieu gastrique, notamment dans le cas des particules cœur-couronne. Les deux systèmes (alginate et alginate-silice) ont permis une meilleure colonisation dans les conditions du colon par rapport aux LGG libres, non-encapsulées. De manière très intéressante, alors que métaboliquement inactives dans les conditions du tractus gastro-intestinal supérieur, les LGG libérées à partir de microparticules silicatées stimulent leur métabolisme une fois mises dans les conditions du colon, où ils dépassent la communauté d'autres espèces de *Lactobacillus*.

Pour clore cette étude, tout en ouvrant le champ d'applications de ces microparticules cargo de probiotiques, la survie des bactéries encapsulées dans deux boissons, un jus de pomme et une bière alcoolisée à 5% a été évaluée. Après un stockage à 4°C pendant une semaine, les bactéries encapsulées ont vu leur viabilité décroitre légèrement, tout en

gardant une valeur convenable pour leur potentielle consommation. Ce résultat montre que, contrairement aux études antérieures de la littérature, la bière contenant 5% d'alcool pourrait être considérée comme matrice alimentaire de probiotiques, tout comme le jus de pomme.

Cette deuxième approche a permis d'obtenir plusieurs résultats positifs: (i) obtenir des particules monodisperses; (Ii) permettre la croissance des cellules dans les micro-compartiments, qui ouvre des possibilités d'exploration de nouveaux systèmes tels que les microréacteurs, (iii) avoir une concentration initiale plus importante de cellules au sein du meme cargo et donc un apport plus important de cellules viables aux intestins, dans le cas de l'administration de probiotiques par la voie orales, (iv) la simplicité de la stratégie de synthèse, (v) avoir une stabilité mécanique supérieure des billes par rapport aux microgels d'alginate seuls. De plus, ces microparticules presenteraient un intérêt non seulement comme cargo dans des produits alimentaires, mais aussi à des produits cosmétiques ou nutraceutiques. En effet, un dentifrice contenant des probiotiques pour équilibrer le microbiota bucal ou une crème exfoliante avec des probiotiques à libérer sur la peau sont quelques idées potentielles pour valoriser ce matériau. Au-delà du domaine des probiotiques, les microparticules pourraient avoir un intêret dans les implants de cellules eucaryotes, les amplificateurs de cellules bactériennes du sol, l'addition ponctuelle de bactéries dans un processus industriel suivi d'une filtration facile du support hors du système. La fabrication du vin ou le traitement de l'eau sont des exemples de champs d'application, parmi beaucoup d'autres.

Des études complémentaires concernant les particules cœur-couronne pourraient être entreprises pour: (i) étudier la fonctionnalité des LGG libérées dans le côlon. Est-ce que les bactéries conservent leurs propriétés d'adhérence ou les LGG libérées relanceraient-elles leur métabolisme au niveau du site ciblé? (ii) suivre la viabilité bactérienne dans des poudres lyophilisées pendant plus de 3 semaines, (iii) adapter la stratégie en tenant compte d'un environnement exempt d'oxygène afin d'appliquer la stratégie à la prochaine génération de probiotiques, qui sont essentiellement strictement anaérobes, (iv) utiliser différents types de précurseurs de silice tels que le glycérol ou les précurseurs préhydrolysés pour effectuer l'enrobage de silice. Étudier leur impact sur le métabolisme des bactéries encapsulées, (v) moduler la quantité de précurseur de silice ajoutée dans

l'étape de minéralisation afin d'évaluer la robustesse mécanique de ces supports et d'évaluer la désintégration des billes. Une certaine stabilité mécanique est en effet exigée dans certains processus de production.

En conclusion, l'encapsulation des bactéries probiotiques en vue d'une libération contrôlée au niveau du tractus gastro-intestinal reste un sujet de recherche compétitif et stimulant, non seulement au niveau académique mais aussi industriel. Le marché des probiotiques devrait atteindre 36,7 milliards de dollars d'ici 2018. De nouveaux fournisseurs d'aliments aux probiotiques sortiront de la boîte-à-idées et pousseront les limites des techniques d'encapsulation actuelles.

5. GENERAL CONCLUSIONS AND PERSPECTIVES

This PhD work is inserted in a European network called BIBAFOODS. It is an international and powerful consortium of researchers who work in leading institutions across Europe: Portugal, Spain, France, Germany, Belgium, Denmark and Sweden. One of its main objectives is to develop colloidal delivery systems for bioactive compounds, such as probiotic bacteria and enzymes, resulting in eventual potential carriers for functional foods. Overall and in brief, the collaborations were very productive due to the complementary and specific expertise available within the partners. For instance, the present work took advantage of the rheology and *in vitro* gut model knowledge from partners at University of Algarve (Bruno Medronho) and University of Ghent (Tom van de Wiele), respectively.

Accordingly, the goal of the present PhD study was to develop food compatible microcarriers encapsulating a model probiotic bacterium: *Lactobacillus rhamnosus* GG. In order to accomplish such task, alginate and silica were chosen as organic and inorganic polymers, respectively. Two entrapment strategies were adopted therefore to obtain the hybrid alginate silica microparticles: emulsification and electrospraying coupled with a silica coating step.

In the **emulsification strategy**, the facile one-pot water-in-oil (W/O) emulsion is composed of $CaCl_2$ and sodium alginate with sodium silicate in the water phase along with miglyol in the oil phase and PGPR as stabilizer. Beads of about 10-20 μm in size were successfully obtained after a 6 h synthesis at room temperature. Despite the fact that we observed entrapped LGG with the TEM and CLSM techniques, the bacteria hold only little viability when being assessed with DNA intercalating dyes. Additionally, the disintegration of the material in gastrointestinal conditions was not achieved. The combination of both results directed us to the conclusion that such composite material could be employed in the encapsulation of other molecules of interest, but it is not suitable for cells, more specifically LGG. The formation mechanism of those beads was in any case investigated with the aid of SEM, NMR and rheology. Remarkably, in situ linear rheological experiments are observed to be sensitive to the different formulations of the W/O emulsions and gave valuable insights on the formation mechanism. Calcium

is observed to drive not only the formation of the alginate network but also tunes the final morphology of the calcium silicate shell, *i.e*. smooth vs. perforated beads, while the concentration of the silica precursor is driving the formation of robust round beads. Interestingly, the alginate network can be strengthened by interaction with silicate aggregates, and this can happen above a critical calcium concentration.

The key appealing factors of this synthesis are related to the cost-effectiveness and green-label of the silica source, the monodispersity of the final material along with the stability of the W/O emulsions. Additionally, as humans are not able to detect particles below 25 µm and the mouthfeel is a decisive parameter in food matrices development, the interest of such a carrier is rather tremendous. Nonetheless, optimizations in separating the alginate-silica particles from the concentrated emulsion as well as scaling-up the synthesis are two major priorities when considering future studies. In resume, this fairly simple reverse emulsion route constitutes an innovative approach with potential application in the encapsulation of water-soluble biomolecules compatible with basic pH.

The second strategy consists in obtaining alginate microbeads of about 220 µm in size in a first step via **electrospraying**, and further coating them with silica in an aqueous solution containing Tween 40 as porogen. In order to store the microcarriers with high cell viability for longer periods of time at room temperature, freeze-drying appears as the best current option. Sucrose was chosen as cryoprotectant to enhance the cells protection during the drying, and therefore avoiding primarily water crystals growth within the alginate matrix. By adding the disaccharide the sizes of the beads doubled, probably due to the increased viscosity of the electrosprayed solution. Importantly, a high viability of LGG was maintained in both alginate and alginate-silica during 3 weeks at room temperature (at least $3.4\ 10^{10}$ CFU g^{-1} and $4.1\ 10^{8}$ CFU g^{-1}, respectively). These results are in line with the total cell counts of products momentarily in the market in Europe ($\geq 1.0 \times 10^{9}$ CFU g^{-1}, Winclove 505 Adult).

In the following stage of the research, the viability of the released bacteria from freeze-dried material was evaluated in an *in vitro* batch SHIME model (simulator of the human intestinal microbial ecosystem). It was revealed that microencapsulation efficiently protected LGG from the low gastric pH, especially in the case of silica-coated beads. Both

encapsulation systems (alginate and alginate-silica) allowed for a better colonization of the colon compared with free LGG. Interestingly, although metabolically inactive in the upper GIT, LGG released from silica coated beads boost their metabolism once they arrive in colon conditions, where they outcompete the community of other *Lactobacillus* species.

To conclude the work, the viability of released LGG from the freeze-dried carriers was briefly investigated in apple juice and beer at 4 °C during one-week. Opposing prior research, it was concluded that beer containing 5 vt% of alcohol could be a suitable matrix for probiotics delivery likewise is apple juice.

The core-shell approach has several positive outcomes: (i) monodispersity of the material; (ii) cells growth within the micro-compartments, which paves opportunities for exploring new systems such as microreactors, (iii) larger initial density of cells in a single carrier allowing a greater amount of cells arriving viable to the intestines in the case of oral probiotics intake, (iv) simplicity of the synthesis strategy, (v) superior mechanical stability of the beads when compared to alginate beads alone. Additionally, its interest is not only in possibly adding these carriers to thicker food products, but also in cosmetics or nutraceuticals. Indeed, toothpaste containing probiotics to balance the oral microbiota or an exfoliating cream with probiotics to be released on the skin are few potential ideas for such material. Beyond the probiotics field, their interest fall within eukaryotic cells implants, soil bacterial cells enhancers, punctual bacteria addition in an industrial process followed by easy filtration of the carrier out of the system. Wine making or water treatment are examples of fields with potentiality along these lines, among many more.

There are surely perspectives also for future research when it comes to this core-shell strategy. They are mainly: (i) Study the functionality of the released LGG in the colon. Does it keep its adhesion properties or does the released LGG revive its lactic acid production in the targeted site? (ii) Follow the bacteria viability of the freeze-dried powders for more than 3-weeks, (iii) Adapt the strategy taking into consideration an oxygen-free environment in order to apply the strategy to the next generation of probiotics, which are essentially strict anaerobes, (iv) Use different types of silica precursors such as glycerol or pre-hydrolyzed ones to perform the silica coating. Investigate their impact on the

metabolism of the encapsulated bacteria, (v) Tune the quantity of the silica precursor added in the coating step in order to assess the mechanical robustness of these carriers and evaluate more closely the coating disintegration. Mechanical stability insights may be of interest for products holding clear-cut requirements during their production processes.

As a final remark, encapsulation of probiotic bacteria targeting a release in the guts remains a challenging research topic, although the growth forecast for this market is expected to reach $36.7 billion by 2018. Novel probiotic food carriers will emerge from out-of-the-box thinking and pushing the boundaries of current encapsulation techniques.

APPENDIX I:

CHARACTERIZATION TECHNIQUES

APPENDIX I: CHARACTERIZATION TECHNIQUES

Scanning Electron Microscopy (SEM)

The scanning electron microscopy provides information on morphology, topology and composition of a given sample. Consequentially, this technique is useful for the understanding of microscopic structures. The images are produced by scanning the material with a raster pattern, line-by-line scanning, using lenses to direct a focused beam of electrons onto a sample. These electrons interact with the atoms composing the sample at various depths. Backscattered, primary and secondary electrons and photons of characteristic X-rays are types of signals resulting from such interaction. In the case of the secondary electron imaging, which is the most standard detection mode, emission of secondary electrons from very close to the sample surface allows very high-resolution images of the sample's topography and details of less than 1 nm in size can be revealed. As a result of a very narrow electron beam, SEM images hold a large depth of field and a 3D appearance is the outcome. When it comes to magnification, a range between 10 to more than 500 000 times is of possibility. Such fact highlights its potential as a technique if compared to the best light microscopes that hold a 250 times lower magnification power.

In the conventional SEM imaging, the material must be electrically conductive, at least surface-wise, as well as electrically grounded in order to prevent charge accumulation. If a sample is nonconductive, it is usually coated with gold or carbon using either a low vacuum sputter coating or a high vacuum evaporation.

In the present work, the observations were performed with a HITACHI S4800 microscope with an accelerating voltage of 3.0 or 5.0 kV and working distance of about 8 mm. Samples were carbon-coated under vacuum before observation unless otherwise specified.

Transmission Electron Microscopy (TEM)

The transmission electron microscopy allows the user to examine fine details as small as a single column of atoms on a sample. The image is obtained from the interactions

happening during the passage of an electron beam accelerated by a high voltage through an ultra-thin sample. The transmitted light beam is analyzed and information on the crystal structure of the matter is obtained via the diffraction properties of the electrons. Alongside, the contrast of the images is a result of the absorption of electrons by the material, the thickness of it and its composition.

In our case, the technique targeted the observation of local arrangement of pores in a sample and the presence of entrapped bacteria within the material hybrid matrix. To observe the arrangement of the pores, the sample powders were dispersed in a bi-component resin (BDMA and Araldite®) that harden for 3 days at 60°C. Ultra-thin slices of 80 nm were cut with a microtome (Leica) and were placed on a holey carbon grid coated with copper. To observe the entrapment of bacteria within a hybrid matrix, the sample preparation is more arduous and already mentioned on the experimental chapter. In the sample preparation, oolong tea extracts (OTE) and lead citrate are used for enhancement of the contrast of cell components, as osmium tetraoxide (OsO_4) does not provide enough high contrast. Thus, the aromatic polyphenols of OTE react with peptide bonds and acts as an adjunct to aldehyde fixation. Aldehyde creates covalent bonds between protein and tissues anchoring them to the cytoskeleton of the organism. This step is called fixation. It brings rigidity to the biological tissues preventing them from decay, *i.e.* autolysis or putrefaction.

In the present work, the observations were performed with a Philips/FEI CM200 200 keV.

Confocal Laser Scanning Microscopy (CLSM)

The confocal laser scanning microscopy allows the direct study of thick living specimens with a minimal sample preparation, which often resumes in the employment of fluorescent markers. It overcomes limitations of the traditional fluorescence microscopy in terms of image's optical resolution, especially in respect to sample depth. CLSM uses a point illumination on a sample and a pinhole in an optically conjugated plane in front of the detector, fact that excludes out-of-focus signals. This way only the fluorescence close to the focal place is identified. However, only one point in the specimen is illuminated at a time and scanning over it with a regular raster, line-by-line

scanning, is compulsory. A positive peculiarity of this technique is the possibility in combining successive slices of different depths of a thick sample and obtaining a global 3D image (z-stack).

Staining the cells with the right fluorescent dyes and in suitable proportions is the core of a successful imaging. Essentially, fluorophores are fluorescent markers utilized to detect the expression of proteins and nucleic acids that accept light energy from a light source, a laser for example, at a certain wavelength and re-emit it at a longer wavelength. When the light is absorbed, electrons become excited and move from a resting state to a maximal energy level called the excited electronic singlet state (excitation stage). Conformational changes of the fluorophores happen in sequence and the electrons fall to a more stable, but lower, energy level allowing some of the absorbed energy to be released in form of heat. Subsequentially, the electrons fall back to the resting state releasing the remaining energy as fluorescence (emission stage). A single fluorophore can repeat such cycle several thousand times.

Our observations were carried out with a Leica TCS SPX AOBS CLSM. Images at a 315 µm side length square pixel size were obtained for each case in 1024 x 1024 matrices at 40x magnification (numerical aperture = 0.8). Fluorescence emissions were recorded within an airy disk confocal pinhole setting (Airy 1). Each channel was acquired sequentially. First channel detection was set from 492 to 525 nm with a 482 nm excitation laser line. Second channel detection was set from 597 to 716 nm with a 535 nm excitation laser line.

Flow Cytometry (FC)

The flow cytometry technique allows measurements of individual particles, often cells, that enter in a first stage the 3D space of a sample line holding a diameter only a bit larger than most of the cells. With the help of a fluidic system, a stream of single particles is ordered within a sheath fluid and pushed through the illumination source stage, allowing the analysis of one individual cell at a time. If the particles are labeled with fluorophores, quantitative and qualitative data is obtained via light scattering emissions using commonly lasers as light sources. Light that is scattered in the forward direction (FSC), mostly up to 20° offset from the laser beam's axis, relate to the

particle's size. Side scatter (SSC) providing information on relative complexity, granularity and internal structures for example, can be obtained with light measurements done at approximately 90° angle to the excitation line. Generally speaking, flow cytometers use separate channels and detectors, nowadays photomultiplier tubes (PMT) are utilized, to detect emitted light and such features will vary according to the instrument and manufacturer. Optical filters control the specificity of the detection, blocking and transmitting certain wavelengths at the same time. They are mainly three: long pass (allowing light through above a cutoff wavelength), short pass (allowing light below a cutoff wavelength) and band pass filters (allowing light within a specific narrow range of wavelengths known as band width). The use principle of fluorophores work in the same way as already mention for the CLSM technique.

Our experiments were performed using a CyAn ADP LX device equipped with a 50-mW Sapphire solid-state diode laser (488 nm). Green and red channels were collected with photo-multiplier tubes (PMT) using 530/40 and 613/20 band pass filters, respectively. Forward (FS) was collected with a 488/10 band pass filter. Two fluorescent dyes, SYBR Green I and Propidium iodide (PI), were used in combination to access the intact and damaged LGG cells.

Polymerase Chain Reaction (PCR) and Quantitative Polymerase Chain Reaction (qPCR)

Polymerase chain reaction is an efficient technique used in molecular biology to amplify a single or a few specific segments of DNA or RNA strands across several orders of magnitude. There are three clear steps in a typical PCR cycle, and each cycle doubles the load of the targeted DNA. As a preliminary step, the DNA must be extracted from a sample. Then the three main steps (denaturation, annealing and extension) can take place. During the denaturation, the temperature rises above 90 °C for few seconds in order to break the relatively weak hydrogen bonds holding the complementary bases together. The double-stranded DNA is therefore separated into two single strands. In the next step, the temperature decreases to 50 – 64 °C for few seconds allowing the annealing of the primers to the single-stranded DNA templates. A very specific sequence of genetic code is encoded within the primers (man-made oligonucleotides targeting a specific bacteria, group or so on). Two primers (forward and reverse) are used at this

stage in order to copy each newly separated single strand of DNA. The primers should bind perfectly to a complementary part of the template. At this stage, two separated DNA strands, with sequences marked off by primers, are ready to be copied. In the third main step, the temperature increases approximately to 72 °C and the extension occurs. The nucleotides, known as dNTPs, in solution are added to the annealed primers by the DNA polymerase, and a new strand of DNA is therefore created. The cycle restarts since 30 to 40 repetitions are commonly necessary in a PCR amplification step to gather enough material.

In conventional PCR, DNA qualification can be done at the end of the above-mentioned three steps by loading the amplified DNA in an agarose gel and performing an electrophoresis. On the other hand, in quantitative PCR (qPCR), the amplification is monitored in real-time and quantification happens simultaneously with the aid of fluorescent markers. Commonly it is used non-specific dyes that intercalate with any double-stranded DNA.

In our PCR case, we used primers targeting lactobacilli (667R and 0159F) and total bacteria (518R and 338F-GC). Additionally, qPCR was performed on a StepOnePlus Real-Time PCR system with lactobacilli primers (04R and 05F), total bacteria primers (518R and 338F) and SYBR Green as the non-specific fluorescent dye.

Denaturing Gradient Gel Electrophoresis (DGGE)

The denaturing gradient gel electrophoresis can be seen as a molecular fingerprinting method that separates PCR-generated DNA fragments according to their mobilities under increasingly denaturing conditions and a uniform electric field. Differing DNA sequences of many dominant microorganisms are obtained with a PCR of environmental DNA. Yet the fragments often have similar sizes lower than 600 base pairs resulting in a single DNA band when running the conventional agarose gel electrophoresis. The outcome is therefore non-descriptive. With the DGGE technique, PCR products encounter a linearly increasing gradient of a chemical denaturant (usually a mixture of formamide and urea) as they migrate through a polyacrylamide gel. The weaker melting domains of the double-stranded DNA begin to denature upon certain threshold denaturant concentration, what slows drastically the migration. More

precisely, A-T pairing (2 hydrogen bonds per pairing) is less stable than G-C pairing (3 hydrogen bonds per pairing). DNA fragments richer in GC will be more stable, remain double-stranded until facing higher denaturant concentrations and therefore migrate farther down the gel. Often, a GC rich sequence is incorporated into one of the primers used in the PCR to modify the melting behavior of the fragment of interest and improve the fragments separation. To reveal the bands, the gel is stained with a DNA binding fluorescent dye and visualized under a UV light.

As a rule of thumb, distinctive bacteria have differing sequences of DNA, thus they will denature at different denaturant concentrations culminating in a pattern of bands. Theoretically each band represents a clear-cut bacterial population present in the initial community. The fingerprint can be uploaded in databases to elucidate microbial structural differences, community profiles, and so on. Additionally, specific target microorganisms can be studied since a breadth of PCR primers is available nowadays. As well as the technique can identify constituents representing only 1% of the total community.

Our DGGE experiment was performed using the INGENYphorU System and we targeted lactobacilli and total bacteria with the primers, 667R/0159F and 518R/338F-GC, respectively. We also used SYBR Green as fluorescent dye.

DNA extraction

DNA extraction is a procedure allowing the purification of DNA via physical and chemical steps. Firstly, the sample of DNA has to be exposed out of the cells. For such, a lysis buffer containing surfactants, salts, a chelating agent and a polymer is added to tubes holding the DNA samples and glass beads. The tube is shaken vigorously. The salts will provoke the clumping of debris as proteins, lipids and RNA, which are discarded after the solution's centrifugation step. Secondly, exposed DNA is purified further with a phenol-chloroform extraction. Phenol denatures further proteins present in solution. After another centrifugation step, denatured proteins stick to the organic phase while nucleic acids stay in the aqueous phase. Chloroform removes phenol residues from the solution. A freezing step of purified DNA in sodium acetate and isopropanol aids in precipitating the DNA. In sequence, the solution is centrifuged, supernatant discarded

and TE buffer (tris-EDTA buffer) is added to DNA pellet. This buffer will solubilize the DNA material and protect it from degradation.

Sanger Sequencing

Sanger sequencing is an *in vitro* DNA replication based on the selective addition of chain-terminating dideoxy nucleotides (ddNTPs for adenine, cytosine, guanine and thymine) by a DNA polymerase. The DNA fragments, usually up to about 900 base pairs, are separated with a capillary electrophoresis process. The classical method requires a DNA sample, a DNA primer, DNA polymerase, ordinary DNA nucleotides (dNTPs) and four dye-labeled chain-terminating dideoxy nucleotides. The latter nucleotides lack a 3'-OH group necessary in the formation of the phosphodiester bond between two nucleotides, resulting in cessation of the DNA extension when a modified ddNTP is incorporated into the sequence. In short, four separate sequencing reaction vessels will contain the DNA sample, DNA polymerase, the primer, all four dNTPs, but only one of each ddNTPs. The mixtures are heated in order to pull apart the double-stranded DNA, then cooled to allow the primer to bind onto the single DNA strand. In sequence, the temperature raises again to the optimal enzyme temperature (around 72 °C) allowing it to synthesize a new DNA starting from the primer. The polymerase will continue adding nucleotides to the strand until it happens to add a ddNTP. At this stage, the extension ends. This process is repeated in a number of cycles. When the cycling is completed, it is guaranteed that a dye labeled ddNTP will have been incorporated at every single position of the targeted DNA fragment in at least one reaction; therefore the vessel will contain fragments of different lengths. Finally, they run as a result of an electric field through a thin tube containing the gel matrix. Short fragments, such as the ones containing only one nucleotide after the primer, will move faster within the matrix followed by the next-smallest fragment, and so on. The fluorescence for each dye label will be detected, and a series of peaks in fluorescence intensity are shown in a chromatogram, which the DNA sequence is read from.

A service provider at University of Ghent ran our Sanger sequencing and reported the result.

Rheology

Rheology is a relevant tool on the understanding of the physical properties of a given material, primarily in the solid and the liquid state, but also soft matters such as gels, suspensions, emulsions, colloids or melted polymers. Overall the technique attempts to define a relation between the stress acting on this material and the resulting deformation/flow taking place. This way, the concepts of stress and strain are key to rheological evaluations. Stress (σ) is always a measurement of force per unit of surface area (force/area) and it is expressed in units of Pascal (Pa). The type of stress will be determined by the direction of the force with respect to the impacted surface. Normal stress happens when the force is directly perpendicular to a surface and can be produced during tension or compression. Shear stress occurs when the forces act in parallel to a surface and it is proportional to the shear strain rate (velocity/height).

The viscosity (η) is tendency of the fluid to resist a flow and it is defined by:

$$\eta = \frac{shear\ stress}{strain\ rate}\ (Pa.s)$$

In the case of hydrocolloids capable of forming gels, viscoelasticity (combination of viscosity and gel behavior) can be examined by determining the effect of an oscillation force on the material movement. Stress-strain testing plays a role in studying the behavior of gels and can be categorized as follows: small-strain and large-strain testing. In our case, we will focus on small-strain testing, which is when only a small percentage of the deformation is required to break the sample. An example is the oscillatory test. Gels have viscoelastic properties, therefore dynamic rheological tests in the linear viscoelastic range can provide information on the storage modulus (G'), loss modulus (G'') and loss factor ($\tan\delta = G''/G'$). The G' value measures the deformation energy stored in a sample during a shear process and ends up representing the elastic behavior of the sample. On the contrary, the G'' value measures the deformation energy loss during the shear and represents the viscous behavior of the sample. In resume, if $G' \gg G''$ than the sample has a solid-like behavior and the deformations will be essentially elastic; if $G'' \gg G'$ than the sample behaves in a liquid-like fashion. Figure 65 exemplifies the fluid-like and solid-like behaviors of a material undergoing gelation.

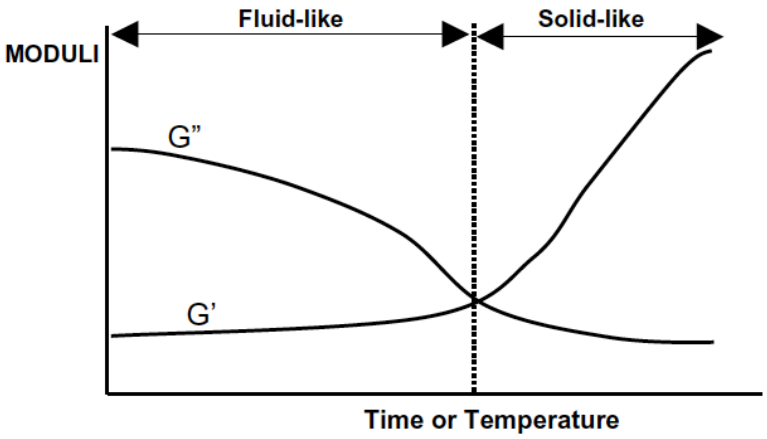

Figure 65: Viscoelastic properties of a material undergoing gelation.

Our rheological measurements were carried out on a HAAKE MARS III rheometer set with a cone-and-plate geometry (35 mm, 1º). A Peltier unit was used to accurately control the temperature, which was fixed at 25.0 ± 0.1 ºC. To minimize evaporation the measuring geometry was closed with an appropriate solvent trap.

We follow *in* situ the evolution of alginate crosslinking, silica precipitation and a sol-gel process measuring shear viscosity over 12 h.

APPENDIX II:
ESPERLUETTE

APPENDIX II: *ESPERLUETTE*

During my PhD studies, I conceived of an idea for a non-profit journal at the university of Lorraine that would acquaint both scientists and liberal arts majors with the exciting scientific research being done on campus. I interviewed PhD students, wrote and edited short, engaging pieces about their work, and paired their stories with striking, original illustrations from local artists. The result has been *Esperluette*, a compact, high-quality science publication. It's a mesmerizing glimpse into research crucial to our collective future and a bridge between the scientific and non-scientific communities of the University of Lorraine and beyond. Please find more info about the crew on our blog: http://esperluettenancy.wixsite.com/esperluette.

All the articles published since the beginning of 2016 can be found in the next pages or online. The explored domains encompass from chemistry, biology, physics and mathematics to informatics, geography, literature and it goes on and on.